Emil A. Edwin

Assessment of Fatigue Damage of Mooring Chain for Mobile Units – with focus on Installation Handling and Corrosion Degradation

Master's thesis in Marine structures

Supervisor: Kjell Larsen

August 2020

Master's thesis

NTNU
Norwegian University of Science and Technology
Faculty of Engineering
Department of Marine Technology

NTNU
Kunnskap for en bedre verden

Emil A. Edwin

Assessment of Fatigue Damage of Mooring Chain for Mobile Units – with focus on Installation Handling and Corrosion Degradation

Master's thesis in Marine structures
Supervisor: Kjell Larsen
August 2020

Norwegian University of Science and Technology
Faculty of Engineering
Department of Marine Technology

NTNU
Norwegian University of
Science and Technology

NTNU
Norwegian University of Science and Technology

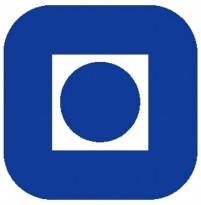

Department of Marine Technology

Assessment of Fatigue Damage of Mooring Chain for Mobile Units – with focus on Installation Handling and Corrosion Degradation

MSc thesis 2020

Emil A. Edwin

Fall 2020

I Assignment Text

I.I Background

The purpose of the mooring system of a Mobile Unit (MOU) is to keep the vessel safely at a required position. It normally consists of 8-12 mooring lines of heavy chain, steel wire ropes and/or synthetic polyester ropes connected to a seabed anchor.

During the past years, the requirements to the mooring and station keeping systems of mobile and permanent units have become more complex;
- The industry is moving into new frontiers (ultra-deep water down to 3000m depth and into arctic areas)
- There are more operations adjacent to other installations (flotel operations and tender support vessel operations)
- The new mobile units are becoming larger and many units are at the end of their lifetime
- There are too many anchor line failures

For MOUs, mooring failure rate is unacceptably high. The investigations show a variety of direct causes covering both inaccurate design, bad quality of mooring line components and lack of personnel competence related to operation of the system. The design practice for MOUs neglects the design check for fatigue completely; control of wear, tear and fatigue cracks are considered to be included in the class societies (e.g.DNV GL) re-certification regime.

The overall objective of this thesis is to improve the understanding of the fatigue degradation of mooring chain for MOUs during installation operations. Particular focus shall be on corrosion degradation and how finite element (FEA) analysis can be used in such assessments.

I.II Scope of Work

- Review relevant procedures and methods for installation and retrieval of mooring lines for mobile units. Propose safe conditions for a typical rig move operation and describe briefly hazards and risk reducing activities
- Review relevant literature and papers on mooring line failures. Make a summary on the main causes for line failures
- Describe state-of-art findings and knowledge related to corrosion degradation of chain by reviewing relevant literature. Propose any activities or changes that can be made to improve the present situation
- Describe briefly the DNV GL's requirements for inspection and re-certification of used chain. Propose improvements or revisions based on 2) and 3)
- Describe how fatigue damage of the mooring chain can be estimated for an installation operation using a frequency domain method and a simple model for mooring line dynamics. Describe in detail the simple model for line dynamics. Propose and describe how a finite element (FE) model of the chain links can be used in the assessment
- Make a finite element model of i) chain links in pure tension and ii) chain links supported by the stern roller of the anchor handler. Calculate the stress distribution and the stress concentration factors. Extent to be agreed with supervisor
- Conclusions and recommendations for further work

I.III General information

All necessary input data for the installation case is assumed to be provided by Equinor. The work scope may prove to be larger than initially anticipated. Subject to approval from the supervisor, topics may be reduced in extent. In the thesis the candidate shall present his personal contribution to the resolution of problems within the scope of work. Theories and conclusions should be based on mathematical derivations and/or logic reasoning identifying the various steps in the deduction. The candidate shall utilise the existing possibilities for obtaining relevant literature.

I.IV Report/Delivery

The thesis report should be organised in a rational manner to give a clear exposition of results, assessments, and conclusions. The text should be brief and to the point, with a clear language. Telegraphic language should be avoided.

The report shall be written in English and edited as a research report including literature survey, description of relevant mathematical models together with numerical simulation results, discussion, conclusions and proposal for further work. List of symbols and acronyms, references and (optional) appendices shall also be included. All figures, tables and equations shall be numerated.

The original contribution of the candidate and material taken from other sources shall be clearly defined. Work from other sources shall be properly referenced using an acknowledged referencing system.

The report shall be submitted in Inspera, as specified by the department of Marine Technology. In addition, an electronic copy (pdf) to be sent to the supervisor.

I.V Ownership

NTNU has according to the present rules the ownership of the thesis results. Any use of the thesis results has to be approved by NTNU (or external partner when this applies). The department has the right to use the results as if the work was carried out by a NTNU employee, if nothing else has been agreed in advance.

I.VI Thesis supervisor:

Prof. II Kjell Larsen, NTNU/Equinor

Deadline: August 15th 2020

Trondheim, January 31st, 2020

Kjell Larsen (sign.)

Emil August Edwin (sign.)

II Acknowledgements

A big thank you to my supervisor, Professor II Kjell Larsen. His guidance has been crucial when navigating through the big jungle of material needed to realize this MSc-thesis. Kjell has showed great interest for my project throughout the whole master period. Every week, there has been scheduled an hour of personal guidance. If problems occurred, there has never been a problem scheduling another meeting. He has put me in contact with his professional network to provide me with sparring partner, if the matter of subject was outside his expertise. All of this has made the whole experience of writing a MSc very enjoyable and educational.

Secondly, I would like to thank Tom Rune Jensen (CSS, Skien) for helping me navigate in SolidWorks. Even though the effort did not yield any results, our communication given me great insight into the world of FEA and SolidWorks.

When the efforts in SolidWorks did not work out, Petter Henrik Holmström (Equinor, SINTEF) stepped in and provided me with excellent guidance and knowledge in Abaqus. The efforts in Abaqus began in the late stages of the thesis and FEA results for this thesis would not have been produced without him, as time was of the essence.

Lastly, I would like to thank COVID-19 and my old and slowly deteriorating computer for robbing me of my summer vacation. This whole experience would not have been the same without you!

III Executive summary

Today's fatigue limit state (FLS) design curve for mooring chains is produced by DNV-GL in form of a SN-diagram based on Noble Denton testing. Noble Denton's testing is performed on small dimension chain (76mm) and all tests are run with 20% MBL mean load. The design curve do not take into account what mean tension the chain in reality experience, but instead only rely on the stress range. The design curve accounts for corrosion in the form of cross section area loss of link (can be formulated as diameter loss).

Most mooring chains usually operate with a mean tension between 5-18% MBL, as a result it is reasonable to ask if the mean tension has any impact on fatigue life. If it does, is it overly conservative to assume 20% MBL mean tension in DNV-GLs design curves? In this thesis we have looked into fatigue testing of new and used mooring chain (mainly performed by Equinor) to try and identify factors that increase and decrease fatigue life of mooring chain which the DNV-GL SN-curve do not include to a sufficient degree or at all.

Testing from the last decade strongly indicate that mean tension in a mooring chain have a big impact on fatigue life. Tests run on used chain with various degrees of wear, corrosion and defects have however shown outstanding fatigue performance when mean tension is lowered. Results indicate that used chain (up to 25 years in operation) can perform just as well or even outperform the results done by Noble Denton, when lower mean tensions are applied.

There has been universal agreement that corrosion has clear negative effect on fatigue life. Pitting and MIC/SRB have been looked upon as the most compromising types of corrosion as they leave sharp geometries and deep pits which is ideal for crack initiation. For MIC/SRB and pitting, DNV-GLs way of accounting for corrosion with diameter loss is sufficient. But, studies also imply that surface roughness from general corrosion might have a just as negative effect on fatigue life as pitting and MIC/SRB, which cross section/diameter loss do not cover to a sufficient degree. Fatigue assessments for AH OPS (52.6% MBL mean tension) performed in this thesis use LIFEMOOR's model to account for corrosion. These assessments showed that corrosion have a negative impact on fatigue life, but parameter sensitivity testing pointed to corrosion as the least impactful parameter w.r.t. fatigue damage. With an increase in fatigue damage of just 16.7% when comparing a new chain to the most severe corrosion grade included in the NORMOOR model. These findings indicate that today's regime for fatigue damage adjustments due to corrosion might then be overly conservative, especially if not adjusted for realistic operational mean tension.

It is not unusual for mooring chain for mobile units to be deployed and retrieved several times annually. As a part of the of the deployment procedure, the anchor fastening and chain is to be tested with a of 52.6% of the chains MBL (DNV-GL). The magnitude of this test load is often much larger than what the anchor and lines will experience before being retired or break. The test is performed by anchor handling vessels and when the load is applied, the chain will be in contact with fairlead and the stern roller of the anchor handling (AH) vessel. Finite element analyses (FEA) showed that peak stress location switched from chain link crown section for a straight chain, to mid straight section for chain over stern roller. The chain over stern roller saw an increase in peak stress of 15.6%. While a stress increase of just 15.6% might seem small, parameter sensitivity testing performed in this thesis showed that chain/stern roller contact increased fatigue damage by 54.5%, with other test parameters for chain and AH operation (OP) being close to optimal. Vargas, Hsu and Lee (2004) [29] suggests that stress concentration factors (SCFs) do not change to a significant extent with an increasing load. So in quantifying the SCF for chain over stern roller, simulations in Abaqus was run with only 10% of MBL and did not see any stresses exceed material yield. This was done to save computational time and get cleaner results.

An AH with a load of 52.6% MBL magnitude applied to a chain over a stern roller will most likely lead to residual stresses, local material damage and permanent deformation. Residual stresses, local material damage and permanent deformations of chain links has negative effects on fatigue life, but quantifying the effect of these is outside the scope of this thesis.

A fatigue damage assessment tool for AH OPS was programmed in MATLAB. Short term environmental conditions were characterized by JONSWAP wave spectra. The script provide the user with the opportunity to define an AH OP and quantify the fatigue damage caused by the OP. The following parameters were varied in fatigue assessments performed in this thesis:

- Water depth
- Wave heading
- JONSWAP defining environmental parameters (H_s & T_P)
- Applied tug pull force (mean tension)
- Chain corrosion grade
- SCF to account for chain geometry

A total of 5376 different AH OPS and their respective fatigue damage values were quantified. A base case with close to optimal chain and AH OP conditions was developed as a reference when quantifying parameter sensitivities.

Increase in relative fatigue damage ref base case:		
Corrosion	Grade 7	16.70 %
Mean tension	52.6% MBL	648 %
Peak wave period	14 sec	6360 %
Significant wave height	4 m	559 %
SCF	1.27	105 %
Water depth	100 m	2120 %
Wave heading	135 degrees	420 %

Table 1: Relative increase in fatigue damage comparing worst case to base case for each parameter. Except for mean tension where base case value is compared to lowest mean tension

In short, fatigue assessments performed in this thesis showed that if AH OPS are performed under close to optimal conditions, it will not have significant impact on fatigue life (a single AH OP exhaust $1.1 \cdot 10^{-4}$ % of total chain life). All operation parameters varied for the worse, do single-handedly increase the fatigue damage by a significant amount. Table 1 shows the impact on fatigue damage by comparing worst case values for each parameter to base case. It is important to note that the worst case values can be considered extreme and that most sensitivities showed an highly nonlinear behavior. As the base case damage is so small, varying just one parameter by itself is not enough to cause noteworthy damage. When multiple parameters are varied for the worse w.r.t. fatigue damage, the effects add up and we can end up seeing significant fatigue life exhaustion within typical AH operational limits. In AH case studies performed in this thesis with parameters within these typical operational limits, an annual fatigue life exhaustion of 2.42% just from AH was found (assuming 4 deployments and 4 retrievals lasting 30 minutes). The industry's expectation for a chain being operational for 25 years [19] will most certainly not be met if the chain is to experience 2.42% fatigue life exhaustion annually from AH OPS alone.

IV Sammendrag

Dagens FLS designkurve for forankringsliner er levert av DNV-GL i form av et SN-diagram. Diagrammet er basert på Noble Dentons testing, som baserer seg på testing av kjettinger med mindre dimensjoner (76mm), der alle testene gjennomført har en middelspenning på 20% MBL. Designkurven tar ikke noe hensyn til hvilke middelspenninger en kjetting i virkeligheten vil oppleve under vanlig bruk og tar kun hensyn til hvilke spenningsamplituder som oppleves. Designkurven redegjør for kjettingens korrosjonstilstand i form av tverrsnitttap for en kjettingløkke (kan reformuleres til diametertap).

De fleste forankringskjettinger opererer med en middelspenning mellom 5-18% MBL, noe som gjør det fornuftig å spørre seg selv om middelspenning har noen påvirkning på utmattingsskade. Hvis dette er tilfellet, er det da veldig konservativt å anta 20% MBL middelspenning i DNV-GLs designkurver? I denne masteravhandlingen har man sett på utmattingstester gjort på ny og brukt kjetting (hovedsakelig gjennomført av Equinor) for å prøve å identifisere faktorer som øker og minsker tretthetslivet til en forankringskjetting som DNV-GLs SN-kurve ikke dekker til en tilstrekkelig grad eller mislykkes med å inkludere.

Testing av kjetting det siste tiåret indikerer sterk korrelasjon mellom høyt middelstrekk og høyere utmattingskade. Tester kjørt med brukt kjetting som innehar forskjellige grader av slitasje, korrosjon og defekter har hatt fremragende utmattingsytelse når middelstrekket i forankringslinen er satt til typiske verdier man vil oppleve under vanlig drift. Resultatene fra testing indikerer at brukt kjetting (opp til 25 år i drift) kan yte like bra eller bedre enn Noble Dentons resultater, når en lavere middelspenning påføres kjettingen under testing.

Det er en universell enighet om at korrosjon har en klar negativ effekt når det kommer til utmatting. Gropkorrosjon og MIC/SRB har vært sett på som de mest kritiske typene korrosjon, ettersom de skaper skarpe geometrier og dype groper som er ideelle startsteder for sprekkdannelse. For MIC/SRB og gropkorrosjon, er DNV-GLs måte å redegjøre for korrosjon med diametertap tilstrekkelig. Men, studier peker også mot at generell overflateruhet pga. korrosjon kan ha minst like negativ effekt på utmattingsliv som gropkorrosjon og MIC/SRB, dette er noe som tverrsnitt/diametertap ikke klarer å ta hensyn til. Tretthetsvurderinger for AH OPS gjennomført i denne masteroppgaven bruker LIFEOORs modell for å redegjøre for korrosjon. Tretthetsvurderingene peker mot at korrosjon har en negativ effekt på utmatting, men testing av parameterfølsomhet utført viste at korrosjon hadde minst effekt på utmatting av alle parameter testet. Med en økning i utmattingskade på bare 16.7% når en ny kjetting ble sammenlignet med en kjetting som innehar LIFEMOORs mest alvorlige korrosjonsgrad. Dagens regime for justering utmattingskade pga. korrosjon kan være for konservativt. Spesielt hvis man ikke justerer for middelstrekkverdier nærmere det kjetting typisk opplever under vanlig bruk.

Det er ikke uvanlig at kjetting brukt til mobile enheter blir utplassert og hentes opp igjen flere ganger årlig. Som en del av utplasseringsprossessen skal kjettingen testes med en påsatt kraft lik 52.6% av kjettingens MBL (DNV-GL). Denne kraften er ofte mye større enn hva en kjetting kan forvente å se før den bryter eller tas ut av drift. Testingen utføres av AH-fartøy og når lasten på 52.6% MBL påføres, så er kjettingen i kontakt med fartøyets aktervalse og føringstrinse. FEA viste at peakstresset i en kjettingløkke forflyttet seg fra løkkens krone for en kjetting i rett strekk over til midten av løkkens rette seksjon når kjettingen var i kontakt med aktervalsen. Kjettingen i kontakt med aktervalse så en økning i peakstress på 15.6%. Selv om 15.6% stressøkning kan virke lite, viste tesingen av parameterfølsomhet en økning i utmattingskade på 54.5% når stressresultatene fra kjetting over aktervalse fra FEA ble brukt (resten av parameter satt til tilnærmet optimale operasjonsverdier). Vargas, Hsu and Lee (2004) [29] peker til at SCFer for kjettingløkker ikke endrer seg nevneverdig når man øker påsatt last. Så når SCF lagd for å redegjøre for kjetting over aktervalse ble kvantifisert i FEA, så ble simuleringer i Abaqus kjørt med kun 10% av kjettingens MBL, noe

som igjen førte til at vi ikke så stressverdier som overgikk kjettingens flytegrense. Dette ble gjort for å spare stimuleringstid og få penere verdier i Abaqus.

Når man i virkeligheten ville påført 52.6% av kjettingens MBL, så ville vi garantert sett stress høyere enn flytegrensen, som ville kunne føre til restspenninger, lokale materialskader og permanente deformasjoner. Restspenninger, lokale materialskader og permanente deformasjoner har en negativ effekt på kjettingens utmattingsprestasjoner i ettertid, men å fastsette effekten av disse er dessverre utenfor omfanget til denne masteravhandlingen.

Et utmattingskade-verktøy for AH OPS ble programmert i MATLAB. Kortvarige vær- og sjøforhold er karakterisert av JONSWAP bølgespektrum. AH OPS utmattingskadeverktøyet gir brukeren mulighet til å definere sin egen AH OP og kvantifisere utmattingskaden operasjonen vil ha på kjettingen. Følgende parameter ble variert i denne masteravhandlingen:

- Vanndybde
- Bølgeretning iht. AH-fartøy
- JONSWAP definerende sjøtilstandparameter (H_s & T_P)
- Påført kraft av AH-fartøy (middelspenning)
- Kjettingens korrosjonstilstand
- SCF som redegjør for kjettingens geometri

Total ble utmattingsverdier kvantifisert for 5376 forskjellige AH OPS. En base case med tett opp mot optimale verdier for AH OPS ble definert som en referanse for å sjekke sensistiviteten til de ulike parameterene.

Increase in relative fatigue damage ref base case:		
Corrosion	Grade 7	16.70 %
Mean tension	52.6% MBL	648 %
Peak wave period	14 sec	6360 %
Significant wave height	4 m	559 %
SCF	1.27	105 %
Water depth	100 m	2120 %
Wave heading	135 degrees	420 %

Table 2: Relativ økning i utmattingskade, når man sammenligner verste verdier iht. utmattingskade med base case. For middelstrekk er base case satt opp mot minste middelstrekk

Kort oppsummert, så forteller resultatene oss at AH OPS utført under tilnærmet optimale forhold fører til neglisjerbar skade på kjettingen (en enkelt AH OP fører til en skade lik $1.1 \cdot 10^{-4}$ % av det totale tretthetslivet). Alle parameter hvis endret for det verre i denne avhanglingen fører egenhendig til drastisk økning i utmattingskade. Tabell 2 illustrerer dette ved å sammenligne worst case verdier for hver parameter med base case. Her er det viktig å huske at worst case verdiene er ekstreme og at sensitivitene for det meste en har ulineær utvikling. Men ettersom skaden fra base case er såpass liten, vil ikke en parameter alene klare å føre til at vi ser betydelig skade av kjettingen. Om man varierer flere parameter for det verre iht. utmattingskade, så vil man kunne se at en signifikant del av tretthetslivet vil kunne gå med. I AH case-studier utført i denne masteravhanglingen, ble det funnet en årlig skade på 2.42% av totalt tretthetsliv kan forekomme bare fra AH OPS utført innenfor typiske operasjonelle grenser. Dette vil med høy sannsynlighet føre til at kjettingen ikke vil oppfylle industriens ønske om 25 år med drift [19].

Contents

List of Tables

List of Figures

14th August 2020

V List of Symbols and Abbreviations

Abbreviation	Definition
CAE	Computer-aided Engineering
CBL	Catalogue breaking load
COG	Center of gravity
CP	Cathodic protection
$DOF(s)$	Degree(s) of freedom
DP	Dynamic positioning
FEM	Finite element method
FEA	Finite element analysis
FL	Fatigue Limit
FLS	Fatigue Limit State
HC	Hydrocarbons
H_s	Significant wave height
MBL	Minimum breaking load
MIC	Microbiologically influenced corrosion
MOU	Mobile unit
MT	Magnetic particle testing
NDT	Non-destructive testing
OPB	Out of plane bending
OPS	Operation(s)
PT	Liquid penetration testing
SCF	Stress concentration factor
SRB	Sulphate reducing bacteria
SW	SolidWorks
RAO	Response amplitude operator

Symbol	Definition	Unit
a	Added mass	kg
A	Area	m^2
A_{link}	Cross sectional area of chain link	m^2
A_γ	Normalizing factor	
a_D	Intercept parameter of the S-N curve	
c	Length of line secant	m
C_d	Drag coefficient	
$d\&D$	Diameter	m
d_{NBi}	Fatigue damage for sea state i	
E	Energy	J
EA	Elastic modulus times area	$GPa \cdot m^2$
F	Force	N
F_{prop}	Propulsion Force from vessel	N
F_w	Environmental forces acting on vessel	N
g	Gravity	m/s^2
h	Water depth	m
H_s	Significant wave height	m
k	Spring constant	N/m
L	Length	m
m	Mass	kg
$n\&N$	Number of cycles	
s	Suspended length of line	m
S	Stress	MPa
SCF	Stress concentration factor	
T	Tension	N
T_2	Mean wave period	s
T_i	Time spent in sea state i	s
T_m	Percentage of MBL	0 - 1
T_p	Peak wave period	s
v	Velocity	m/s
v_{0i}	Mean up-crossing rate	Hz
w	Weight	kg
x, y, z	Directional inputs	m
α	Angle	$^\circ$
ϵ	Directional motion	m
η	Degree of freedom	
$\Gamma(.)$	Gamma function	
ω	Angular frequency	s^{-1}
ω_p	Peak wave frequency	s^{-1}
ϕ	Angle	$^\circ$
φ	Angle	$^\circ$
ρ	Density	kg/m^3
σ	Stress	MPa
σ_{si}	Standard deviation of the stress process	MPa
$\sigma_{T_{line(\omega)}}$	Standard deviation of line tension	N

*Unless specified otherwise

1 Introduction

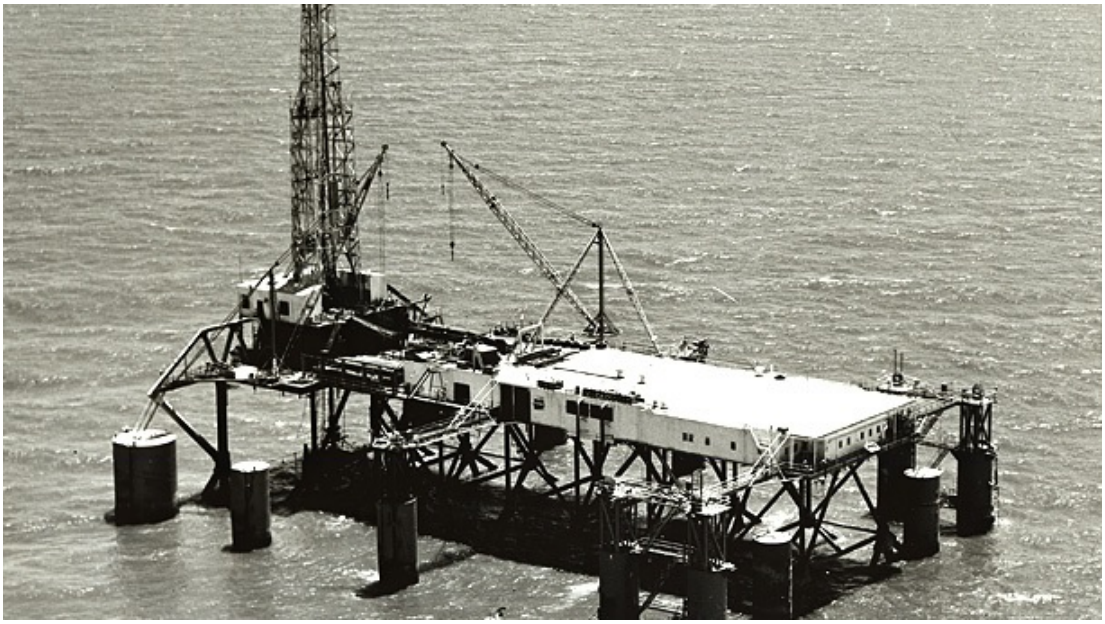

Figure 1: The first mobile drilling platform, Mr.Charlie (1954) [25]

Since the introduction of a mobile drilling rig in the 1950s, the use of mobile units in the offshore industry has increased drastically. The economical benefits of not having to fix platforms to the sea floor with stiff structures and being able to reuse units for different operations are obvious. In later years, drilling at ultra deep water (3000m depth) has become more common. With it, deeper waters and harsher weather conditions follow. To operate in these areas; floatels, semi submersibles, drilling rigs and ship based floaters are needed and keeping them at a relatively fixed location is a must. As a result, the need for sufficient station-keeping has increased. Mooring lines and DP systems is per date the go-to solutions for fixing floating units in the offshore industry.

With anchored units becoming heavier and operations moving out on deeper waters, requirements for improvements in durability has increased. While we've seen great improvements, failure rates have been relatively consistent since year 2000 [30]. While the industry has identified some of factors that impact life span of mooring lines, many stones are still unturned and research on the impact of identified factors is limited to a few topics.

This thesis sets out to introduce the typical life course of mooring lines for mobile units, identify factors which reduce life span and look into inspection/certification regimes. Then the outline some scenarios for a mooring chain during AH OPS using FEA and quantify fatigue damage for the different scenarios.

2 Background

This thesis requires some knowledge about chain and fatigue assessment, hence this chapter is here to give a brief introduction to some important themes and work as references for later chapters.

2.1 Chain classifications

Mooring chains are classified by material grade and link bar diameter. Abbreviations for these will be frequently used throughout this paper. This chapter aim to give an introduction to these dimensions and material grades.

2.1.1 Material grades

Steel grade	*Yield stress* R_e *N/mm²*	*Tensile strength* R_m *N/mm²*	*Elongation* A_5 *%*	*Reduction of area* Z *%*	*Charpy V-notch* *Temperature* [1] *°C*	*Average energy* *J*	*Single energy* *J*
R3	410	690	17	50 [2]	0	60	45
					-20	40	30
R3S	490	770	15	50 [2]	0	65	49
					-20	45	34
R4	580	860	12	50 [3]	-20	50	38
R4S	700	960	12	50 [3]	-20	56	42
R5	760	1000	12	50 [3]	-20	58	44

[1] For grade R3 and R3S, testing may be carried out at either 0°C or -20°C.
[2] For cast accessories, the minimum value shall be 40%.
[3] For cast accessories, the minimum value shall be 35%.

Table 3: Table from DNVGL-OS-E302 showing material properties of different mooring chain steel grades [9]

2.1.2 Link dimensions

- for nominal diameter up to 84 mm: - 2 mm
- for nominal diameter 85 to 122 mm: - 3 mm
- for nominal diameter 123 to 152 mm: - 4 mm
- for nominal diameter 153 to 184 mm: - 6 mm
- for nominal diameter 185 to 210 mm: - 7.5 mm
- for nominal diameter over 210 mm: - 8.5 mm

Table 4: DNVGL-OS-E302s nominal diameters of a mooring chain link [9]

The table shows the nominal diameters of a mooring chain link and their accepted tolerances. The link shall be measure at clamp and bend area unless stated otherwise.

2.2 SN-curve

The SN-curve is a frequently used tool to identify the fatigue life of a structure. The diagram allows you to find the design life one of a structure for a given stress range.

Below you'll find the eq. that the SN-diagram is derived from:

$$N\left(\Delta S\right)^{m} = a \tag{1}$$

$$N = a\left(\Delta S\right)^{-m} \tag{2}$$

To fit the logarithmic scale of the SN-curve, we end up with:

$$log(N) = log(a) - m \cdot log(\Delta S) \tag{3}$$

$\Delta S = stress\ range$
$N = number\ of\ cycles\ spent\ in\ stress\ range$
$a = intercept\ parameter\ of\ the\ SN-curve\ a = 6 * 10^{7}\ for\ studless\ chain$
$m = slope\ of\ the\ SN-curve.\ Varies\ for\ different\ geometries.\ m = 3\ for\ studless\ chain$

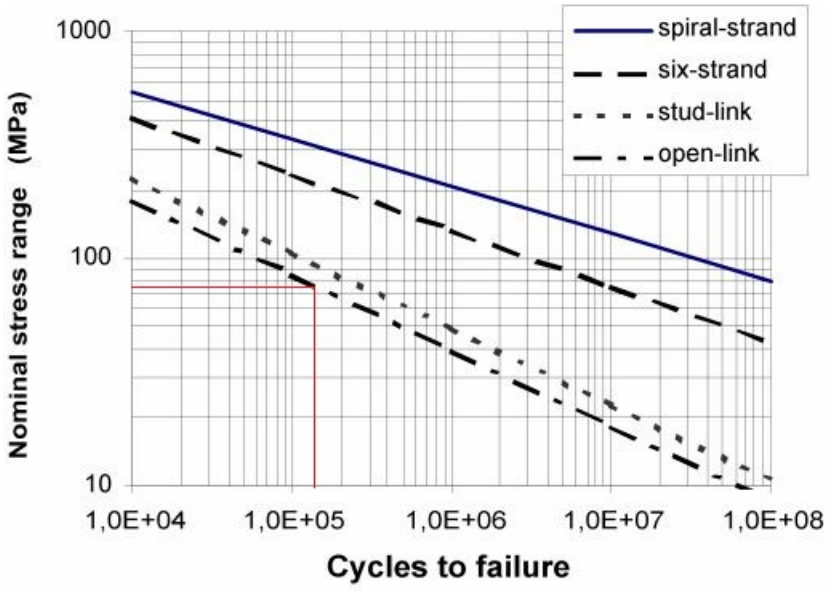

Figure 2: Illustration on how to use DNV-GLs SN-diagram for fatigue in mooring chain[8]

Figure 2 gives an example on how to use the SN-curve. It shows that for a open-link chain with expected nominal stress range of 70 MPa, we can expect a fatigue life of 150.000 cycles. It is important to note that the design curves is moved two standard deviations in the conservative direction from original test curves.

2.2.1 The Miner sum

The Miner sum is widely used in fatigue assessments. If we have a given or expected distribution of stresses and the number of cycles a structure is to operate under each range, the Miner sum can be used to approximate accumulated damage and stress equivalents.

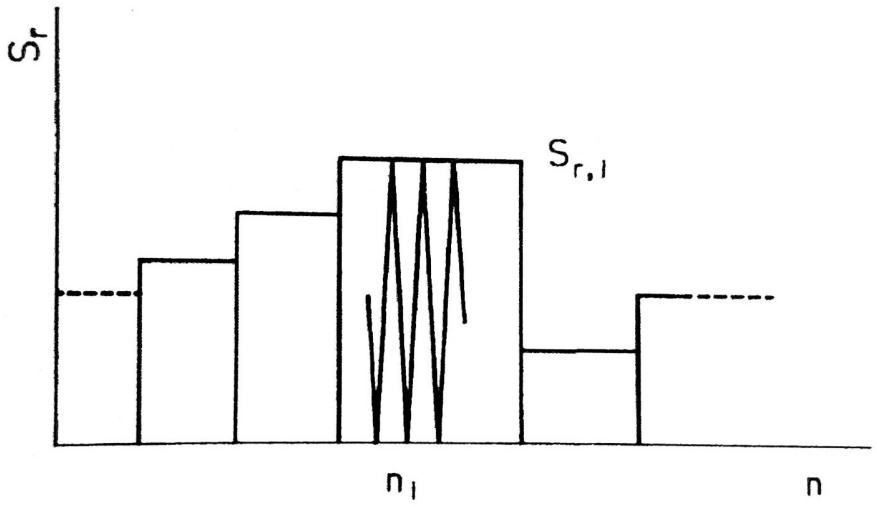

Figure 3: Figure from "Fatigue and fracture in marine structures"[37], illustrating stress ranges and their respective number of cycles in blocks. S_r denoted as ΔS in this paper.

As a structure exposed to marine environment is subjected to many different load spectrum over different time intervals. The Miner sum for equivalent stress is presented in equation (4) (taken from "Fatigue and fracture of marine structures (compendium)"[37], but can also be found in DNVGL-OS-E301).

$$\Delta S_{eq} = \left[\frac{\sum_{i=1} n_i \left(\Delta S_i\right)^m}{N} \right]^{\frac{1}{m}} \tag{4}$$

$\Delta S_{eq} = equivalent\ stress\ range$
$\Delta S_i = nominal\ stress\ range\ for\ load\ cycle\ i$
$n_i = number\ of\ cycles\ spent\ in\ stress\ range\ i$
$N = total\ number\ of\ cycles$
$m = slope\ of\ the\ SN - curve$

As mentioned earlier, the Miner sum is also used to approximate the accumulated damage that occurs over time.

$$D_i = \frac{n_i}{N_i} \tag{5}$$

$n_i = number\ of\ cycles\ spent\ in\ stress\ range\ i$
$N_i = total\ number\ of\ cycles\ in\ fatigue\ life\ for\ stress\ range\ i$
$D_i = damage,\ load\ cycle\ i$

This can be used to calculate the total damage from a set of load cycles by using the Miner sum:

$$D = \sum_{i=1}^{k} \frac{n_i}{N_i} \tag{6}$$

$n_i = number\ of\ cycles\ spent\ in\ stress\ range\ i$
$N_i = total\ number\ of\ cycles\ in\ fatigue\ life\ for\ stress\ range\ i$
$D = total\ damage.\ Equal\ to\ 1\ at\ failure$
$k = number\ of\ blocks\ (fig.3)$

2.2.2 2-parameter Weibull distribution

The Weibull distribution another tool often used in fatigue assessments for marine structures and has been proven for stress spectra. The Weibull presents a closed form equation as a simple alternative to equation (4). The method is an conservative method as it do not take fatigue limits (low stress ranges not leading to defect propagation) into account. The cummulative load spectra for a structure exposed to loads may be described by the 2-parameter Weibull distibution shown below [37]:

$$\Delta S = \Delta S_0 \left(1 - \frac{log(n)}{log(n_0)}\right)^{\frac{1}{h}} \tag{7}$$

$\Delta S_0 = max\ stress\ range\ in\ load\ history$
$n = number\ of\ load\ cycles\ exceeding\ \Delta S$
$n_0 = number\ of\ load\ cycles\ in\ the\ load\ history$
$h = Weibull\ shape\ parameter$

By inserting equation (7) into equation (4), we can derive the following:

$$\Delta S_{eq} = \frac{\Delta S_0}{(ln(n_0))^{\frac{1}{h}}} \left[\Gamma\left(1 + \frac{m}{h}\right)\right]^{\frac{1}{m}} \tag{8}$$

Where table and typical values for h and Γ can be found in Appendix B.

2.3 DNV-GL design curve for fatigue

DNV-GL's design curve for fatigue life in mooring chains is based on a study performed by Noble Denton in 1990's [8]. The test was performed on new chain with smaller dimensions (76mm) of steel grade R3 and R4. A mean load of 20% MBL was used and links broken under testing was replaced and testing continued. So the test included second and third breakages. DNV-GL design curve do not to this date, take into account the effect of mean tension in the mooring lines.

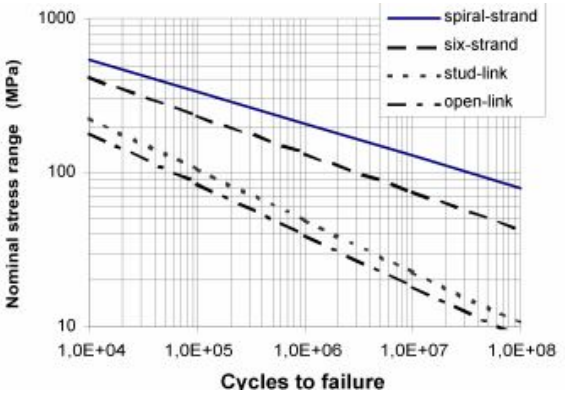

(a) DNV-GL SN design curve for mooring chain [8]

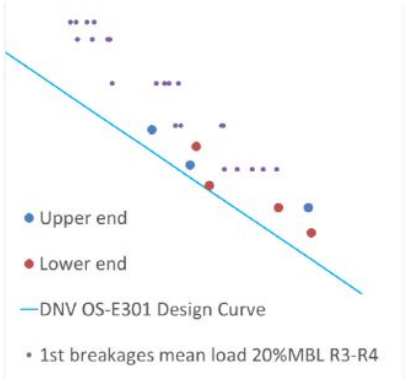

(b) DNV-GL SN-curve (blue) plotted against Noble Denton's first breakage test results (purple) and tests results for a corroded chain (dark blue and red) [39]

Figure 4

In figure 4b you can see that the SN-curve is moved two standard deviations in the conservative direction from the original test results. The background for the DNV-GL design curve for fatigue in mooring chains will be important for discussions in latter chapters.

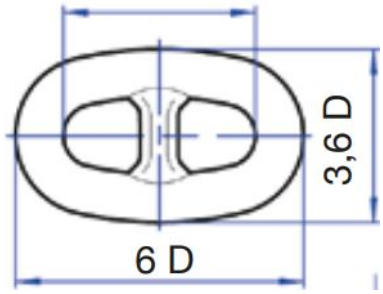

Figure 5: Ramnäs Bruks studded chain [2]

Chain with studs will have a better fatigue performance than studless. If the stud is to go missing the opposite is true. Since there has been many cases of the stud loosening in operation, studless chain has not been as popular a choice in offshore mooring history. Testing results used in this paper is based on studless chains.

3 Installation and retrieval of mooring lines and anchors for mobile units

The life of a chain used for mooring of mobile units is a hectic one. Compared to the chains used for permanent operations, chain for mobile units will often be redeployed and used on many installations before being retired (up to 4 deployments and retrievals annually). Mobile installations also often use smaller dimensioned chain (76 mm) than permanent ones (100 mm +). For mooring lines used for mobile units, we see a lot of line failures. Kvitrud (2014) [18] suggest a failure rate of $2 * 10^{-4}$ per line, per year in the Norwegian sector between 2010-2013. Kvitrud (2014) includes permanent installations its study, but suggest most failures have occurred in chains for mobile units.

Let us imagine a scenario where a drilling rig is to drill some wells at an oil field. In figure 6 we will illustrate the big picture for the operation w.r.t. operation route and anchor handling.

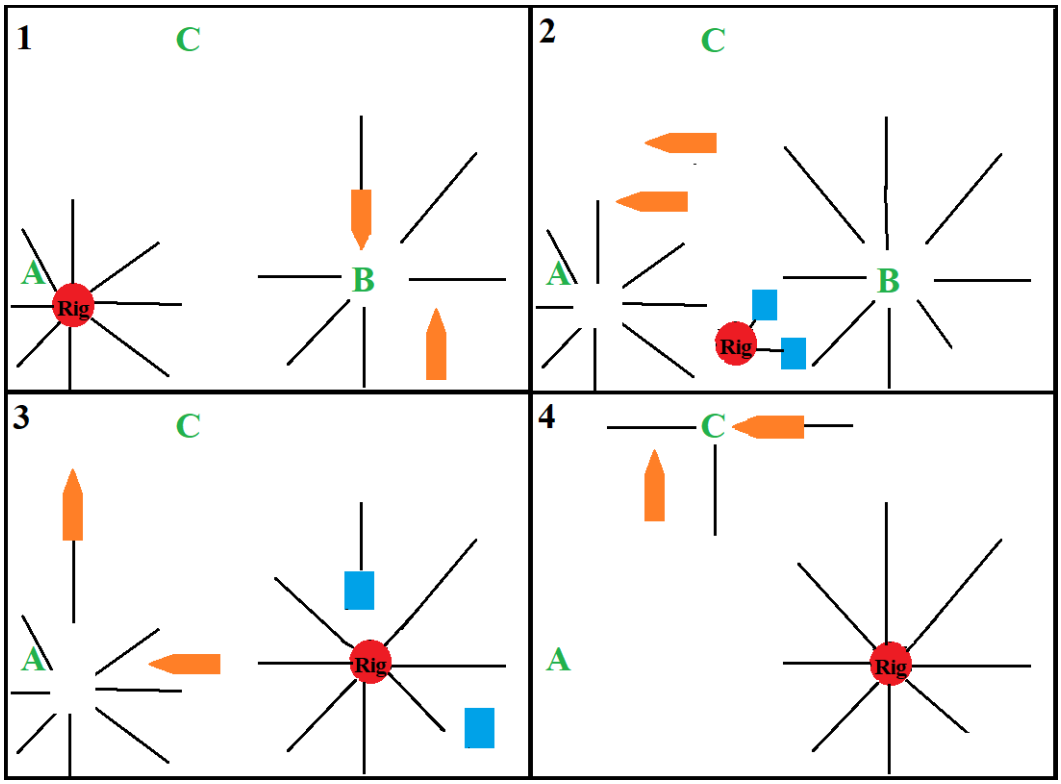

Figure 6: Numbers represent chain of events, letters represent planned operational sites for drilling rig, red dot represent drilling rig, orange boxes represent anchor handlers (crew 1), black lines represent anchor lines and blue boxes represent towing/anchor handlers(crew 2). Illustration made by author.

- **Event 1:** The drilling rig moored at location A and operating. Meanwhile crew 1 is at site B, pre-laying anchor lines for the drilling rig. Before mooring systems can be used, crew 1 performs tests on the lines and their bedding-in in accordance with DNVGL-OS-E301.
- **Event 2:** Drilling rig has completed its operation at site A and crew 2 now de-attach the drilling ring and transports it to site B. Crew 1 moves over to site A, to retrieve anchors and mooring lines.

- **Event 3:** Crew 1 has started the retrieval of mooring lines and anchors, while crew 1 has started the process of connecting the drilling rig to pre-laid mooring at location B.
- **Event 4:** The drilling rig is now operating at location B, while crew 1 is pre-laying anchor lines and performing tests at location C.

While figure 6 might not give an exact representation of how it happens in real life, the big picture is correct. A relevant scenario is that chain for a drilling operation is operational for three months before being retrieved and then out of operation for two weeks, before being deployed, tested and then operational for another three months [19]. That means that and average chain used for mooring of drilling units experience being redeployed and tested up to three times annually.

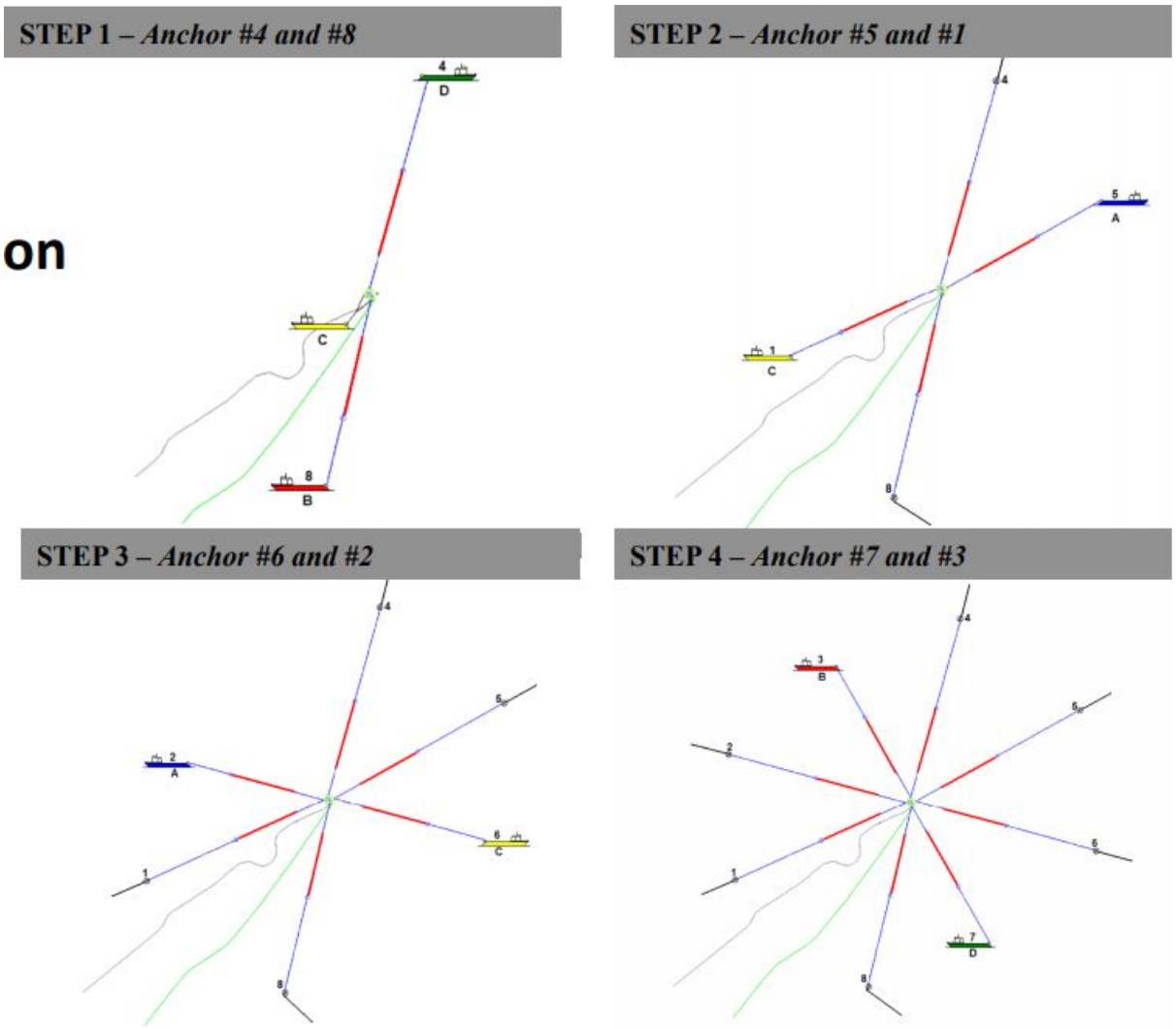

Figure 7: A more detailed illustration of anchor installation [20]

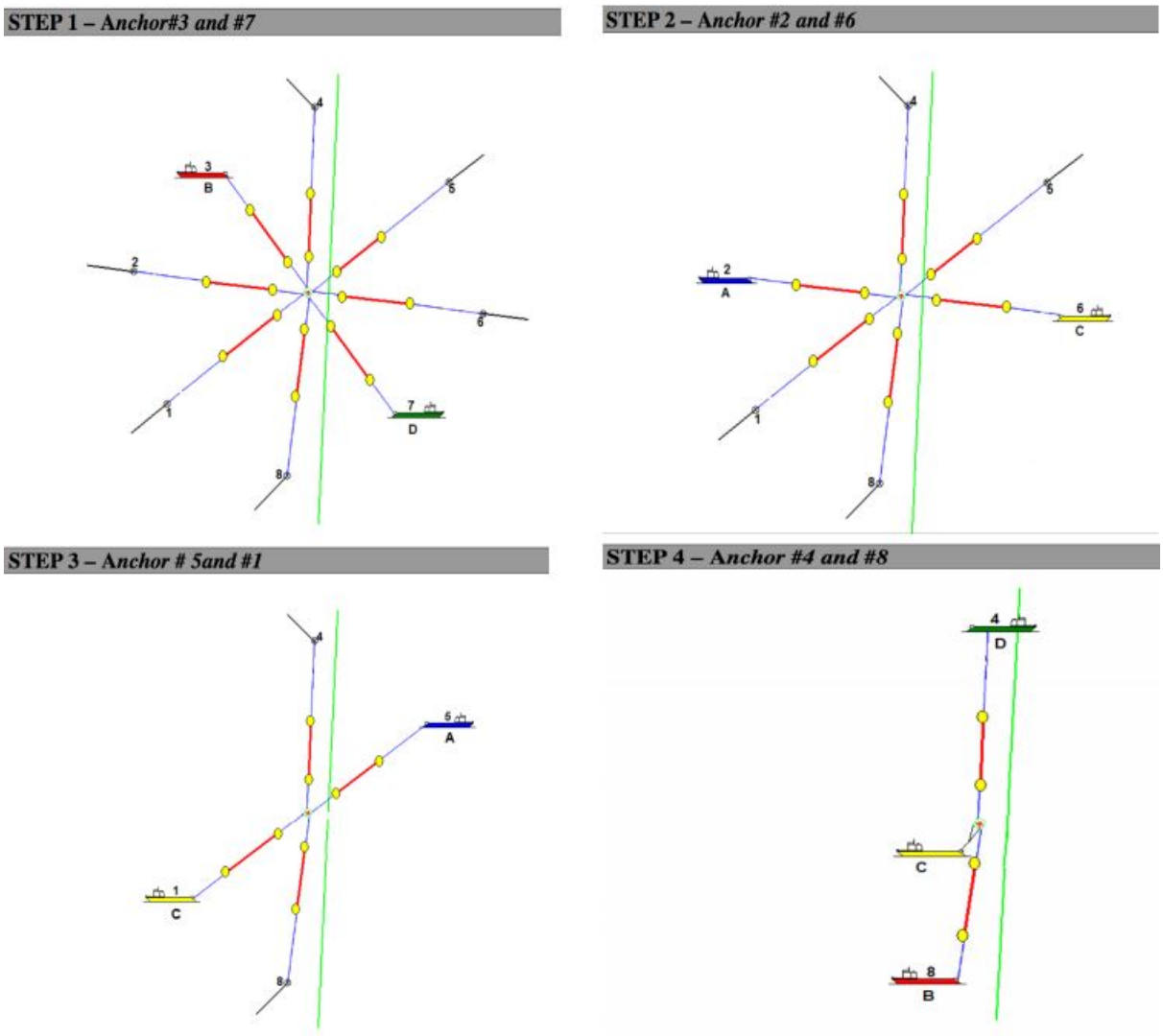

Figure 8: A more detailed illustration of anchor recovery [20]

3.1 Fluke anchors

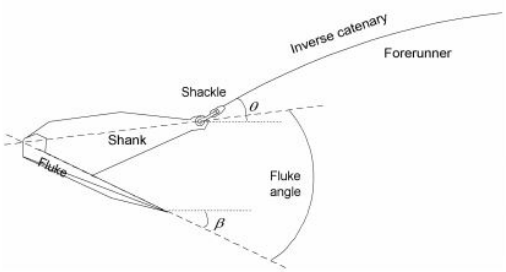

(a) DNV-GL illustration of a fluke anchor and its angle of attack in the sea floor [8].

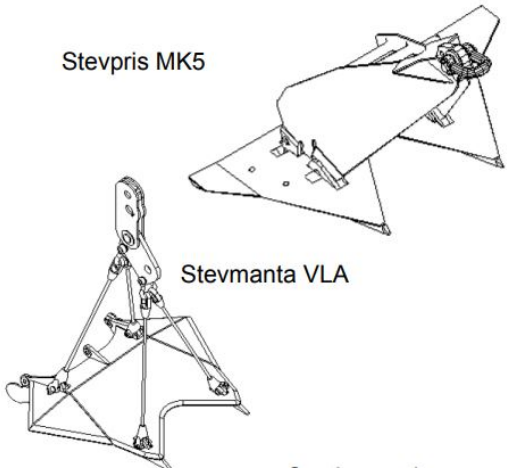

(b) Illustration of fluke anchor (Stevpris MK5) and a plate anchor (Stevmanta VLA) [20]

Figure 9: Illustrations of the most commonly used anchors for mooring chains for mobile units

For mobile units drag based anchors like plate anchors and fluke anchors are often used. But most commonly used is the fluke anchor. It is designed to be easily deployed and retrieved. Both anchors are deployed by dragging them along the sea bed until the plate becomes sufficiently buried into the ground and bedding-in is secured. The bedding-in has good capacity along the dragging direction. The fluke angle shown in fig. 9a is usually between 30-50° as different angles is optimal for different soil conditions. Larger angles are typically effective for clay, as anchor can penetrate deeper and achieve increased resistance.

3.2 Testing of anchor bedding-in and anchor lines

After bedding-in is assumed secured, DNVGL-OS-E301 states that testing has to be performed to assure mooring system integrity and sufficient anchor fastening. This load is to be equal to a 52.6% of the chains MBL [19], this is typically close to the biggest load a system can expect to see over a 100 year period at given location. This load is heavily dependent on the area the chain is operating in and the load is to be applied by the anchor handlers.

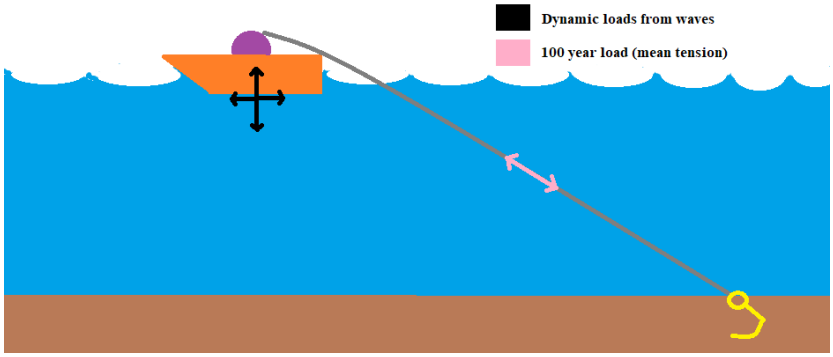

Figure 10: Simple illustration of anchor handlers testing an anchor and line with a 100 year load

The anchor line and anchor bedding-in testing is assumed to last 30 minutes [19]. The same goes for the anchor retrieval. "Statoil and Oddfjell (2017)" [31] show the scope of work for a rig move. For this area, the anchor handler ran tests with a load 200 tons for 10 minutes. Comparing the load with the chains MBL of 612 tons [31], we end up with an equivalent of 33% MBL mean tension under testing. This is lower than recommendations of the DNV guidelines.

3.3 Retrieval of anchors

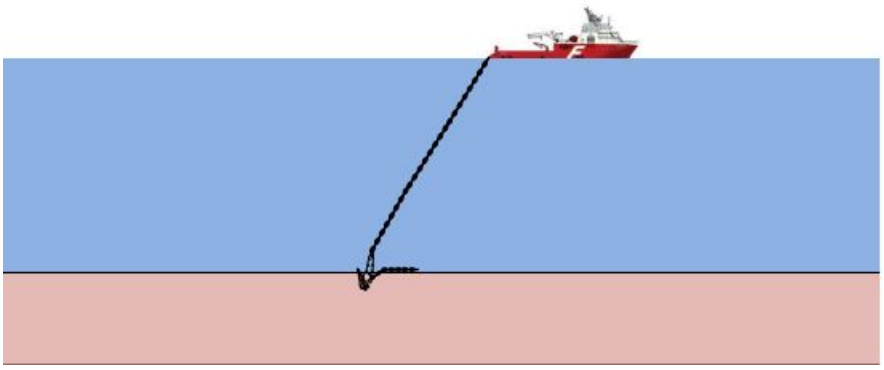

Figure 11: Illustration of anchor handlers retrieving an anchor[31]

The retrieval process of the anchor is basically breaking it free from the soil. As the fastening is weaker in the horizontal direction, it is recommended to retrieve some mooring line before the breaking process starts (illustrated in figure 11). Then you pull in the opposite direction used to fasten the anchor (180°). For the Åsgard operation, a maximum tension in line of 200 tons was to be used to pull the anchor free. This is the same as load applied in testing, indicating that anchor pulling loads and anchor line and bedding-in testing loads can be of the same magnitude. A more detailed walk-through of anchor retrieval for "Rig Move from Mim to Åsgard S" can be found in appendix C.

3.4 Layout of anchor handling vessel

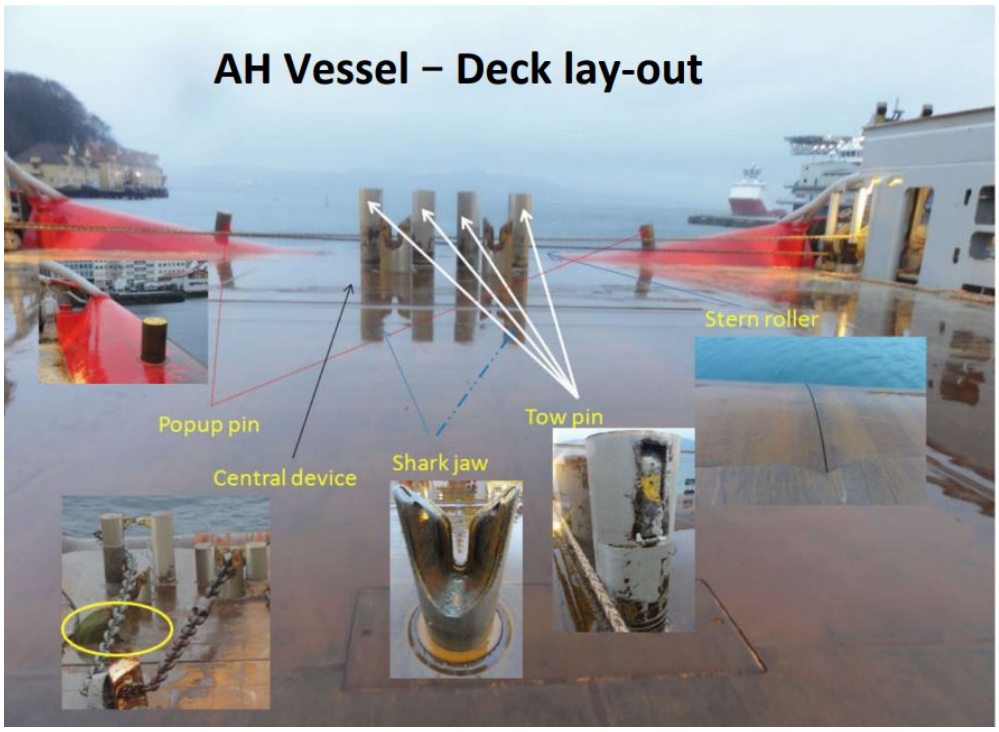

Figure 12: Picture of deck layout of a anchor handling vessel[20]

The layout of the anchor handling vessel is essential to guidance of a chain. With handling forces of large magnitude it is VERY important to have control of the load direction. Potential results of bad layout can be loss of control, capsize, twisting of chain, fatalities/damage of personnel, damage to or break of chain.

3.5 Discussion

This chapter fails to identify the typical magnitude and time span of a 100 year storm compared to anchor line testing with a mean tension of 52.6% MBL. This should be investigated further as we do not know how the values given for the Åsgard rig move compare to AH operations performed in general.

3.6 Further work

The chain undergoes high loads under deployment and retrieval. Work should also be done to identify worst case scenarios geometries between chain links and stern, fairlead etc... FEA run in this thesis will only include one chain/stern roller geometry configuration. It could be that chain links experience worse contacts at other locations of the vessel deck, like in the shark jaw, popup pin etc. displayed in figure 12.

4 Inspection and recertification

Safety in the offshore industry is extremely important as the consequences of failure can be catastrophic. Inspection and certification equipment and structures is an important aspect of maintaining safety and keeping risk low. Inspection and certifications of mooring chains is no exception as failure of mooring system can lead to fatalities, HC spills and major economical loss. The Norwegian petroleum industry routines for inspection and re-certification is currently based on DNVs DNVGL-RU-OU-0300, chapter 3, section 4 and its Appendix D [10]. This summary will only touch upon regulations of mobile mooring systems, and focus on the regulations regarding the chain part of a mooring system.

4.1 DNV regulations for inspection of mooring lines

For inspection of mooring for units not permanently moored, there are two different classifications given by DNV resulting in two slightly different inspection regimes.

- **ME:** "The class notation ME is only issued for mobile units. The ME notation covers all mooring equipment installed on the unit, or belonging to the unit. Rental equipment when rented by the owner, is included in this definition." [10]
- **POSMOOR:** "This type of mooring system is normally applicable for drilling and support units not fixed at one location for a longer period of time." [10]

Where POSMOOR is for a DP assisted system (as an addition to mooring lines). POSMOOR has the same inspection regime as ME for the mooring lines, but have additional regulations that needs to be followed for the DP-systems. POSMOOR will therefore not be discussed further.

4.2 Non destructive testing methods (NDT)

There is many types of NDT, but the most frequently used for mooring chain examination is Magnetic particle (MT) and liquid penetration testing (PT). A brief introduction will be given for the two methods to get an understanding of the process and how they will applied in mooring line examination.

4.2.1 Magnetic particle testing (MT)

MT starts out by running a magnetic current through the object which is to be tested. If there are defects present in the object, current disruption will occur, leading the defects to emit an electromagnetic field. Added magnetic particles will then gather around the defects, making previously hard to detect defects visible.

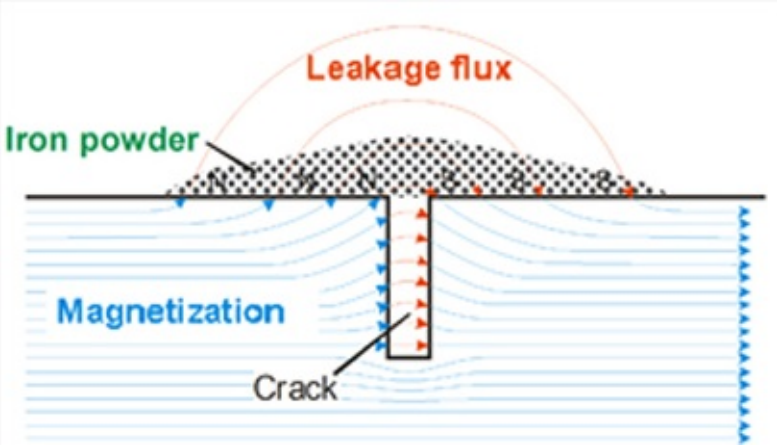

Figure 13: Illustration showing the principle of MT[26]

This method is extremely effective in finding small [33] cracks and defects which makes it perfect for examination of mooring chains. The methods even works through thin coatings. The biggest drawback is that mooring chains have to be retrieved from operation, brought to a dry environment and tested there. This is goes for all NDT methods. MT is by far the most commonly used when assessing mooring chains.

4.2.2 Liquid penetration testing (PT)

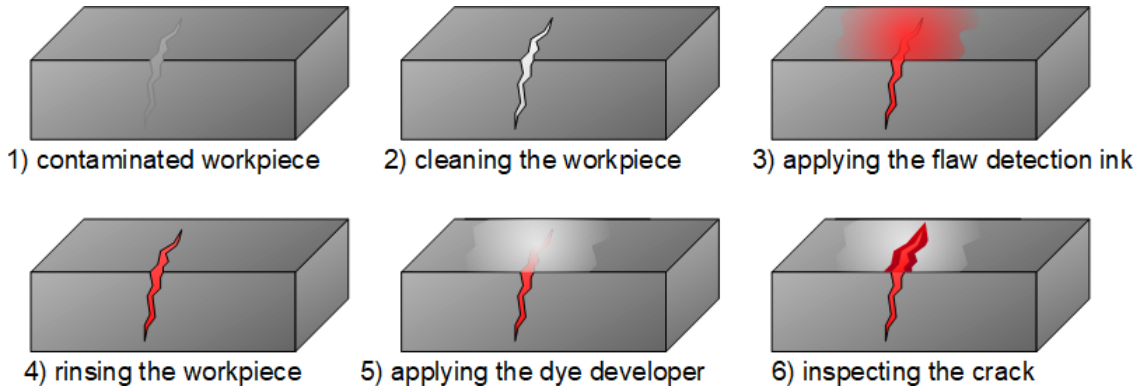

Figure 14: Illustration showing the steps of PT[32]

PT is not as common in examination of the chain itself, but is a recommended practise by DNVGL-RU-OU-0300 for joining shackles. The method is basically filling defects with highly visible fluids that will help visualize the defects. This is a cheap method, but has some shortcoming when inspecting the smaller defects. The method is highly dependant on a thorough cleaning that makes it possible for the liquid to penetrate the defects. Some cracks might even be too small for the method to give a proper indication.

4.3 ME inspection regime

The ME inspection regime consists of (if not any other information is given) an annual - and a complete inspection (every 5 year). Other surveys include continuous and occasional surveys, but these will not be discussed in this thesis.

Annually DNV demands an inspection mainly related to document verification and visual inspection.

- **Documentation:**
  Records and certification for the following shall be reviewed: Maintenance, assembly, service history, calibrations, length tension measurements and winches. The service history holds key info for fatigue damage like position logging, damages (damage potential) and peak and shock loads for the system
- **Visual inspection of accessible parts of mooring system:**
  Here inspection often is done by ROV or personnel on the moored unit. The inspection is to pay extra attention to contact areas of chain to prevent unhealthy loading conditions, wear in chain links, twists of chain (especially in fairlead/windlass area), condition of wire/fibre rope and anchors/anchor bolsters. Should severe damage or maintenance neglect be observed a complete survey (see below) should be carried out.

The complete survey is more extensive in nature and is to be carried out every fifth year if no other instructions are given. As there is a chance of mooring chains having 20 plus years in operation and not having any documentation or history logs, the frame of the complete survey is dependant on these factors.

- **Documentation:** In addition to the documentation requirements for the for the annual survey, the following shall be provided[10]:
  - DNV GL chain certificate
  - Year entering service
  - Bar chart, i.e. length of chain out versus time
  - Information on chain breakages, e.g. position, year entering service, certificate
  - Identification marks on chain
  - Summary of previous repairs
  - Summary of previous survey findings
  - Information on the likely future service of the chain, e.g. if plans to head-to-tail chain, expected length to be over fairleads and windlass, likely area of operations
- **Examination of chain less than 20 years, no failures, w documentation and service history:**
  - 100% visual examination
  - 5% NDT on general chain
  - 20% NDT on chain which has been in way of fairleads over last five (5) years
  - 20% NDT on chain which will be in way of fairleads over next five (5) years.
  - If no documentation or history is available, examination shall be increased to include mechanical testing of each length of chain and NDT increased to cover 20% of the whole

chain.

- **Special requirements for chains older than 20 years:**
  - If all documentation is available, and historical information including previous reports showing no failures and only minor repairs, then the survey extent stated for chain less than 20 years old can remain in place
  - If no documentation is available (i.e. no certificates, unable to identify the chain, unable to ascertain orientation of the chain, which parts have been over the fairleads etc.) then the chain shall be subjected to minimum 20% NDT and mechanical testing of all lengths
  - If documentation review reveals history of defects, then NDT shall be increased to 100% in the areas where defects are found
- **General:**
  - All joining shackles of Kenter or similar design which have been in service for more than five years, shall be dismantled and magnetic particle (MT) or liquid penetrant testing (PT) shall be carried out on all the machined surfaces

Bullet points above are more or less directly taken from DNVGL-RU-OU-0300[10].

4.4 DNV regulations for recertification of mooring lines

For recertification MT is the only accepted method of examination. The added magnetic powder shall cover the whole link, but is to be extra carefully applied in hotspot areas. These hot spots are marked in figure 15 (A,B,C etc.), but also include link shoulder, outer bend region and other areas that might be exposed to mechanical damage for the specific chain.

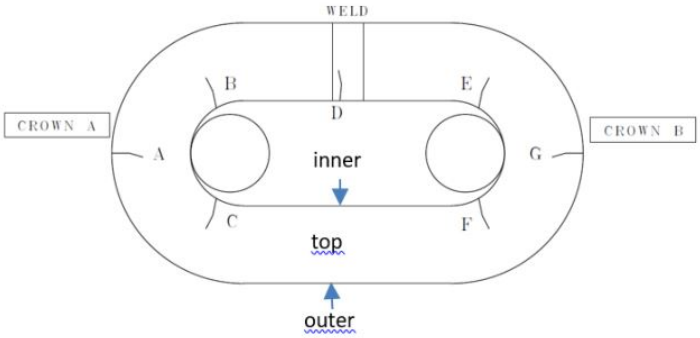

Figure 15: Illustration showing the most common crack initiation points[36]

The diameter of bend area of a link and other exposed areas to rough wear or gouging, is to be measured on 1% of the link for working length of a chain, but can be increase or decreased based on results from visual inspection by a attending surveyor. Also length over 5 links is to be measured every 100m of chain, but can also be be deviated from if attending surveyor can confirm no in-service problems with chain twisting or mismatching with fairlead/windlass and no indications of stretching is made under visual inspections.

MT is to be carried out on 20% of links and diameter measurements on 3% of links over 150m lengths. There is supplementary requirements for MT and diameter measurements for chain that has been or is to be in working contact with fairlead/windlass.

4.4.1 Diameter loss due to corrosion and abrasion

The regulations cover both temporary and position mooring equipment. Temporary equipment is not prelaid for the moored object and therefor not relevant for this thesis. We will only focus on the position mooring.

For position mooring, the acceptance criteria for abrasion and corrosion in links and joining shackles is a loss of up to 10% cross-sectional area for a chain, which corresponds to approx. 5% of the diameter. The mean of two perpendicular measurements is to be taken and checked against the allowance criteria. If these criteria are not met, the chain is to be rejected. Lengths over five links is also not to exceed 23.25 times the diameter.

Defects like cracks and gouges can be removed by grinding. The requirements for the grinded area is a length of six times the depth of the defect along the link and has to have bottom radius of 3 times depth to avoid stress concentrations. Sharp corners of new geometry is not allowed. No more than 10% cross sectional area loss from this process is to be accepted and MT or PT must be used to confirm elimination of defect. If any gross distortions are found in a link, it is to be rejected.

There is also information on inspection of mooring lines with stud and joining shackles, but the inspection of these is not as relevant for this paper. Additional information of stud inspection can be found in Appendix A.

4.4.2 Mooring line failure

In case of mooring chain failure it is important to note if the failure was due to overload and if it was the the extent of the overload. If no irregularities is found ref DNVs DNVGL-RU-OU-0300's Appendix D and DNVGL-OS-E302, local damage on the link is assumed. If not, ten links on each side of the break is to be examined with close visual inspection, NDT and dimension checks of links. If suspected damage to other areas as a result of the break, they shall be examined the same way.

4.5 Discussion

While DNVs regulations for inspection and recertification of mobile mooring systems is very concrete in its structure use clear language, questions can be raised over the practises suggested and if they are sufficient considering the potential outcome of a failure. Considering that mooring chains have to be brought up to land for testing, why only test 5% of the general chain? The cost of bringing up a chain for testing is already large. Why not test more? A chain is only as weak as its weakest link.

Should some more critical sections of the chain be identified and listed as well? Extra requirements for chain in fairlead/windlass is great, but why only 20% of the segment? Could other areas be interesting as well? Corrosion is know to have a negative effect of fatigue life and to be more likely to occur at certain segments of the chain. More research on identifying these areas and adding additional NDT hot spots for the complete survey seems like a good idea. It is understandable that NDT is costly, but could more/larger areas be considered when they are up to inspection?

5 Degradation by corrosion

Figure 16: Chains with varying degree of corrosion[35]

Corrosion is a widespread problem affecting metal structures placed in the sea and marine environments. The corrosion process is often thought about as a even continuous process, but in reality one might experience several types of corrosion on a single unit. For a full length of mooring chain one can expect to see different types of corrosion throughout it's length.

While corrosion in general is unwanted, there is big differences in damage impact. The most problematic types of corrosion for structural integrity and fatigue life is originally assumed to be the ones which result in a localized area of attack, as these attacks make good initiation points for cracks to develop.

5.1 Corrosion protection

There are many types of corrosion protection on marked. This thesis sets out to identify the most commonly used protection methods and the extent of their use on mooring chain.

5.1.1 Coating

Coating is a cheap and effective way of protecting metals from corrosion. The main protection barrier of coating is insulating the the metal from the corrosive environment. It may also include sacrificial metal to give a cathodic protection effect if a breach in the coating should occur. With the mooring lines dynamic nature, wear is common. Because of this coating on mooring chains has a very limited corrosion protection effect. To do maintenance on a mooring chain coating, one would need to retrieve the chain and treat it in a dry environment. This makes maintenance a costly affair. So by being both costly and ineffective, organic coating is not used for mooring chains.

While some chain suppliers might offer thermal sprayed aluminium coating (anode material), this is mostly done for chain operating in the splash zone as chain in this area is know to be extra exposed to corrosion. It is very important that assessments are made to assure that hydrogen embrittlement do not occur (see next subsection about cathodic protection)

5.1.2 Cathodic protection

Cathodic protections is another commonly used corrosion counter measure. By attaching a sacrificial anode or applying a direct current to the part or assembly that needs protection, corrosion protection is achieved.

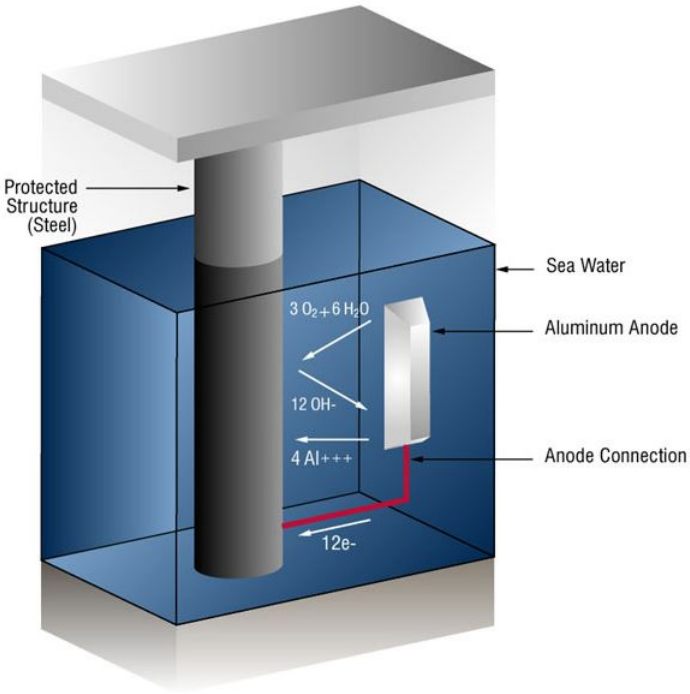

Figure 17: Cathodic protection represented by an aluminium sacrificial anode [4]

Figure 17 demostrate how a sacrificial anode works. What the figure do not capture as well is that anodes have a limited range which it can protect (same for applied direct current). To cathodically protect a full mooring chain, one would require an even distribution of anodes to be implemented over the length of the chain. Also worth mentioning is that anodes is a limited resource and have to be replaced ever so often. Installing maintaining anodes or implementing direct current system for a mooring chain is extensive and costly operation.

Hydrogen emrittlement is another unwanted effect that can occur when cathodically protecting mooring lines. Hydrogen embrittlement has a negative effect on fatigue life. While cathodic protection of mooring chains is not a normal practise, there are instances where the chain can indirectly be protected. A good example is a chain in contact with a ship hull with CP. One would originally think of this as a good thing, but with current introduced to high strength steels the three conditions for hydrogen embrittlement can be fulfilled (see figure 18).

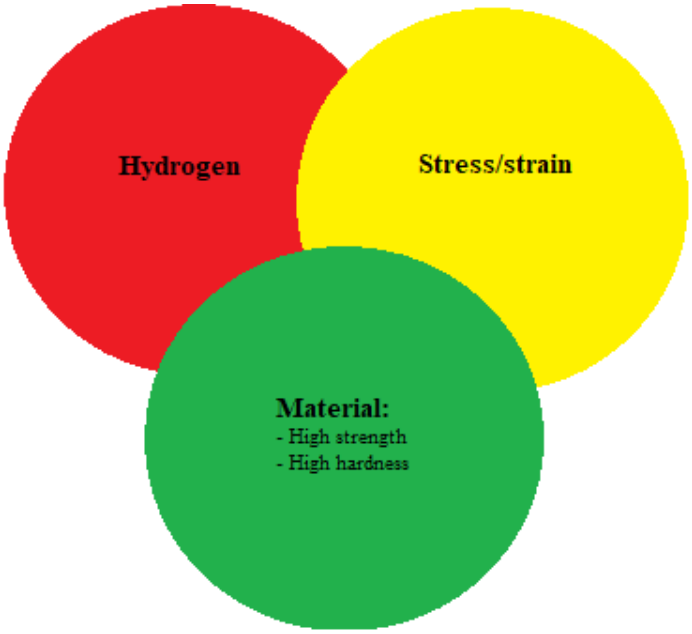

Figure 18: The three factors needed for hydrogen embrittlement to occur

Figure 18 show how CP might induce hydrogen production. With the chains being made of high strength steels and being exposed to both external and residual stress [9], adding hydrogen will often lead to high strength metals showing reduced strength and brittle behavior in crack propagating areas. This is a highly unwanted effect and hence cathodic protection should be avoided.

5.1.3 Todays mooring lines corrosion protection

We can conclude that corrosion protection on mooring lines is hard to implement. Most corrosion reducing measures are done when choosing material for the chain. Choosing the right material composition too secure as uniform corrosion as possible and avoid more critical corrosion phenomena like pitting corrosion. Material compositions are industry secrets and hard to come by. Therefore, this topic will not be further elaborated upon.

5.2 Types of corrosion affecting mooring chains

Mooring chains are used all over the world at depth up to around 3000m. The type and degree of corrosion is highly dependant on the environment of which the chosen material is placed in. The list of factors is long, but for mooring chains, chloride content, oxygen, bacteria and pollutants are the more dominating. Following a chain from top site moored object to anchor, we will see different environments as depth increases. For fatigue assessments it interesting to know how all parts of a chain performs, but most important is identifying the most compromised parts.

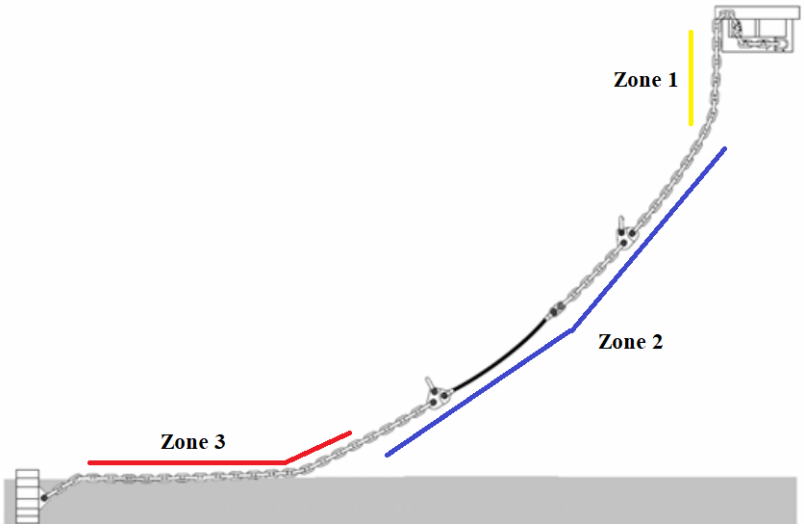

Figure 19: Image illustrating the three main zones in which we see different extent and types of corrosion. Important to note that this is a sketch and that segments are not up to scale [39]

5.2.1 Zone 1: Splash zone

This section is often referred to as the splash zone and chain in this area is often subjected to substantial corrosion. Corrosion here is a result of water levels rising and falling and erosion from waves, weather and colliding debris. We also have increased access to oxygen from the air and temperatures are often higher in the upper water levels and the air. Marine growth is likely to occur in this zone as well, which MIGHT bring some MIC with it. Rough surface is to be expected.

5.2.2 Zone 2

Figure 20: Typical corrosion found in zone 2. Picture of chain used at Åsgard A [14]

The corrosion in zone 2 is mainly uniform and the oxide layer created helps prevent further corrosion. Calcites also help form a protective layer. As we seen in figure 20, the corrosion is minimal and very uniformly distributed. One might see tendencies to pitting, but pitting in this region is very uncommon and (mostly) not severe compared to zone 1 and 2. In light of effect on fatigue life, this part of the chain is not as interesting in fatigue life assessments.

5.2.3 Zone 3: Seabed

This zone is a bit more complex due to its geometry w.r.t the seabed and its dynamic nature. One could say the chain experiences different environments and therefore we often see different extent and types of corrosion over this segment. Microbiologically Influenced Corrosion (MIC) due to Sulphate Reducing Bacteria (SRB) is typically a form of corrosion we find in zone 3. This corrosion is caused by sulphate bi-product made by sulfate eating bacteria and typically causes pitting with sharp edges, good for crack initiation.

Figure 21: Characteristic worst case pits made from MIC/SRB [38]

5.3 Inspection of used anchor chains

In 2016 and 2017 Equinor retrieved a full length seabed chain that had been operating in the north sea for 20 years to inspect the corrosion of this chain segment and perform fatigue testing w. special focus on the effect of MIC caused by SRB.

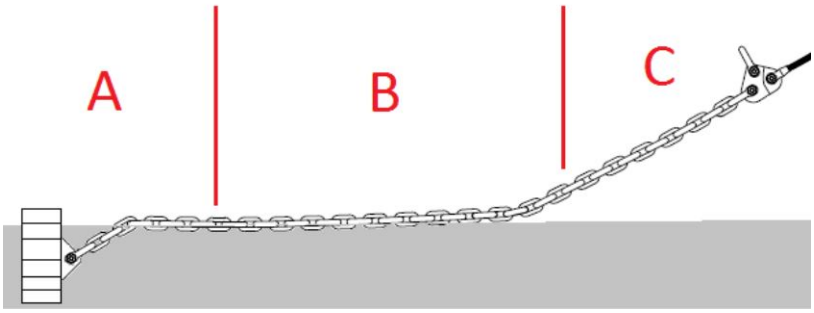

Figure 22: Principal sketch of the seabed chain: Lower part (A) is always on the seabed. Middle part (B) is moving in and out of the seabed, while the upper part (C) is always in the water column [39]

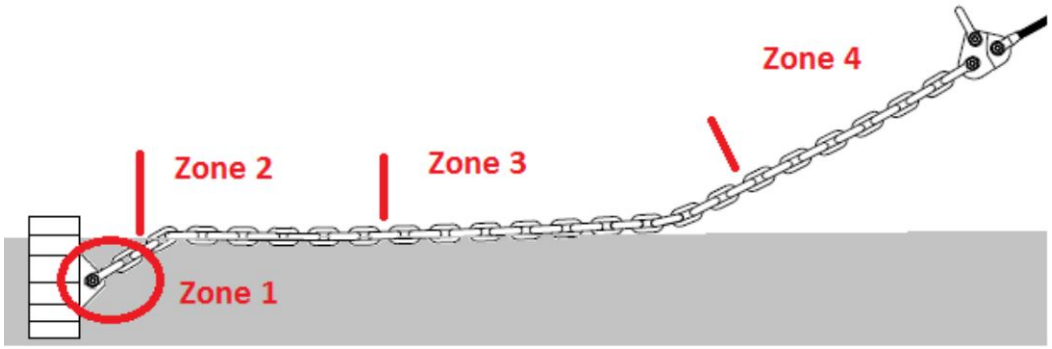

Figure 23: Sketch showing the approximate position of the corrosion condition zones for the chain retrieved by Equinor in 2016 and 2017 [39]

Below is listing of Equinors findings of corrosion by visual inspection in the zones indicated in figure 23. These zones are not the same as in in figure 19. Findings in"Øystein Gabrielsen, T. Liengen, and S. Molid (2018)" [39] states:

- **Zone 1:** Part of chain closest to suction anchor, with no significant corrosion. This condition covers the first 18 links closest to anchor
- **Zone 2:** Lower part with corrosion attacks 3-4 mm deep, width of varying size from a few mm to large sections. The condition starts with full effect on link 19 from the anchor, and slowly disappear towards the middle part of the chain
- **Zone 3:** Middle part with no significant corrosion
- **Zone 4:** Upper part with mixture of increased roughness due to general corrosion and some shallow pits. The condition gradually changes from the middle part with worse condition at the upper end. Note that the general corrosion does not include a significant material/diameter loss, but has a significant rougher surface than middle part chain without significant general corrosion

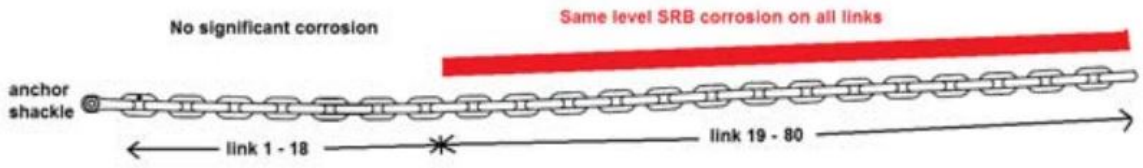

Figure 24: Sketch showing corrosion attack on chain closest to anchor (zone 1 and zone 2), retrieved with the suction anchor in 2017 [39]

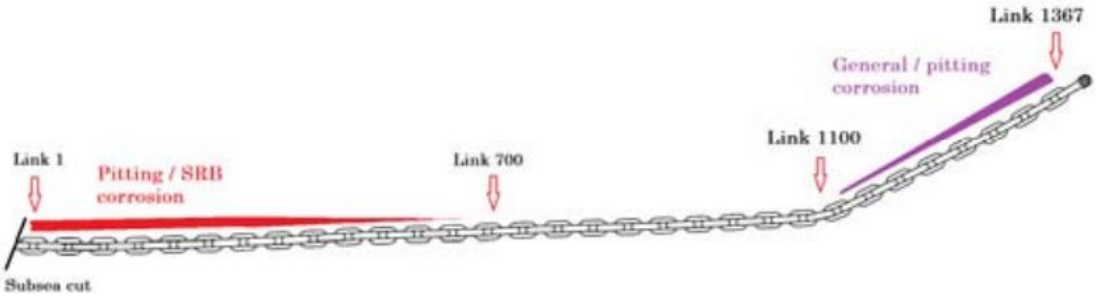

Figure 25: Sketch showing corrosion attack on part of seabed chain retrieved in 2016. Red and purple indicates level of corrosion attack in Zone 2 (red) and Zone 4 (purple). Note that corrosion attacks in Zone 2 and Zone 4 both decreases towards Zone 3 [39]

Øystein Gabrielsen, T. Liengen, and S. Molid (2018) [39] concludes the following on why we see the different types of corrosion:

- **Zone 1:** Low corrosion as the oxygen content is low for the buried part of the chain. Oxygen used by general corrosion or microbial activity. SRB present but not active.
- **Zone 2:** Severe corrosion observed. This part was buried, but closer to the surface. Movement have supplied nutrients and sulfate to SRB and indicies made that dissolved oxygen supply have created generalized corrosion. SRB corrosion dominating. Steady state corrosion of 0.2 mm/yrs.
- **Zone 3:** Positioned on seafloor, but often lifted off. Movement prevented deposits and thin calcite layer works as corrosion protection. Calcite layer is also reason for gradually increase to zone 2 and 4.
- **Zone 4:** As zone 4 is lifted from the seabed, nutrients for SRB is limited, but still present. General and local corrosion is also present. Some protection from calcite layer is in place. Stabelized to 0.05 mm/yr

5.4 Effect on fatigue

It is important to consider corrosion in fatigue life assessments as fatigue is intertwined with crack initiation and growth. Different types of corrosion leave different types of geometries in the metal. Uniform corrosion and rounded corrosion pits is not as critical as the sharp geometries that pitting -, crevice - and MIC SRB corrosion leave behind. Looking at figure 21 we can clearly see the sharp edges, but also observe significant diameter loss in local areas.

As mentioned in chapter 2, DNVs SN-curves for fatigue life is based on testing of new chains in air [8]. As of for now, the SN-curves only take into account diameter loss of chain (implemented in the calculations for stress) and there is good reasons to believe that this is not an accurate way of portraying corrosion and its effects on fatigue life. While there is still not much work on to which degree different types of corrosion affect fatigue life some studies have been conducted on corroded chains from different segments with varying degrees of corrosion and time in operation. Figures below show a list of chains and their specifications and plot their performance next to the DNV SN-curve. This is taken from "Øystein Gabrielsen, T. Liengen, and S. Molid (2018)"[39], one of the more relevant fatigue tests on chain with focus on corrosion. The tests have been conducted by Equinor and DNV GL.

Test #	Corrosion type / zone	Mean load	Load Range
1	Zone 2	11.9 %MBL	+/- 4.3 %MBL
2	Zone 2	11.9 %MBL	+/- 3.9 %MBL
3	Zone 2	11.9 %MBL	+/- 5.2 %MBL
4	Zone 2	11.9 %MBL	+/- 3.5 %MBL
5	Zone 4	11.9 %MBL	+/- 4.8 %MBL
6	Zone 4	11.9 %MBL	+/- 5.6 %MBL
7	Zone 4	11.9 %MBL	+/- 3.9 %MBL

Table 5: Fatigue test conducted by DNV GL on chain used for 20 years, showing test parameters [39]

Important to note is that the tests were performed on different segments from the same chain. Zone 2 inhibited more localized pitting attacks and while zone 4 had a more general corrosion, which can be described as rougher surface and less significant material loss. A more detailed corrosion description can be found in under in chapter 5.2.3.

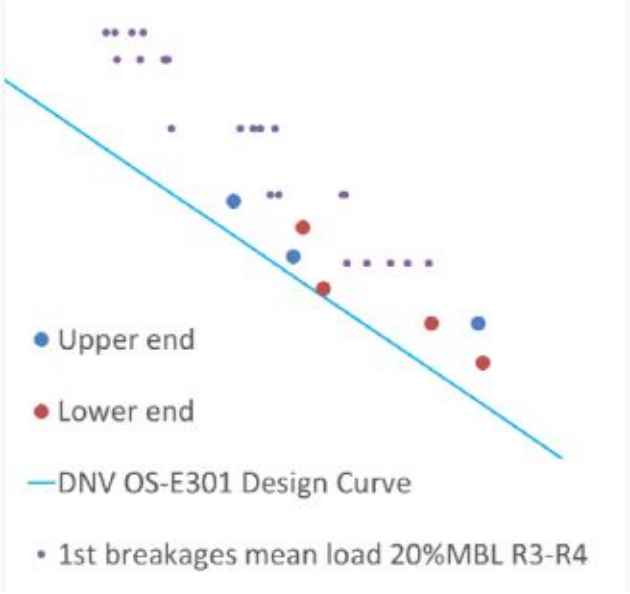

Figure 26: Test result plotted along DNVs SN-curve and the test results it is based upon [39]. Red represent Zone 2 and blue Zone 4. X and Y axis is not included, but x axis represent cycles and y axis stress range.

All the chain segments pass the DNV requirements, BUT it is very important to note that the mean load is much lower(11.9% MBL) than for the tests that DNVs curve (20% MBL) is based upon. Thus indicating that corrosion has a negative effect. Comparing the results, the difference between the two test chains segments (red and blue) is less than expected. Pitting and SRB attacks would be expected to lead to higher stress concentrations and thus more decrease in fatigue life than what just a general rough surface. Findings in "Øystein Gabrielsen, T. Liengen, and S. Molid (2018)" [39] indicate that surface roughness might affect fatigue life just as much as SRB and pitting. This indicates that DNV-GLs way of accounting for corrosion with diameter loss is outdated.

5.5 For further investigation

The sample size for this test is still very small and no clear conclusion can be drawn about the effect of different corrosion types effect on fatigue life. The only certainty is that corrosion in general clearly has a negative effect. As "Øystein Gabrielsen, T. Liengen, and S. Molid (2018)" [39] indicate that surface roughness has just as negative effect on fatigue life as pitting corrosion (pit depth is easily translated to diameter loss), another question occur. Is the fatigue life reduction caused by corrosion adequately represented by diameter loss (in SN- diagram)? With "Øystein Gabrielsen, T. Liengen, and S. Molid (2018)"'s indications, more testing should be done to better understand the mechanics and effects of different corrosion conditions on fatigue life.

Another consideration is the high mean load of 20%MBL that the DNV curve is based on (ref chapther 2. An interesting question: Is reasonable to extend the fatigue life for corroded chain if more realistic loading conditions, especially mean load (typically 5-18%MBL [19]) is applied?

For further investigation it would be interesting to see if it is possible modify a SN diagram to more precisely represent corrosion based on:

- Type of corrosion present
- Pitting/crack depth and location instead of diameter loss
- General surface roughness
- Corrosion condition vs. realistic loading conditions

6 Findings from existing testing and studies

While there isn't much certainty in fatigue assessment of mooring chain, tests and studies from the last decade have given some good indications which factors affect fatigue life and how we can improve the way we select, dimension, use and inspect mooring chains. This chapter sets out to summarise the findings from testing and studies.

6.1 Fatigue cracking initiation

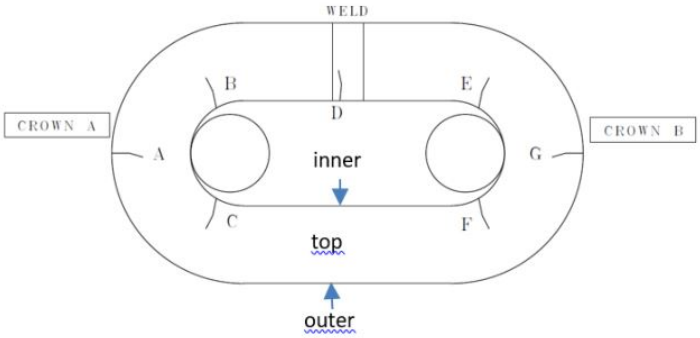

Figure 27: Illustration showing the most common crack initiation points.[36]

The locations marked by letters in fig. 27 show some the most common crack initiation points, but link shoulder, outer bend region (mostly studded chain) and other areas that might be exposed to mechanical damage for the specific chain should also be included. A, B, C, E, F and G all represent areas where we expect to see higher stresses (see fig.28) than in the rest of the link. While at B, C, E and F interlink wear is also expected.

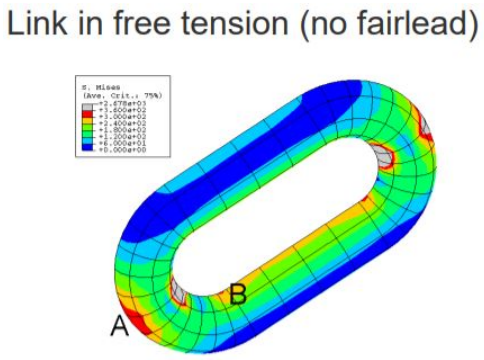

Figure 28: Illustration of von Mises stress distribution of chain in pure tension [17]

Point D in figure 27 is also marked as welding lead to material defects and act as good crack and corrosion initiation areas. Even if post treatment like heating to release residual stress and grinding to avoid sharp geometries is applied, one can never completely eliminate the damage done by welding.

6.2 Chain link dimensions and material grade

As mentioned earlier, the SN-curve design curve from DNV-GL is only based on testing of 76mm chain, grade R3 and R4. As mooring chains vary in size and steel grade, Y.-H. Zhang and P. Smedley (2019) [36] sets out to test chains of higher diameters (127 mm) and steel grades (R4 and R5) and compare them to DNV-GLs (Noble Denton) and smaller dimension chains (76 mm).

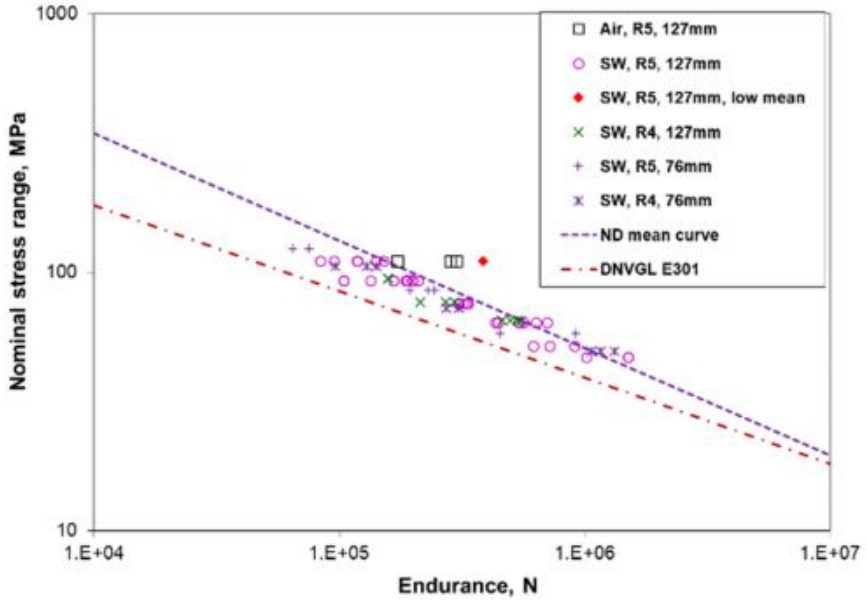

Figure 29: Test results plotted in a SN-diagram with varying chain dimensions and material grades [36]

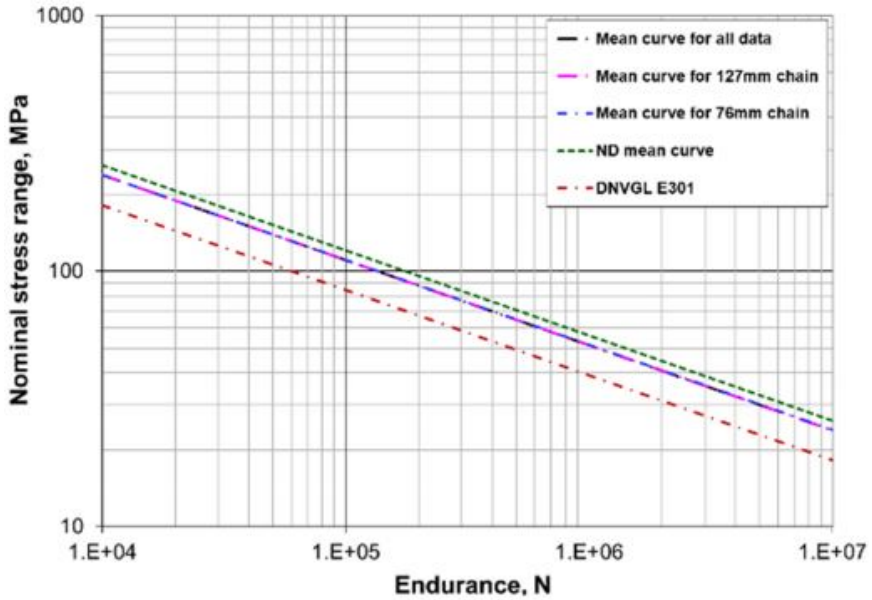

Figure 30: Test results mean curve plotted in a SN-diagram with varying chain dimensions and material grade [36]

All tests except one was run with a mean load of 20% MBL, the same as Noble Denton. We can see in figure 29 that the material grades seems insignificant for fatigue performance. The test result are also relatively close to the Noble Denton curve. So no significant difference in fatigue performance was found when plotting for nominal stress range. It is important to notice that 20% MBL for R5 is higher than for R4, R3 etc. and that one would expect to see higher steel grades perform better than lower grades if test was performed with an absolute mean load (not based on a percentage of MBL).

Some of the same observations was made for chain dimensions. When plotted in an SN-diagram, there was good agreement in fatigue performance for the different chain dimensions. But as a bigger diameter will lead to lower stresses inside the link, indications are: higher fatigue performance for larger dimensions if tested for the same absolute load range. This conclusion is supported by "J. Fernández, W. Storesund and J. Navas (2014)" [13].

6.3 Fairlead contact and interlink wear

Chain condition	Bend	Crown	Straight	Other
"As new" surface Varying interlink wear	6	17	-	1
Corrosion pits or "rough" surface	-	22	1	-
Total	6	39	1	1

Table 6: Fatigue break positions for "as new" and corroded chain from OMAE2017-61382 [22]

Table 6 indicates that fatigue break is almost guaranteed to start at the crown. Corroded chain all failed at the crown. For "as new" chain, the tests show that initiation at crown is most likely, but that the inside of the bend also can occur. For "as new" chain breaks inside bend, anomalies from manufacture was the main suspect. What we can draw from this is that anomalies can be important if the chain is subjected to high loads and it's condition is "as new". But as surface roughness from corrosion occurs later in a chains life, initiation point will most likely move to the crown.

The tests did not show any break strictly due to the wear. The initiation started in pitted or anomalies from production. One could argue that the diameter loss from wear is a contributing factor for break, but wear alone was not the sole reason in any of the test performed in "K. Larsen, Øystein Gabrielsen, and S.-A. Reinholdtsen (2017)". The test size is small, so this is not a conclusion, but more an indication.

"K. Larsen, Øystein Gabrielsen, and S.-A. Reinholdtsen (2017)" present one test result on a chain with fairlead wear. This link actually broke in wear dent (see figure 33.)

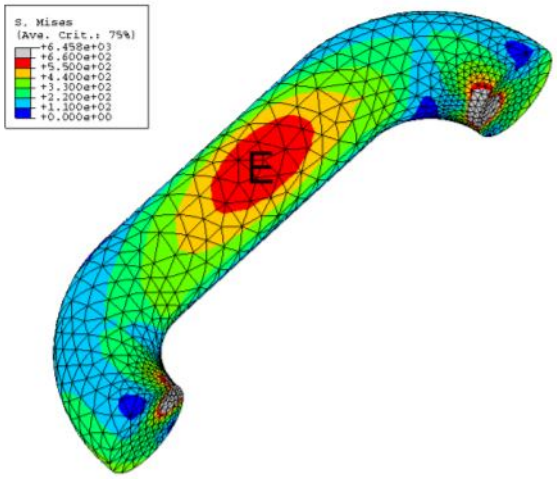

Figure 31: Stress distribution for a chain link mispositioned in fairlead [22]

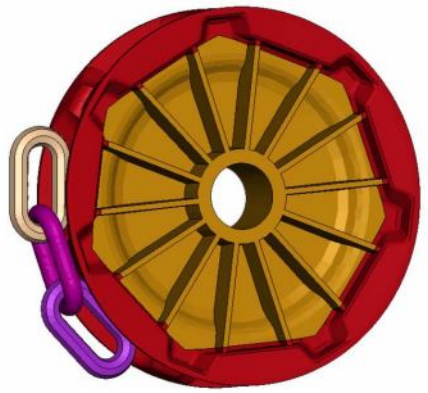

Figure 32: Chain position in fairlead [22]

Research on chain with deformations from fairlead/link contact fatigue performance is very scarce. From CAE simulation results (ref. figure 31), we can assume stress distribution will shift drastically, when comparing pure tension in link to tension with some out of plane bending introduced. In figure 31 higher stresses than for pure tension (ref figure 28) is observed at a new location. A chain link that has been exposed to a loading situation like the one in figure 31 is likely to have residual stresses in the material and contain micro cracks. This situation of deformation from fairlead/link contact similar to the ones we might see from testing and retrieval described in chapter 3. Only that the load from anchor line and anchor testing procedure is most likely much higher than what the chain can expect to see in operation.

Figure 33: Link with failure in wear dent. Break in white circle. [22]

6.4 Mean tension

As mentioned in chapter 2, the SN-diagram from DNV-GL is based on Noble Denton's (2002) research which is ran with a mean tension of 20% MBL, hence it does not take mean tension into account. As already implicated earlier in this paper, mean tension might be a big factor in fatigue life.

Test	Years in operation	"Type"	Condition	2011-2018	2019 ->
A	12	Platform	Wear	4	
B	10	Platform	Pitting	6	
C	9	Platform	Wear	9	
D	4	Platform	Fairlead wear	4	
E	12	Platform	Wear	4	
F	14	Seabed	SRB	4	
G	5	Platform	Pitting	4	
H	16	Platform		3	
I	18	Seabed	Pitting	9	
J	17 / 21	Seabed	SRB	8	
K	12	Platform	Pitting	5	
L	21	Platform	Wear	3	
M	19	Seabed	SRB	7	3
N	19	Interm.	General corrosion	4	
O	19	Seabed	SRB	4	3
P	19	Seabed	SRB		10

Table 7: List over fatigue test planned and conducted by Equinor. Only first breakages[38]

Equinor has run multiple tests on chains with different wear, time in operation etc. over the years (ref. table 7). The initial reasoning for testing has varied and so has the mean tension. In OMAE2019-95083, employees at Equinor tries to categorize and understand data from earlier tests w.r.t mean tension. This has been done because mean tension of a mooring line in operation is between 5-18% and maximum 20% MBL [19]. If mean tension has a big impact on fatigue, the assumption of 20% MBL might seem overly conservative if mean tension potentially is as low as 5% MBL under operation. It is important to remember that the DNV-GL SN-curve is moved two standard deviation from the original mean curve, which is also of conservative nature.

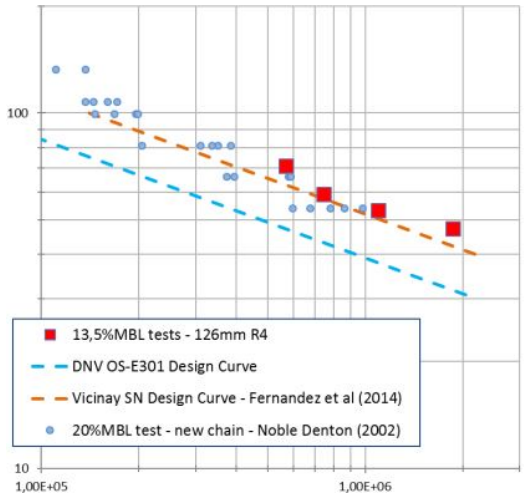

(a) SN-diagram for R4 126mm chain with uniform corrosion and significant interlink wear. 13.5% MBL mean load [38]

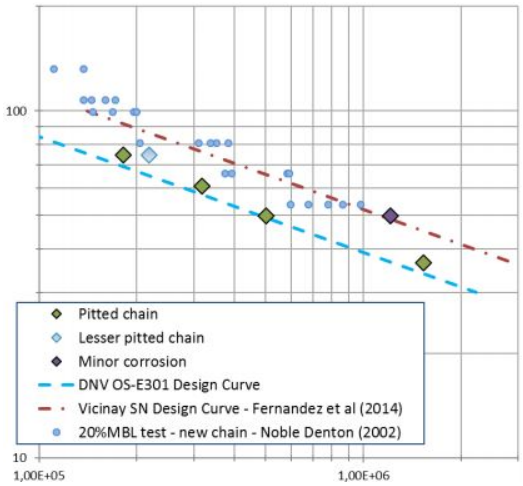

(b) SN-diagram for R4 126mm chain with rough surface and pitting corrosion. 16% MBL mean load [38]

Figure 34

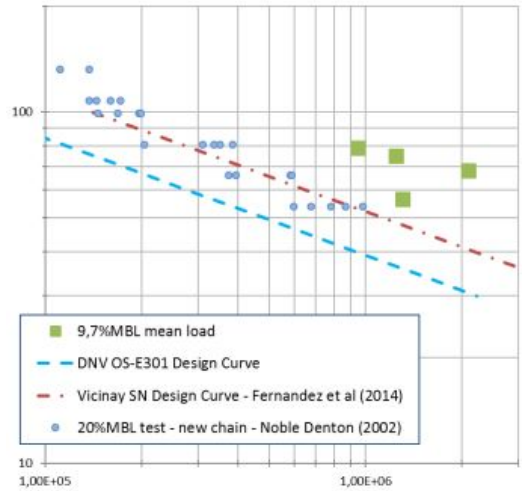

(a) SN-diagram for without uniform corrosion and limited wear run with low mean load. 9.7% MBL mean load [38]

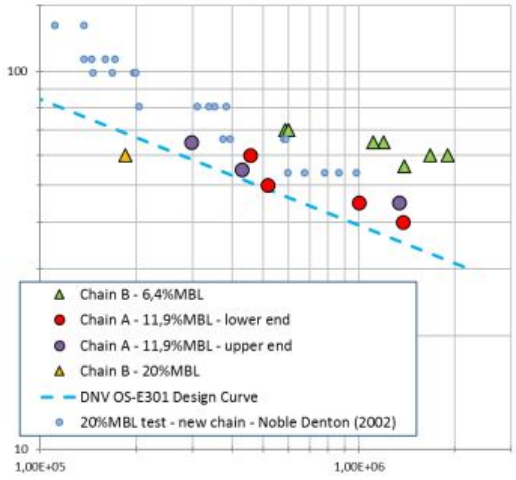

(b) SN-diagram for chain with 4 mm deep pits tested with different mean loads. 11.6%, 6% and 20% MBL mean load [38]

Figure 35

The results presented in figure 34 and 35 all indicate the same trend. A lower mean load increases fatigue life drastically and surface roughness decrease fatigue life. If mean load did not have any impact, we would expect the fatigue life of corroded chain to be at best equal or less than the mean curve from Noble Denton. The test results indicate that used chain can outperforming Noble Dentons result for new chain given a low mean tension.

Another test was run on segments from the same chain (chain C in table 7) with significant corrosion with varying mean load, but the same maximum load:

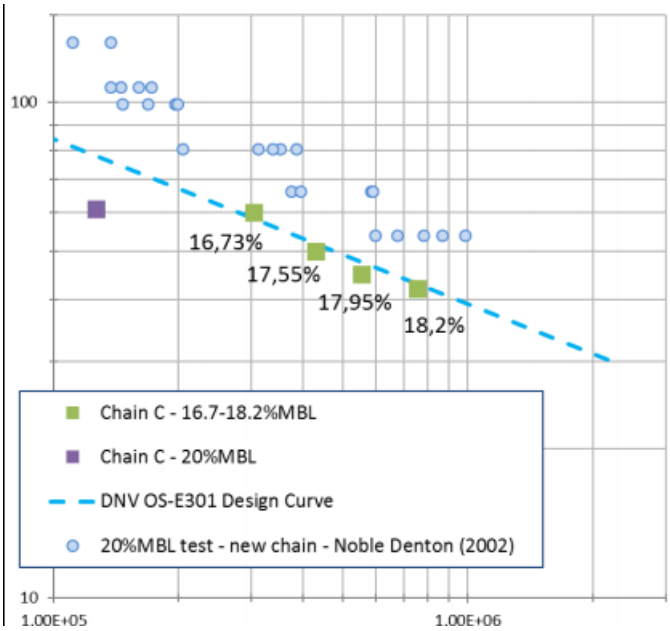

Figure 36: Tests with varying mean load, but the same maximum load done on chain with 4mm SRB corrosion[38]

In figure 36, stress amplitude was decreased with increasing mean load. Figure 36 shows increase in fatigue life with a increased mean tension, BUT (again) stress amplitude was decreased. The purple dot was run with the 20% MBL mean tension, but the same stress amplitude as the 16.73% MBL mean tension segment. Here we see a dramatic decrease in fatigue life, boosting the hypothesis that mean tension is plays a big role in fatigue assessment.

6.5 Discussion

It is hard to draw any conclusions, as the results that we have looked upon have different goals for their testing and the result pool from testing is still not big enough. Testing rigs and the way testing have been performed also varies some, but from the writers understanding, not to a big extent.

Even though the general condition of the same type of corrosion, defect, wear etc. may appear the same for different chain segments, deviations will appear in testing. Manufacturing, geometry, location and extent of wear/defect/corrosion is important factors as it potentially have huge impact on fatigue life.

Why mean tension has an impact on fatigue life is still up to discussion, but some common conceptions have been established. Initially in a chain link there is a complex set of residual stresses from forging, processing and proof loading. These stresses can be compressive or tension. When a crack or defect is present, these residual stresses might help to open the crack and lead to crack propagation. Or, if they're compressive help prevent crack propagation. For mean tension in a chain, it can only be tension. With a higher mean tension, these cracks/defects will open up, resulting in fatigue life loss.

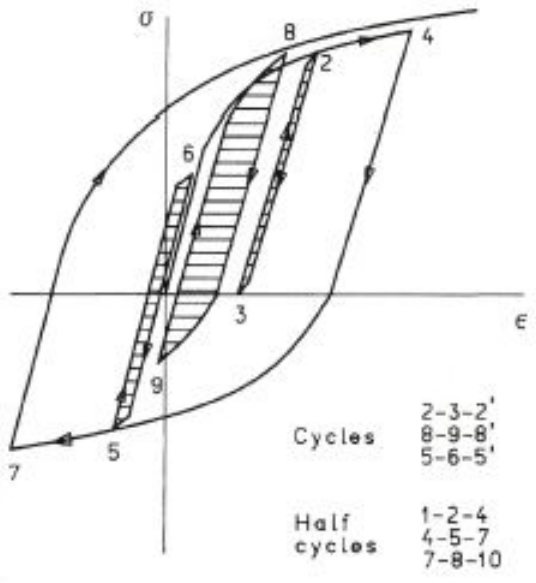

Figure 37: Illustration of load cycles plotting strain against stress[37]

As illustrated in figure 37, a load cycle might compression and tension. In general, the part of a cycle below the x-axis (compression) do not contribute to reduction in fatigue life. With a higher mean tension, we increase the time a cycle spends in tension and its magnitude, hence increased crack propagation. From here, we can drawn the conclusion that a higher mean tension in the line will lead to a reduction in fatigue life.

6.6 Conclusion

All the bullet points below should not be taken as conclusions, but good indications:

- Chain break initiation points are most likely to occur in the areas with the highest stress concentrations
- Defects from manufacturing might lead to break of "as new" chains
- Interlink wear do not seem to alone lead to break unless extensive, but speeds up the process if fairlead damage, rough surface and/or production anomalies is present
- Research on damage from fairlead wear is scars, but existing research indicate that it negatively affects fatigue life and might lead to failure
- A higher mean tension leads to reduced fatigue life

7 Defining the model for line tension (AH process)

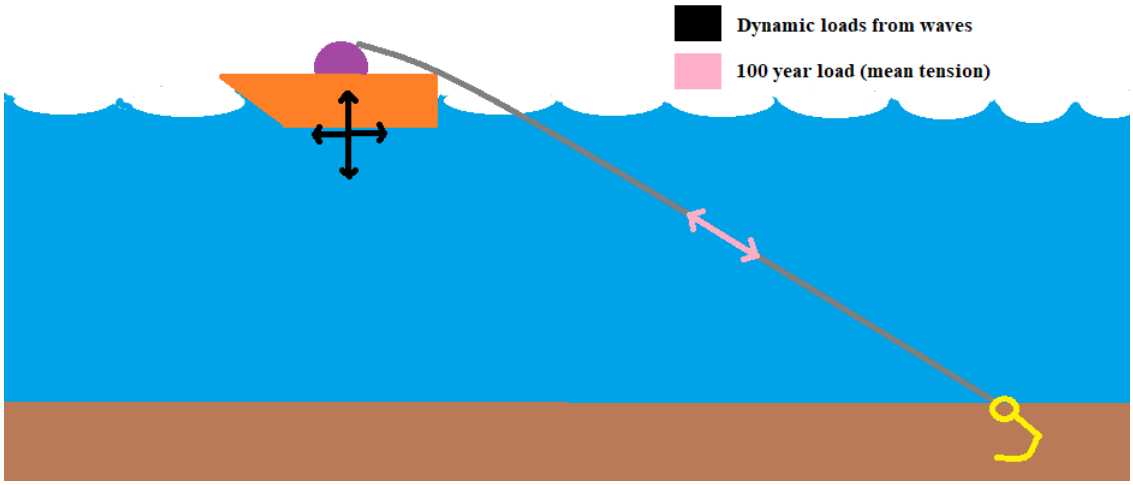

Figure 38: Simple illustration of anchor handlers testing an anchor and line with a 100 year load and dynamic loads from waves on vessel

In chapter 3 negative effects on mooring chain fatigue life from anchor handling is described. Especially testing of anchor fastening and chain after deployment is believed to be damaging for the chain. As the extent of the damage done to the chain by performing mooring line deployment and retrieval is not very well documented, we aim to recreate this process in FEA to quantify hotstop stresses, stress distributions and quantify the fatigue damage. To start, we will need make a model that estimate the tension applied to a mooring chain caused by this process.

By combining a set of RAOs with weather data, we set out to find a RAO for dynamic line tension dependant on wave frequency ($T_{dyn}(\omega)$).

$$T_{dyn}(\omega) = RAO_{COG} \cdot RAO_{stern} \cdot RAO_{\epsilon} \cdot RAO_{ktot} \cdot \zeta_s \tag{9}$$

$T_{dyn}(\omega) = Amplitude\ stress\ (N)$
$RAO_{COG} = Vessels\ directional\ responses\ to\ waves\ at\ COG\ ,\ 6\ DOF\ (m/m)$
$RAO_{stern} = Translation\ of\ movement\ at\ COG\ to\ stern\ ,\ 3\ DOF\ (m/m)$
$RAO_{\epsilon} = Stern\ movement\ in\ tangential\ direction\ at\ stern\ ,\ 1\ DOF\ (m/m)$
$RAO_{ktot} = Total\ line\ stiffness\ as\ a\ function\ of\ wave\ frequency\ ,\ 1\ DOF\ (N/m)$
$\zeta = Wave\ amplitude\ (m)$

7.1 Defining the motions

As mentioned earlier, our case study will feature an AH vessel with a constant propulsion to test the anchor line. To estimate the maximum tension the mooring chain might experience, it is necessary to include line tension induced by the motions that the vessel will experience.

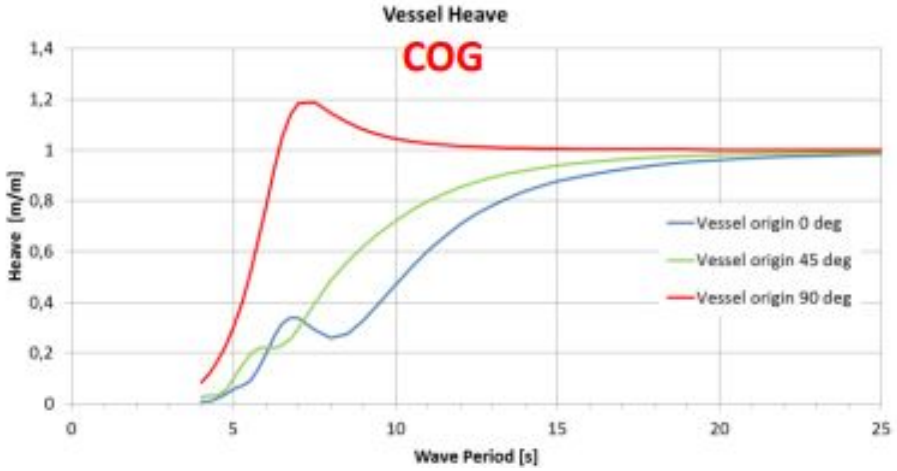

Figure 39: Example of a RAO for heave motion at COG of a vessel for different wave headings [20]

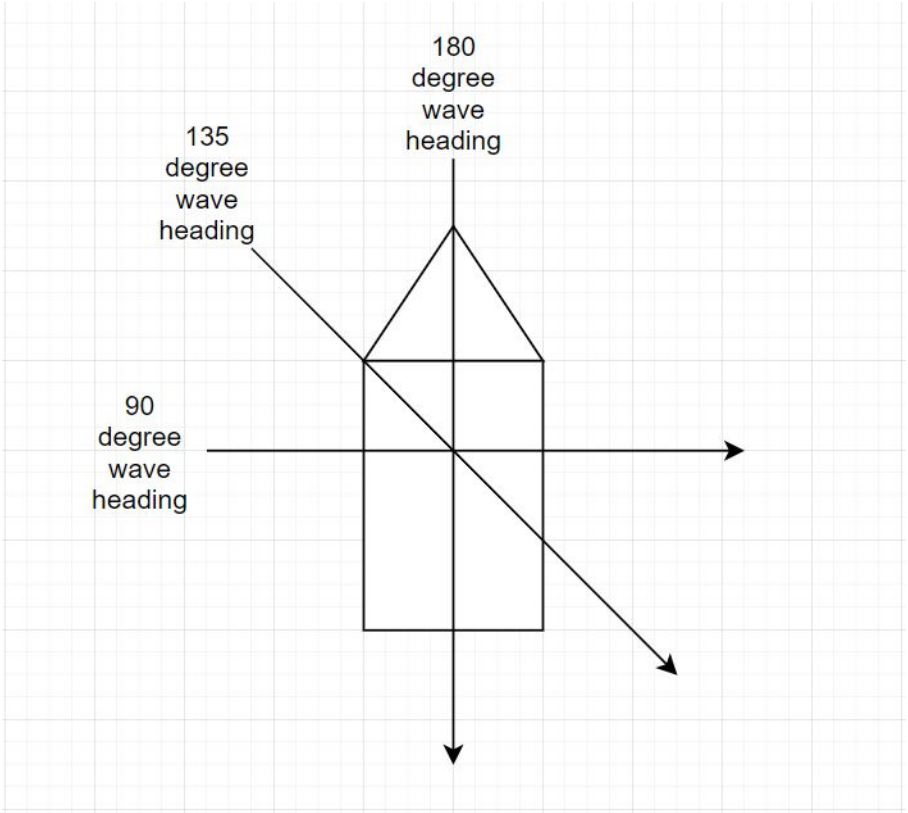

Figure 40: Defining the angles of wave headings. For this case; only 135°and 180°wave headings will be considered in this thesis

The RAOs are unique for each vessel and is calculated by use of first order hydrodynamic analysis tools or, alternatively, estimated from small scale model tests. Figure 39 shows how a specific vessel will respond in heave motion for different wave frequencies and wave headings.

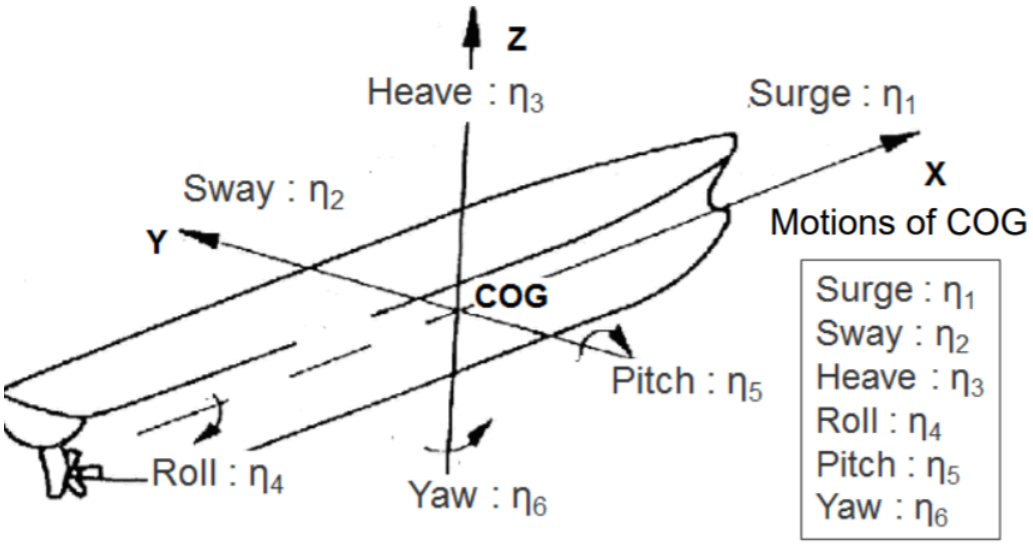

Figure 41: Illustration of a vessels DOFs around a right handed coordinate system fixed in the vessels COG. [20]

So with the RAOs for a vessel it is possible to estimate the vessels response for a chosen DOF by producing a wave heading and wave period.

Most RAOs are for the COG of the vessel, but often we want to see the response of another coordinate, which will differ from the COG's. It is also important to remember that a vessel responds in 6 DOFs and that the rotational DOFs will contribute to movement in x-, y- and z-direction when looking at a point other than the COG. "O.M. Faltinsen (1990)" states that the motion of any point of a body can be written as:

$$s = \eta_1\mathbf{i} + \eta_2\mathbf{j} + \eta_3\mathbf{k} + \omega \times \mathbf{r} \tag{10}$$

$$\omega = \eta_4\mathbf{i} + \eta_5\mathbf{j} + \eta_6\mathbf{k} \tag{11}$$

$$\mathbf{r} = x\mathbf{i} + y\mathbf{j} + z\mathbf{k} \tag{12}$$

i, **j**, **k** are unit vectors along x- , y- and z-axis respectively. This means:

$$s = (\eta_1 + z\eta_5 - y\eta_6)\mathbf{i} + (\eta_2 - z\eta_4 + x\eta_6)\mathbf{j} + (\eta_3 + y\eta_4 - x\eta_5)\mathbf{k} \tag{13}$$

In this paper , we want to look at the midpoint at the stern and are only interested in motions the x- and z-directions. As a result, we can neglect all motions in **j**-direction and set y = 0. We end up with the following expression:

$$s = (\eta_1 + z\eta_5)\mathbf{i} + (\eta_3 - x\eta_5)\mathbf{k} \tag{14}$$

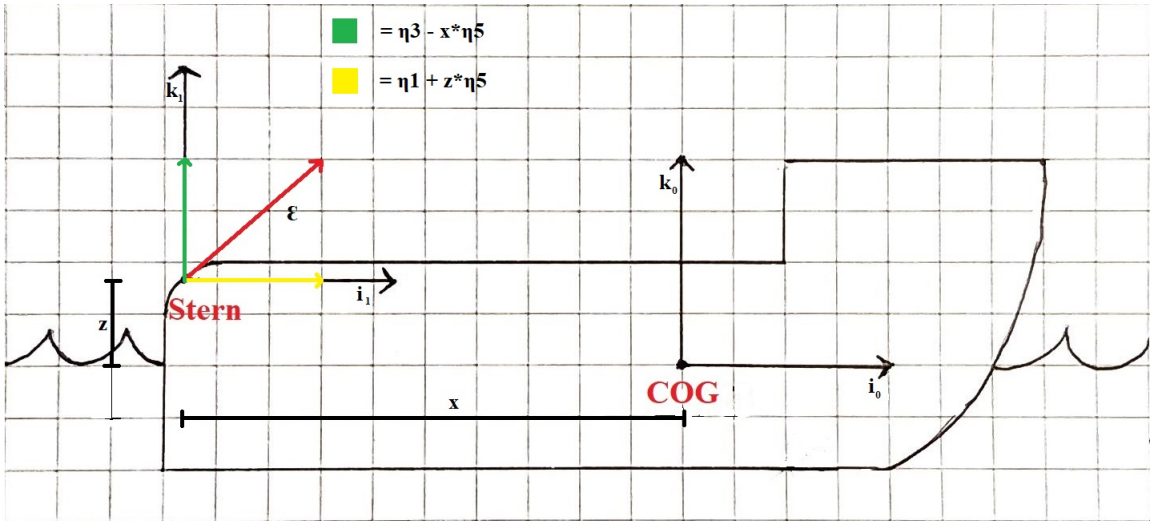

Figure 42: Illustration of how we use equation 14 to find motions at stern based of a RAO for the COG. ϵ is the resultant movement in tangential chain direction at stern.

Lastly, we want the motion in tangential chain direction at stern (ϵ) illustrated in figure 42. This is calculated for each wave frequency taking the relative phases into account:

$$\epsilon = \sqrt{i_1^2 + k_1^2} = \sqrt{(\eta_1 + z\eta_5)^2 + (\eta_3 - x\eta_5)^2} \tag{15}$$

Important to note that in our case, motions are then corrected for by the entry angle of the mooring line, φ shown in figure 50. For more detail on how to calculate φ, see chapter 7.2.3.

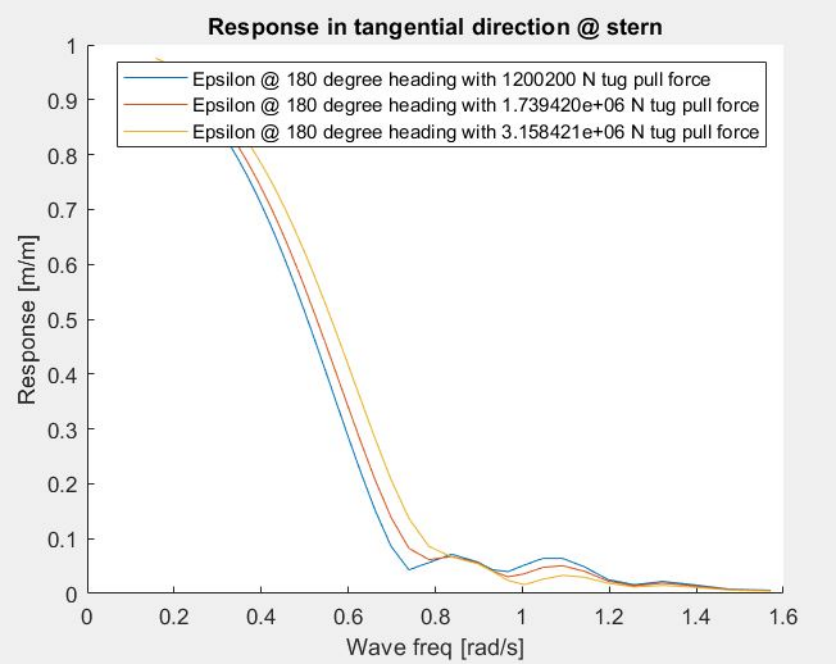

Figure 43: AH vessels response in tangential direction (RAO_ϵ for different AH pull forces and a constant water depth of 100 m

7.2 Defining the Stiffness and line tension

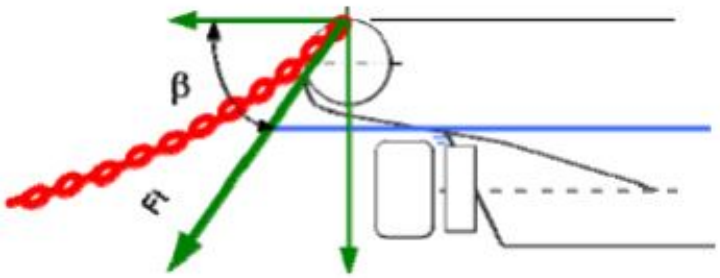

Figure 44: Decoupling forces from anchor testing [20]

We need to quantify the loads from waves and the vessel. The applied vessel pull force is set to 52,6% of the chains MBL as described in DNVGL-OS-E301 [8] [19]. The idea is to treat the chain as a spring with a stiffness given by the material by using the equation:

$$F = k \cdot x_i \tag{16}$$

$k = stiffness$
$x_i = distance\ in\ direction\ i$

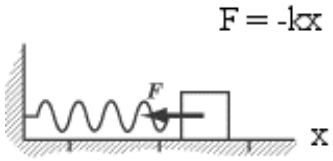

Figure 45: Concept of a spring[7]

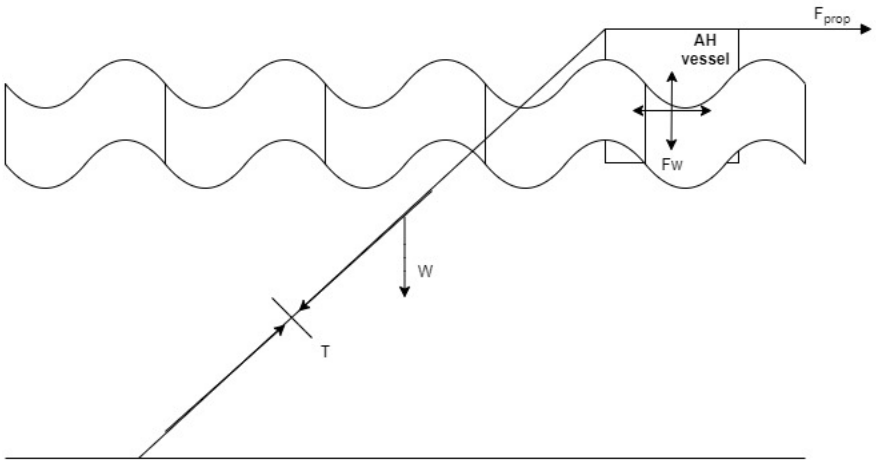

Figure 46: Model of the forces acting on the mooring line when checking anchor bedding-in. F_w in this figure represent a collection term for wave, wind and current forces.

7.2.1 Defining the stiffness (k)

The total stiffness (k_{tot}) of the system concists of:

- Elastic Stiffness
- Geometric stiffness

And are related to each other in the following way

$$\frac{1}{k_{tot}} = \frac{1}{k_{geometric}} + \frac{1}{k_{elastic}} \tag{17}$$

In reality the geometric stiffness is a bit more complicated as it also contains dampening. We can illustrate the anchor line as a system of springs and dampers. Important to note is that springs contribution to stiffness is dependant on distance (x). Dampening has an impact on the lines behaviour as well, but this parameter is dependant on line velocity.

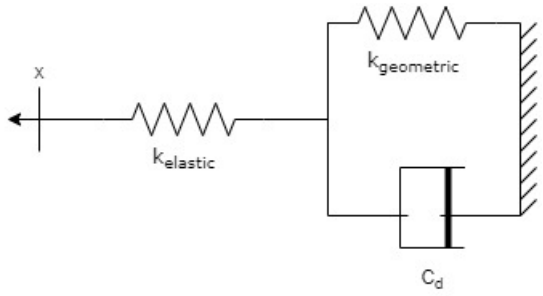

Figure 47: Illustration of anchor line as a set of springs and dampers

With a higher stiffness, moving a moored object will require a higher force than for lower stiffness systems. It is important to define the model i figure 47 correctly, as the stiffness affects low-frequency motions of moored unit and the dynamic tension in the mooring line.

7.2.2 Elastic stiffness

The elastic stiffness is a material parameter and will be defined by the material chosen and the length of the chain.

$$k_{elastic} = \frac{EA}{L} \tag{18}$$

$E = Young's\ modulus\ of\ material\ (GPA)$
$A = Cross\ sectional\ area\ (m^2)$
$L = Active\ length\ of\ chain\ (m)$

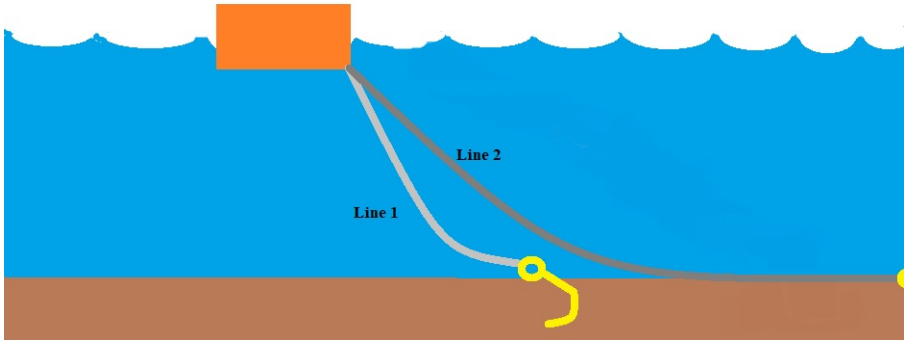

Figure 48: Picture illustrating two different mooring line configurations for mooring the same unit.

In figure 48 two different mooring configurations. As the elastic stiffness is dependant on length (ref. equation (18)), line 1 will have a higher elastic stiffness than line 2. Equation (18) provide mooring systems planners with a good tool to adjust mooring system stiffness for different operations. By applying line configuration 2 (figure 48), with a longer chain segment resting on the sea floor, elastic stiffness is reduced without adding too much weight to the moored system. Note that if friction between sea floor and chain is high enough, the elastic stiffness is only dependant on the length of the chain which is not stuck in the seabed.

7.2.3 Geometric stiffness

Geometric stiffness is related to the chain weight e.g. the equivalent weight w.r.t. the chains position and weight magnitude.

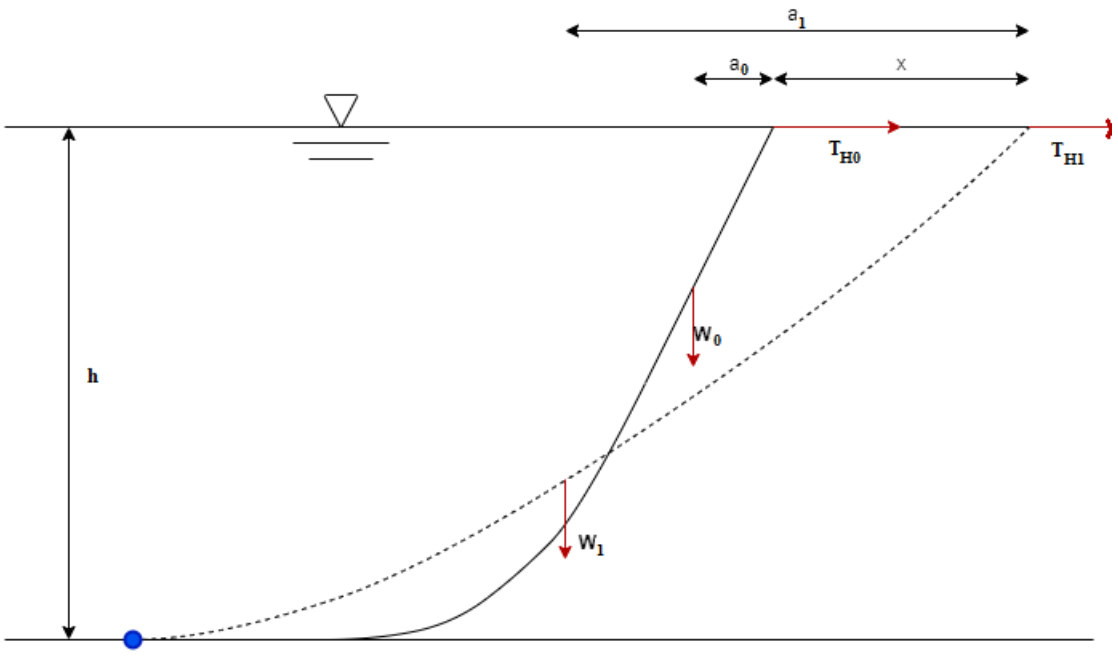

Figure 49: Demonstration of geometric stiffness

Figure 49 shows how the position of a moored unit change the resultant weight. It might be hard to see in the figure that we have a change in magnitude as well, as more chain will be lifted from the seabed in case 1. Assuming that the we have equilibrium in figure 49 around the moored object, we can derive the following equation for the two different positions:

$$T_H \cdot h = W \cdot a \tag{19}$$

$h = Depth\ (m)$
$a = Moment\ arm\ for\ resultant\ weight\ (m)$
$W = Resultant\ weight\ (N)$
$x = Horizontal\ offset\ (m)$

To find the necessary parameters to start calculations, the catenary equations [6] is frequently used. The equations assume a flat seabed and neglect bending stiffness effects.

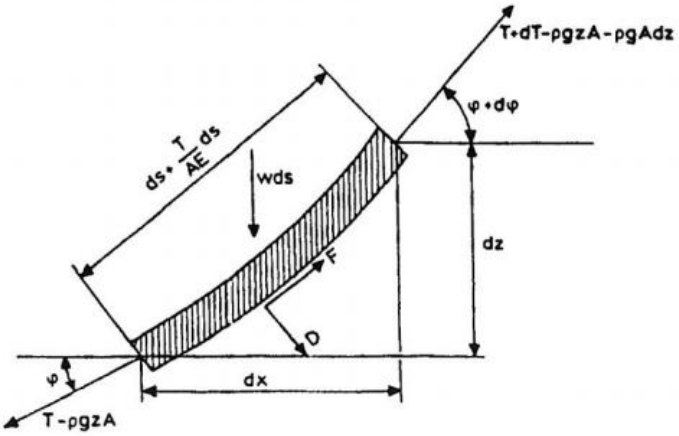

Figure 50: Figure illustrating how terms are expressed in integration form [6]

$D\ and\ F = Hydrodynamic\ forces\ on\ element\ per\ unit\ length\ (N/m)$
$\rho = Density\ (kg/m^3)$
$w = Constant\ submerged\ line\ weight\ per\ unit\ length (N/m)$
$\varphi = Angle\ (^\circ)$
$A = Cross\ section\ area\ (m^2)$
$E = Elastic\ modulus\ (GPa)$

By summing up the moments in figure 50, we can develop the following equations:

$$dT - \rho g A dz = \left[w \cdot sin(\varphi) - F(\frac{T}{EA}) \right] ds \tag{20}$$

$$Td\varphi - \rho g A z \varphi = \left[w \cdot cos(\varphi) + D(1 + \frac{T}{EA}) \right] ds \tag{21}$$

Equation 23 and 24 both ignore F, D and elasticity for simplification reasons. As lines get longer, elasticity in particular get increasingly important. Then modifications to the equations should be considered.

The distance (x) from touchdown point to moored unit is found by using:

$$x = \frac{T_H}{w} \cdot \ln \left[1 + \frac{h \cdot w}{T_H} + \sqrt{\left(1 + \frac{h \cdot w}{T_H}\right)^2 - 1} \right] \tag{22}$$

We can now derive the suspended line length (s) and water depth (h):

$$s = \frac{T_H}{w} sinh(\frac{wx}{T_H}) \tag{23}$$

$$h = \frac{T_H}{w} \left[cosh(\frac{wx}{T_H}) - 1 \right] \tag{24}$$

From here, we can derive the static line tension as an equation based on s and h:

$$T = \frac{w\left(s^2 + h^2\right)}{2h} \tag{25}$$

and for the horizontal (T_H) and vertical forces (T_z):

$$T_z = ws \tag{26}$$

$$T_H = T \cdot cos\varphi \tag{27}$$

Now we can find our geometric stiffness ($k_{geometric}$) using the catenary equations and terms found in figure 46:

$$k_{geometric} = \frac{T_{H1} - T_{H0}}{x} \tag{28}$$

This is only the geometric stiffness and do not account for dampening and is hence not sufficient. We will solve this in chapter 7.2.4.

7.2.4 Total line tension

As illustrated in figure 47, there is a viscous drag part implemented into the spring/damper system of a mooring line. Drag is a phenomenon that occurs when moving an object through a fluid. Drag is a dampening effect that is dependant on the moving objects geometry and velocity. So with a increasing velocity, we will see an increased resistance to the movement. Drag mainly consist of viscous friction in the fluid, which scales linearly with velocity if flow is laminar and squared if flow is turbulent. For this chapter we assume turbulent flow around the mooring line.

To get the motion-to-tension transfer, an analytic method and a estimate for line drag resistance described in "K. Larsen and P.C. Sandvik (1990)" [21] is chosen. The following equations, text and figures is taken from "K. Larsen and P.C. Sandvik (1990)" [21] unless specified otherwise.

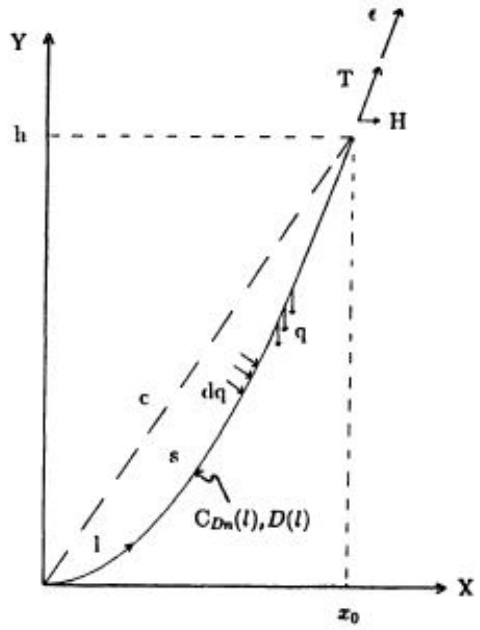

Figure 51: Illustration of a fully submerged mooring line [21]

Symbol description for figure 51:
$T = Upper\ end\ line\ tension\ (static)\ (N)$
$H\ (T_H\ in\ later\ calculations) = Horizontal\ tension\ component\ (N)$
$\epsilon = Tangential\ top\ end\ motion\ (m)$
$c = Length\ of\ line\ secant\ (m)$
$s = Suspended\ length\ of\ line\ (m)$
$q\ (w\ in\ later\ calculations) = Submerged\ weight\ of\ line\ (N/m)$
$h = Water\ depth\ (m)$

We can describe the mooring line segment shown in figure 51 with the following equations:

$$y = \frac{T_H}{w} cosh\left(\frac{xw}{T_H}\right) \tag{29}$$

$$s = \sqrt{h\left(2\frac{T}{w} - h\right)} = \sqrt{h\left(2\frac{T_H}{w} + h\right)} \tag{30}$$

For the horizontal distance from touchdown to upper part of chain (x_0):

$$x_0 = \frac{T_H}{w} ln\frac{s+h}{s-h} = \frac{T_H}{w}\alpha \tag{31}$$

$$\alpha = ln(\frac{s+h}{s-h}) \tag{32}$$

We can describe the change in horizontal distance as a expression of change in equation 30 and 31 (ds and x_0):

$$dx = dx_0 - ds \tag{33}$$

Combining equations 29 - 33 and differentiating we can get the increase in line tension as an expression of top end motion (ϵ) in tangential direction of line:

$$\frac{dT}{d\epsilon} = \frac{T_H \cdot ws\,(T_H + ws\alpha - wh)}{(T_H + wh)\,(wsx_0 - 2T_H h)} + \frac{T}{w}\frac{dw}{d\epsilon} \tag{34}$$

which again can be translated to:

$$k_G(\omega) = k_S + k_C(\omega) \tag{35}$$

$k_G(\omega) = Frequency\ dependant\ geometric\ stiffness$
$k_S = Static\ catenary\ stiffness$
$k_C(\omega) = Stiffness\ due\ to\ drag\ resistance$

The first term in equation 34 represent linearized catenary stiffness of a inelastic line in the direction of the top en tangent and the second part reflects drag induced tension. dw is given as average drag load per unit length for a top side excitation $d\epsilon$.

The term for linearized catenary stiffness k_S (equation 35) is self explanatory and only require us to insert problem specific values. For the term $k_C(\omega)$, the determinator is still in need of some explanation. "K. Larsen and P.C. Sandvik (1990)"[21] gives states the following derivation:

According to figure 51 average drag force per unit suspended length is

$$\frac{dw}{d\epsilon} = \frac{F_C(\omega)}{s} = \omega^2 \frac{\int_0^s CDN(l) u_n(l, \epsilon^*)^2 dl}{s \cdot \epsilon^*} \tag{36}$$

$F_C(\omega) = Total\ frequency\ dependant\ drag\ force\ on\ line\ (N)$
$u_n(l) = Displacement\ normal\ to\ line\ tangent$
$\epsilon* = Magnitude\ of\ chosen\ \epsilon\ for\ linearization$
$CDN(l) = Drag\ factor$

$$CDN(l) = \frac{1}{2}\rho C_{Dn}(l) D(l) \tag{37}$$

$C_{Dn} = Drag\ coefficient\ normal\ to\ line$

Solving the integral in equation 36 analytically for a single line segment, the average drag force per unit suspended length is

$$\frac{dw}{d\epsilon} = 0.53\omega^2 CDN \left[\beta - \frac{\beta^2 + 4}{4} ln(\frac{\beta + 2}{\beta - 2})\right]^{-2} \tag{38}$$

where

$$\beta^{-1} = \frac{T_H}{sw}\left[\frac{h}{c} ln(\frac{h + c}{x_0}) + \frac{x_0}{c} - 1\right] \tag{39}$$

As we want to evaluate the maximum geometric stiffness, we introduce a transfer function to the geometric part of the stiffness

$$k_G(\omega) = k_{S0} sin(\omega t) + k_{C0}(\omega) cos(\omega t)\,|cos(\omega t)| \tag{40}$$

Where the maximum value for $k_{Gm}(\omega)$ is found from differentiation

$$\begin{gathered} k_{Gm}(\omega) = k_{S0},\ if\ k_{S0} \geq 2k_{C0} \\ otherwise \\ k_{Gm}(\omega) = \left[(\tfrac{k_{S0}}{2k_{C0}})^2 + 1 \right] k_{C0} \end{gathered} \tag{41}$$

So by correcting for elastic stiffness (k_E), we get a term for complex top motion-to-tension transfer function, $k_{tot}(\omega)$ operating as a total stiffness based on angular frequency of waves for the system described in figure 47

$$k_{tot}(\omega) = \frac{k_{Gm} k_E}{k_{Gm}(\omega) + k_E} \tag{42}$$

One can expect to see the total stiffness approach the elastic stiffness for higher wave frequencies. When high wave frequencies are present, drag locking is a phenomenon often occurring. Drag locking keeps the chain locked in motion, making the geometric stiffness practically ineffective, hence the total stiffness approaches the elastic stiffness.

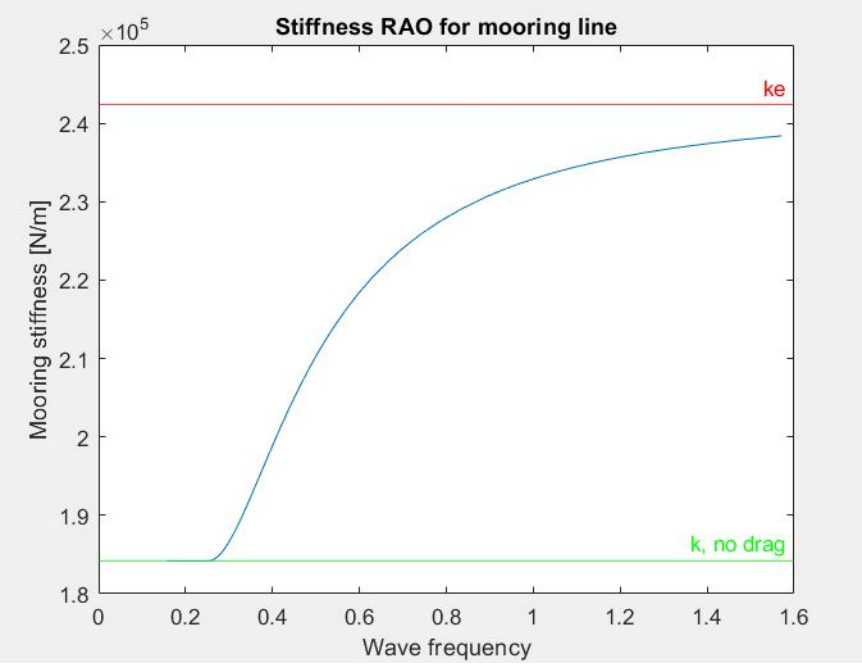

Figure 52: Plot showing how the total line stiffness changes with different wave frequencies. $T_H = 3163kN$, $h = 100m$, 76 mm R4 grade chain.

By multiplying the tangential motion (ϵ) found in chapter 7.1 with the maximum total system stiffness ($k_{tot}(\omega)$) we get the maximum dynamic line tension.

$$T_{dyn.max} = \epsilon \cdot k_{tot}(\omega) \tag{43}$$

Total maximum is then:

$$T_{tot.max} = T_{dyn.max} + T \tag{44}$$

Where T is the static line tension found in equation (25)

8 Defining the model for fatigue damage

To quantify the damage of the AH process for a given duration and weather data for a given geographic area, we need to define a model. As the AH process is a relatively short process, a single sea state can be assumed for the whole operation. Also, low- frequency content of the whole stress process can be neglected for the AH process and hence a narrow-banded assumption can be made.

This chapter will therefor revolve around equation (45) from DNVGL-OS-E301 [8] and defining its parameters:

$$d_{NBi} = \frac{v_{0i} T_i}{a_D} \left(2\sqrt{2} \cdot \sigma_{si} \cdot SCF_{goemetry}\right)^m \Gamma\left(\frac{m}{2} + 1\right) \tag{45}$$

$d_{NBi} = Fatigue\ damage\ for\ state\ i$
$v_{0i} = Mean\ up-crossing\ rate\ (Hz)$
$T_i = Duration\ of\ sea\ state\ i\ (s)$
$a_D = Intercept\ parameter\ of\ the\ S-N\ curve$
$m = Slope\ of\ S-N\ curve$
$\sigma_{si} = Standard\ deviation\ of\ the\ stress\ process\ (MPa)$
$SCF_{goemetry} = Stress\ concentration\ factor\ to\ account\ for\ chain\ geometry$
$\Gamma(.) = Gamma\ function$

8.1 Frequency response method

To get the standard deviation of the stress process and the mean up-crossing rate, there is a need to define a spectra of line tension the mooring chain will experience. To get the tension spectra we use the frequency response method [12]:

$$S_{T(\omega)}(H_s, T_p) = |\epsilon(\omega)|^2 \cdot |k_{tot}(\omega)|^2 \cdot Sj(H_s, T_p) \tag{46}$$

In chapter 7 we defined RAOs $\epsilon(\omega)$ and $k_{tot}(\omega)$ ($H_T(\omega)$ in equation (42)) for the total line stiffness. $Sj(H_s, T_p)$ is a JONSWAP spectrum, which we will further explain in chapter 8.1.1.

8.1.1 JONSWAP spectra

The JONSWAP spectra (Joint North Sea Wave Observation Project) is a sea spectrum model based the on Pierson-Moskowitz's model. It models energy content and distribution over a frequency range of a given sea state [5].

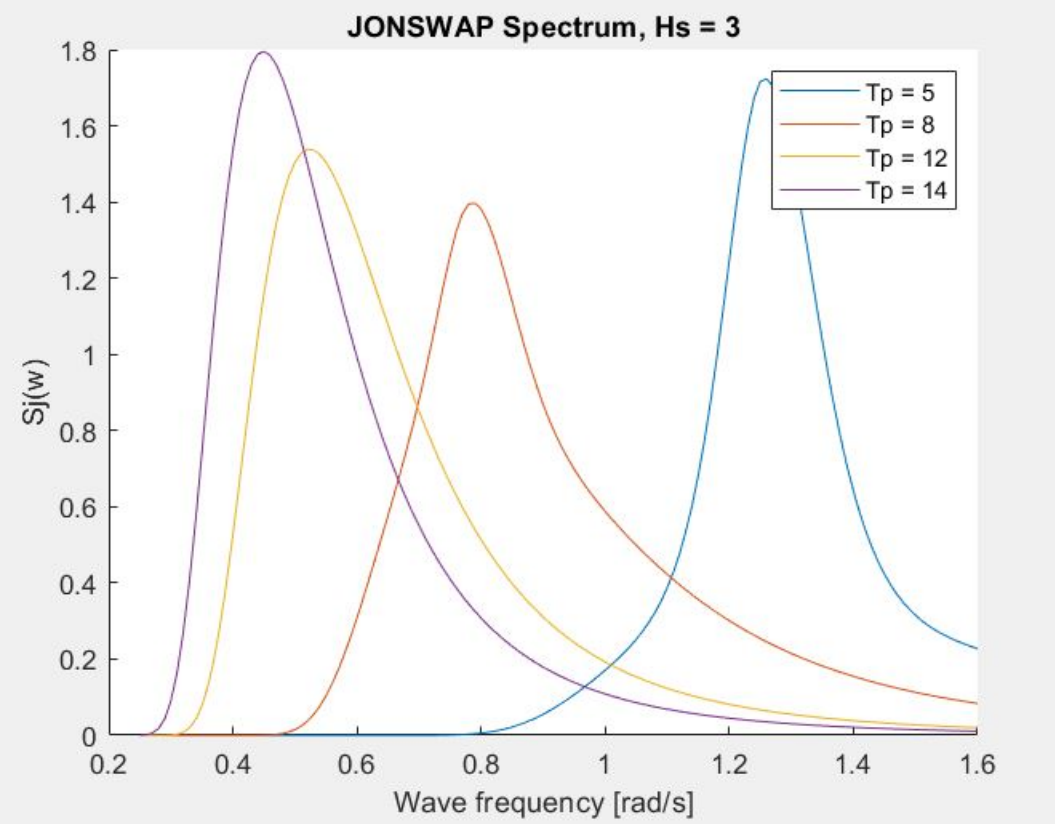

Figure 53: Example of JONSWAP plots made by author. Constant significant wave height and varying peak period

The JONSWAP spectra is defined by the following equation:

$$S_J(\omega) = A_\gamma \cdot \frac{5}{16} \cdot H_s^2 \omega_p^4 \cdot \omega^{-5} exp(-\frac{5}{4}\left(\frac{\omega}{\omega_p}\right)^{-4}) \cdot \gamma^{exp\left(-0.5\left(\frac{\omega-\omega_p}{\sigma\omega_p}\right)^2\right)} \tag{47}$$

$S_J(\omega) = JONSWAP\ spectra$
$\gamma = Non-dimensional\ peak\ shape\ parameter$

$$\gamma = 5,\ for\ \frac{T_p}{\sqrt{H_s}} \leq 3.6$$

$$\gamma = exp\left(5.75 - 1.15\frac{T_p}{\sqrt{H_s}}\right),\ for\ 3.6 < \frac{T_p}{\sqrt{H_s}} < 5 \tag{48}$$

$$\gamma = 1,\ for\ \frac{T_p}{\sqrt{H_s}} \geq 5$$

$H_s = Significant\ wave\ height\ (m)$
$\omega_p = \frac{2\pi}{T_p} = Peak\ wave\ frequency\ (rad/s)$
$\omega = Wave\ frequency\ (rad/s)$
$\sigma = Spectral\ width\ parameter$

$$\sigma = \sigma_a = 0.07,\ for\ \omega \leq \omega_p$$

$$\sigma = \sigma_b = 0.09,\ for\ \omega > \omega_p \tag{49}$$

$A_\gamma = Normalizing\ factor$

$$A_\gamma = \frac{0.2}{0.065\gamma^{0.803} + 0.135} \tag{50}$$

8.2 Standard deviation of stress process (σ_{si}) and mean up-crossing rate (υ_{0i})

To find the fatigue damage for the AH process, we need to find the standard deviation of stress process (σ_{si}) and mean up-crossing period (υ_{0i}) displayed in equation (45).

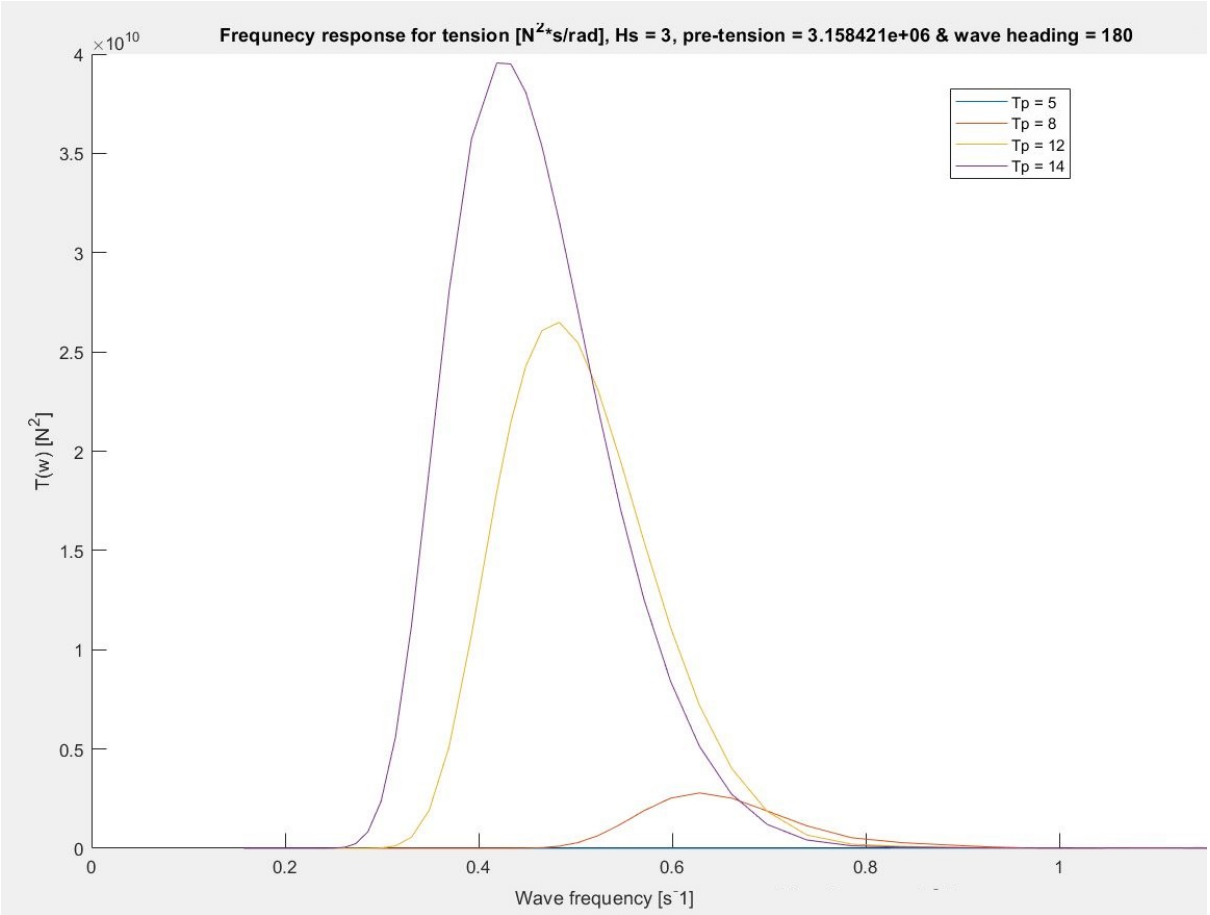

Figure 54: Tension spectra plots using equation (46)

Figure 54 displays four tension spectra (described in chapter 8.1). By integrating tension spectra over a chosen frequency interval, one can obtain the line tension variance :

$$Var(T_{line}(\omega)) = \int S_{T(\omega)}(H_s, T_p)d\omega \tag{51}$$

And now the the standard deviation for line tension can be found ($\sigma_{T_{line}(\omega)}$):

$$\sigma_{T_{line}(\omega)} = \sqrt{Var(T_{line}(\omega))} \tag{52}$$

By dividing standard deviation for line tension ($\sigma_{T_{line}(\omega)}$) by the cross sectional area of a given chain, we get the Standard deviation of the stress process (σ_{si}):

$$\sigma_{si} = \frac{\sigma_{T_{line}(\omega)}}{A} \tag{53}$$

Where it is important to remember that the area is $\frac{2D^2\pi}{4}$, where D is the dimension of the chain.

The mean up-crossing rate is defined as:

$$v_{0i} = 1/T_2 \tag{54}$$

where T_2 is the mean wave period and is defined as (O.M. Faltinsen (1990)) [12]:

$$T_2 = 2\pi\sqrt{\frac{m_0}{m_2}} \tag{55}$$

We calculate the m-values the following way:

$$m_k = \int \omega^k S(\omega)\, d\omega \tag{56}$$

with $k = 0$ and $k = 2$, respectively and $S(\omega)$ defines the spectra.

8.3 Accounting for mean line tension and corrosion

In chapter 5 and 6, the effect of corrosion and mean line tension on fatigue was discussed. The chapters concluded that corrosion and and mean tension affects the fatigue life of the chain, but did not provide any means for quantifying the effects.

LIFEMOOR KPN (NTNU/SINTEF, et al.) and NORMOOR JIP (DNVGL, et al.) are ongoing projects that working on ways to account for mean line tension and corrosion in SN-diagrams. As of per now, a mooring lines SN-curve is defined as (for more, see chapter 2.2):

$$log(N) = log(a) - m \cdot log(\Delta S) \tag{57}$$

$\Delta S = stress\ range\ (MPa)$
$N = number\ of\ cycles\ spent\ in\ stress\ range$
$a = intercept\ parameter\ of\ the\ SN-curve\ ,\ a = 6 \cdot 10^7\ for\ studless\ chain$
$m = slope\ of\ the\ SN-curve.\ Varies\ for\ different\ mooring\ configrations.\ m = 3\ for\ studless\ chain$

Where the intercept parameter (a) is a mooring line type specific constant. The NORMOOR JIP (DNVGL, et al.) projects implement the effects of corrosion and mean line tension on fatigue life by adjusting the intercept parameter (a). DNVGL: "Analysis of Chain Fatigue test Data", report 2020-0386, rev. A (April 4th 2020) [11] gives the following equation:

$$log(a) = 12.057 - 0.00628 \cdot \sigma_{mean} - 0.0117 \cdot corr \tag{58}$$

where,

$$\sigma_{mean} = \frac{T_m \cdot MBL}{A_{link}} \tag{59}$$

$MBL = Chains\ minimum\ breaking\ load\ (N)$
$T_m = Percentage\ of\ MBL\ (Between\ 0-1)$
$A_{link} = \frac{D^2\pi}{2}\ (mm^2)$

Category	Description
1	New chain (only mild corrosion)
2	Some scattered pitting, less than 1 mm.
3	Larger areas affected, pittings around 1 mm deep.
4	Large area affected by pitting, 1-3 mm deep, the deeper sharper in nature. Crown area affected.
5	Severe and widespread pitting, up to 4 mm, but somewhat less than for category 6.
6	Severe and wide spread pitting, 3-6 mm.
7	Severe and widespread pitting, 3-6 mm and deeper. Crown heavily attacked, sharp and deep pittings.

Table 8: LIFEMOOR projects categorization of *corr* values based on corrosion present on mooring chain [1]

Table 8 shows how *corr* (equation (58)) is defined (labeled as *Category* in table 8). Type of corrosion is typically determined by visual inspection.

As the LIFEMOOR and NORMOOR projects are ongoing, no publications are yet released. The information used in this chapter was received by email on a need to know basis.

8.4 Stress concentration factor

In equation (45), the $SCF_{geometry}$ term is added to DNVGL-OS-E301s [8] original term. If $SCF_{geometry}$ is not added, the fatigue results would be for a straight chain with only interlink contact. This thesis aims to quantify fatigue damage for a chain over the stern roller of a AH vessel. For a chain over a stern roller it is expected to see redistribution and higher peak values of stress in the chain link, than in a straight chain. Hence, we need to quantify SCFs to account for the chain/stern roller contact.

8.4.1 Stress concentration factors for stud-less mooring chain in fairleads

In 2004 a rapport was developed to check the SCFs of stud-less chain in contact with a fairlead by using FEA (Vargas, Hsu and Lee (2004)) [29].

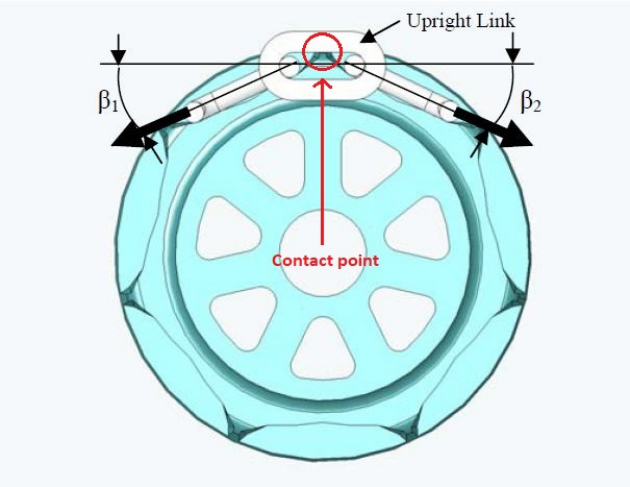

Figure 55: Display of scenario checked in (Vargas, Hsu and Lee (2004)) [29]. Quantifying SCFs for different loads and load directions (β_1 and β_2)

One expects to see the highest SCFs in the areas where fatigue cracks appear and failure appears. The rapport therefor concentrate on stresses in chain link bend, crown and straight section (see chapter 6.1). The rapport defines a SCF for the crown, bend section and straight section:

$$SCF_{location} = \frac{\sigma_{max.location}}{\sigma_{nom}} \tag{60}$$

$SCF_{location} = SCF\ for\ given\ location$
$\sigma_{max.location} = Highest\ stress\ at\ given\ location\ for\ a\ given\ line\ tension\ (MPa)$
$\sigma_{nom} = Nominal\ stress\ in\ given\ location\ for\ a\ given\ line\ tension\ (MPa)$

where,

$$\sigma_{nom} = \frac{T}{A_{link}} \tag{61}$$

and $\sigma_{max.location}$ is found with FEA.

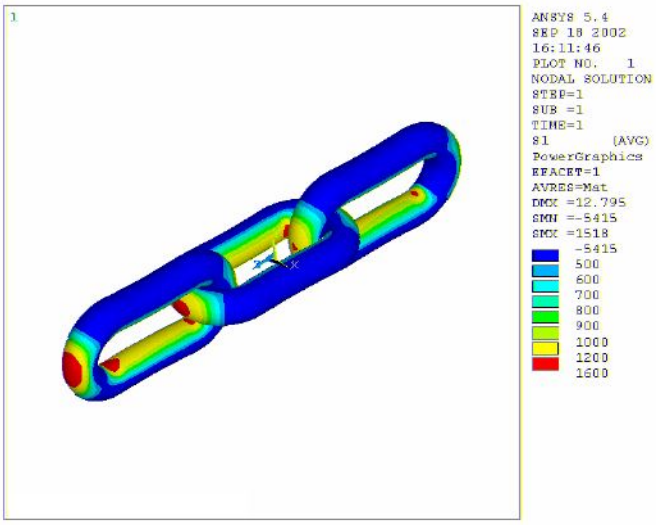

Figure 56: Stress plot for a straight chain loaded with 60% MBL [29]. Analysis performed in ANSYS

The paper runs FEA on a straight chain under tension and a chain placed in a fairlead with the same line tension. By inputing the FEA stress results into equation (60), SCFs for a straight chain and chain in fairlead is calculated for bend, crown and straight section. By dividing the highest SCF value quantified from chain in fairlead FEA with the highest SCF from straight chain FEA, we obtain a final SCF that accounts for chain/fairlead geometry:

$$SCF_{max.fairlead} = \frac{SCF_{fairlead.max}}{SCF_{straight.max}} \tag{62}$$

The most critical SCF calculated with equation (62) is the SCF used as input into equation (45). This approach for defining SCFs will be used for all the following calculations of SCFs.

Straight Chain Model: Bend Section Location

% CBL	6.2%	10.0%	30.0%	45.0%	60.0%
ABAQUS medium refinement	133.3	216.2	646.3	967.5	1287.1
SCF	3.73	3.73	3.71	3.71	3.70
ABAQUS higher refinement	133.5	216.6	647.3	968.6	1288.7
SCF	3.74	3.73	3.72	3.71	3.70
PUSNES Pro/Engineer	130.0				
SCF	3.64				
CosmosWorks	134.8				
SCF	3.77				
NEL ANSYS		216.9	650.6	975.9	1301.2
SCF		3.74	3.74	3.74	3.74

Table 9: SCFs for straight chain with varying line tension. Using different simulation packages and mesh elements and sizes [29]

Vargas, Hsu and Lee (2004) [29] tested the chain configurations with different line tensions and concluded that line tension (up to 60% MBL) has minimal to no significant effect on SCFs for both straight chain and chain in fairlead and that lower line tensions lead to the highest SCFs. For more details and SCF tables, see Appendix D.

Vargas, Hsu and Lee (2004) [29] recommend a small $SCF_{max.fairlead} = 1.15$ compared to DNV's 2.50, but warns that this result is only applicable for the specific chain and fairlead used in the study. The $SCF_{max.fairlead} = 1.15$ will still be used as one of SCFs in later fatigue assessments. Even though the fairlead/chain contact do not resemble the chain/stern roller contact for an AH process.

8.4.2 Structural Analysis of 84 mm R5 Stud Chain Over Stern Roller and Winch Drum by Vicinay Marine

In 2019, Vicinay Marine was tasked to run FEA analysis on studded, 84mm, R5 grade mooring chain after Equinor had experienced breakage in two chains during retrieval of the mooring chain with an AH vessel. The chain section that broke had been in contact with the AH vessels stern roller and winch drum and deformation from the contact was observed. Vicinay Marine ran analysis on a straight chain, over stern roller and winch drum. All scenarios was run with loads of 100, 200, 300, 400 and 500 tons.

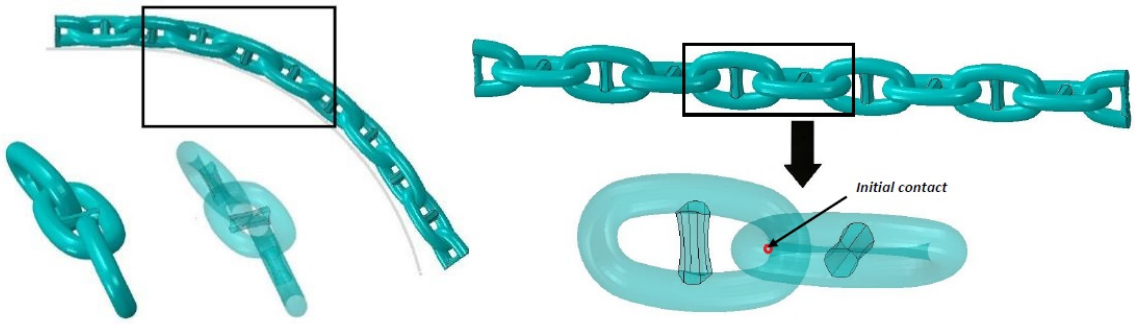

Figure 57: Display of relevant scenarios checked by Vicinay Marine [23]

We can derive SCF_{max} for studded, 84mm, R5 grade mooring chain over by using the approach described in chapter 8.4.1.

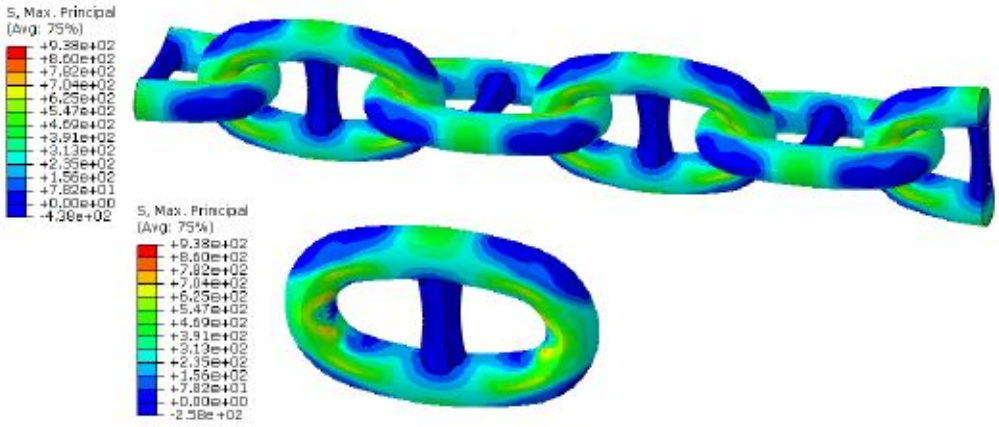

Figure 58: Visualization of stress for straight chain loaded with 100 tons [23]

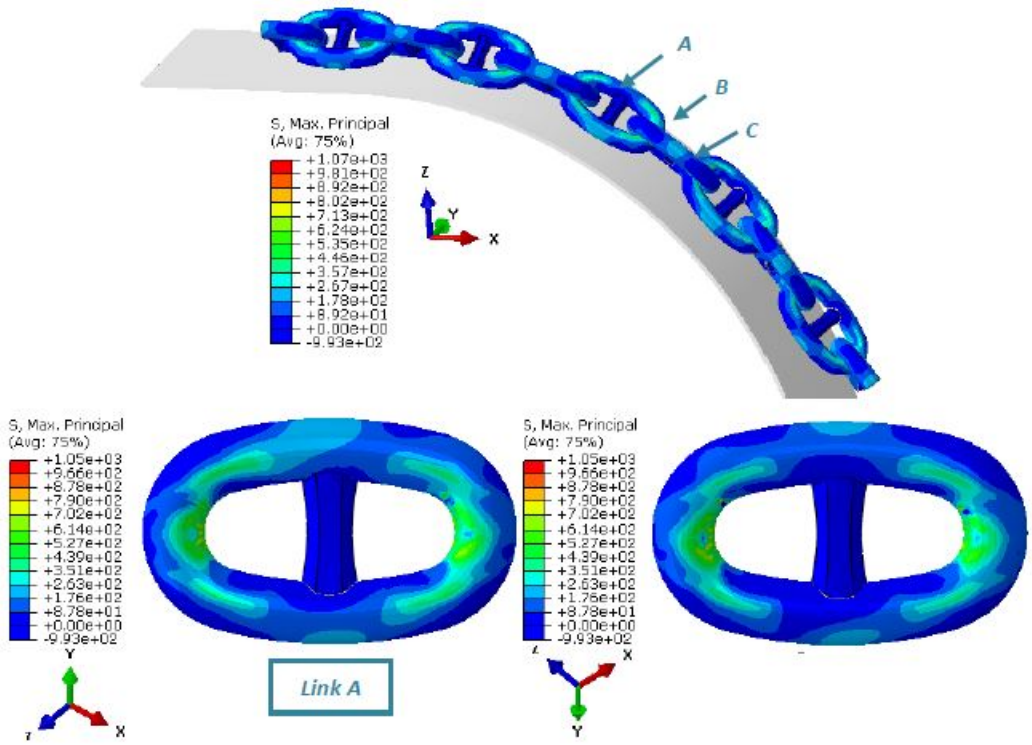

Figure 59: Visualization of stress for chain over stern roller loaded with 100 tons [23]

The rapport is confidential and does not provide any hard values, only stress visualization with colour chart values. Access to more detailed data from the analysis was not obtained, so stress values had to be read from figures like figure 58 and 59. This results in a loss of accuracy as the colour chart takes relatively large stress steps between colours and pinpointing the exact location of stress values proved challenging.

Comparing the stress distributions in figure 58 and 56 we also see that the stud has a big impact. In Vargas, Hsu and Lee (2004) [29] the highest stress was found in the crown. In Vicinay Marine's analyses (2019) the inner bend is the location for the highest stress. As the stud relives the crown and creates higher stresses at the bend and on the mid part of the straight section. This is important to take into account when assessing the fatigue damage results calculated with the SCF_{max} from the Vicinay Marine rapport.

STRAIGHT PULL SCF at givenchain link location				
Load [tons]	Crown	Bend	Straight	Straight no pin area
100.00	1.69	4.99	4.00	2.00
200.00	1.77	4.42	2.65	1.33
300.00	1.77	3.03	2.27	1.01
400.00	1.77	2.36	1.97	0.98
500.00	1.93	2.10	1.75	0.96

Table 10: Straight chain SCFs for given location and load. Performed by reading stress values from visual stress plots in Vicinay Marine (2019) [23]

Chain over stern roller SCF at given chain link location				
Load [tons]	Crown	Bend	Straight	Straight no pin area
100.00	2.78	6.33	3.72	1.99
200.00	2.69	5.59	1.86	1.34
300.00	2.33	3.99	1.93	1.23
400.00	2.49	2.99	1.75	1.15
500.00	2.33	2.55	1.60	1.27

Table 11: Chain over stern roller SCFs for given location and load. Performed by reading stress values from visual stress plots in Vicinay Marine (2019) [23]

Resulting SCF:				
Load [tons]	Crown	Bend	Straight	Straight no pin area
100.00	1.64	1.27	0.93	0.99
200.00	1.52	1.26	0.70	1.01
300.00	1.32	1.32	0.85	1.22
400.00	1.41	1.27	0.89	1.17
500.00	1.21	1.22	0.91	1.32
SCF.max.vicinay	1.27			

Table 12: Local $SCF_{location.max}$ for given location and $SCF_{max.vicinay}$ to account for geometry. Performed by reading stress values from visual stress plots in Vicinay Marine (2019) [23]

As you can see in table 10, 11 and 12 an area called "Straight no pin area" was added. This location was added as the stud increases the stress located on the mid upper side of the straight section. It was desirable to check if the SCF for this location could be compared with the straight section in Vargas, Hsu and Lee (2004) [29] paper. In short, the magnitues of the area specific SCFs are not comparable. But, SCFs obtained from the Vicinay Marine (2019) [23] and Vargas, Hsu and Lee (2004) [29] (see Appendix D) share the trends of relatively constant or decreasing SCFs with increasing loads. Some values deviate from the pattern, but that is to be expected when collecting stress values from coloured stress visualization plots. Comparing studded chain to studless chain is not optimal, as the stress distribution in the link will be different and is likely the reason largest magnitude SCFs for chain over stern roller occur at the bend location instead of the crown in the Vicinay study.

Using equation (62) we get $SCF_{max.vicinay} = 1.27$. This is a value used in further fatigue damage assessment.

9 FEA analysis

Fatigue damage on mooring chain is quantified in a MATLAB script, based theory introduced earlier in this thesis. In thesis , we only use FEA to quantify SCFs that account for the geometry of a chain over a stern roller (see chapter 8.4.1). No fatigue analysis in FEA software was performed.

9.1 Geometry of chain over stern

For this paper we recreate a 76mm chain with R4 grade steel laying over the stern with a medium sized radius (1250 mm) [3] stern of an AH vessel performing testing of chain and anchor bedding-in. The need for an analysis of a straight chain under the same tension is also needed to quantify the SCF_{max} described in chapter 8.4.1.

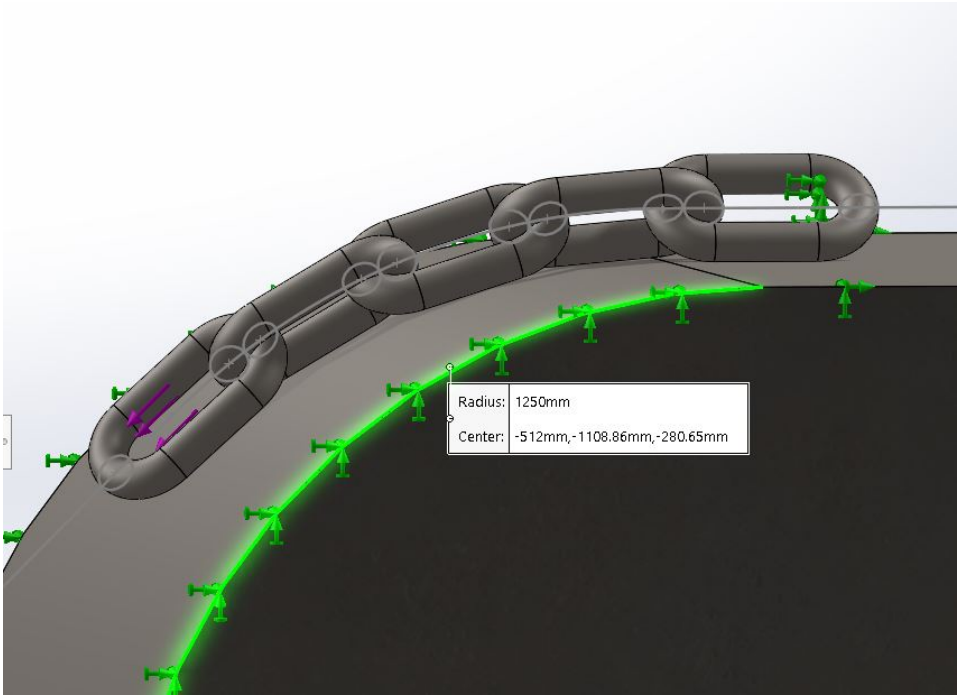

Figure 60: Display of chain over stern roller in SolidWorks.

9.2 Software

It was originally intended that Abaqus was to be used for simulation and modelling. As of 12 march 2020, NTNU Tyholt was closed as a measurement to halt the COVID-19 pandemic. With NTNU Tyholt closed, the plan to use in-house expertise in Abaqus proved to be difficult and time consuming. After consulting the distributor of CAE software SolidWorks in Norway (PLM group) and the SW forums, indications were that the analysis should be doable in the SW software. As the author had some previous experiences with the software, SW was initially chosen instead of Abaqus.

9.3 SolidWorks

Solidworks provides CAD and FEA integrated in the same interface. It is known for being user-friendly, one of the better professional CAD tools for making parts and assemblies. SW provides the possibility to create a non-linear dynamic analysis with an implicit solver. This problem has a lot of contact surfaces, moving parts and a possibility of stresses exceeding material yield. Running static problems in SW is considered a fast and accurate alternative. SW is in general not considered the best alternative for non-linear dynamic simulations (especially not for more complex models). As mentioned earlier, reassurance from PLM-group and SW forums that this problem was doable in SW simulations still made it the initial software of choice. The procedures in the following chapters on defining the model and simulation in SW was applied to both the straight chain and chain over stern analysis.

9.3.1 Implicit solver

An implicit solver works in the artificial time space 0-1, where the number of time increments is initially user defined. It is an iterative technique looking for global equilibrium of the system. If the system can't find equilibrium at the given time step, the solver reduces the time step and tries again. This will be repeated until equilibrium is found or the a user defined minimum time step is reached and the analysis is aborted [40].

Implicit solvers are known to be the best alternative for scenarios that occur over multiple seconds in real time. But important to note is that if a model contain multiple parts, contact surfaces and few constraint limiting the parts movement, equilibrium can be hard to obtain. When equilibrium is hard to calculate, iterations become many and time steps very small. This often leads to long simulation times or the analysis not converging [24].

9.3.2 Material model

Property	Value	Units
Elastic Modulus	206999.9944	N/mm^2
Poisson's Ratio	0.3000000119	N/A
Tensile Strength	850	N/mm^2
Yield Strength	580	N/mm^2
Tangent Modulus	20700.00026	N/mm^2
Thermal Expansion Coefficient		/K
Mass Density	7850	kg/m^3
Hardening Factor		N/A

Figure 61: Material properties in SW

The material properties in table 61 are collected from the Rämnas product catalogue for chains [2]. Some of the values have negligible errors due to numerical computations. Attempts were done to get the complete stress/strain curve from Rämnas and other chain manufacturers, but were unsuccessful. Instead the tangent modulus shown in table 61 was introduced. The tangent modulus kicks in with 10% of the linear elastic regime slope, when yield magnitude is reached. This is not an optimal solution, but sufficient for this thesis.

9.3.3 Contacts

SolidWorks offers four types of contact. No penetration, bonded, allow penetration and shrink fit. As we don't expect to see any penetration, there is no shrink fits present and the bonded condition "glues" contact surfaces together, no penetration was the only contact definition suitable for this analysis. No penetration with surface-to-surface condition was applied to all sections that has the possibility to come in contact with each other. Efforts were made to make the stern roller into a rigid body shell, but was not successful. Therefor mesh and contacts for the stern roller was also defined.

9.3.4 Mesh

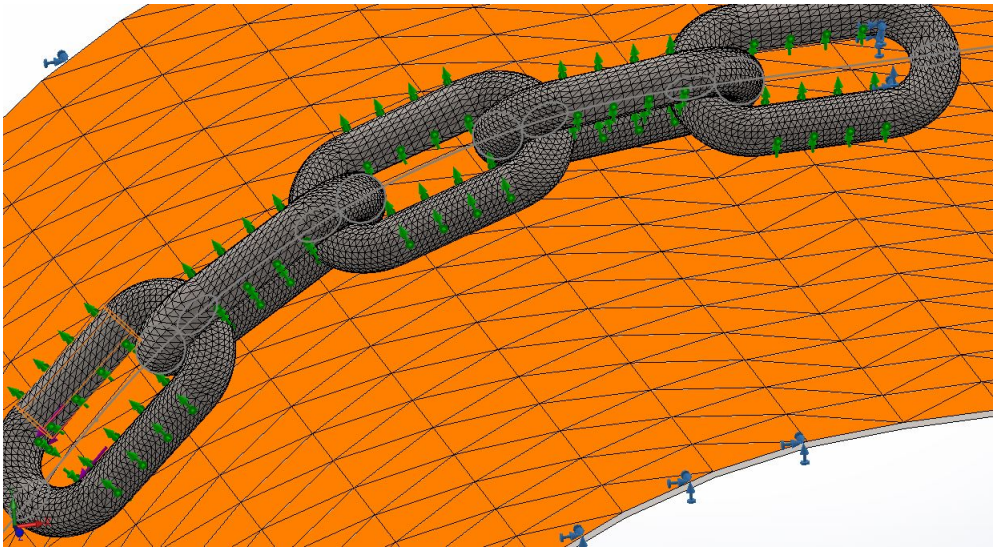

Figure 62: Display of final chain mesh in SW

As SW is not the most suited program to run non-linear dynamic analysis with many contact surfaces, the finest mesh possible was selected for contact surfaces in consultation with Tom Rune Jensen (CSS, Skien) [16]. The elements are tetrahedral elements as this the only elements SW only offers. Multiple simulations were run for both straight chain and chain over stern roller with coarser meshes, but the simulations failed.

9.3.5 Fixtures and loading

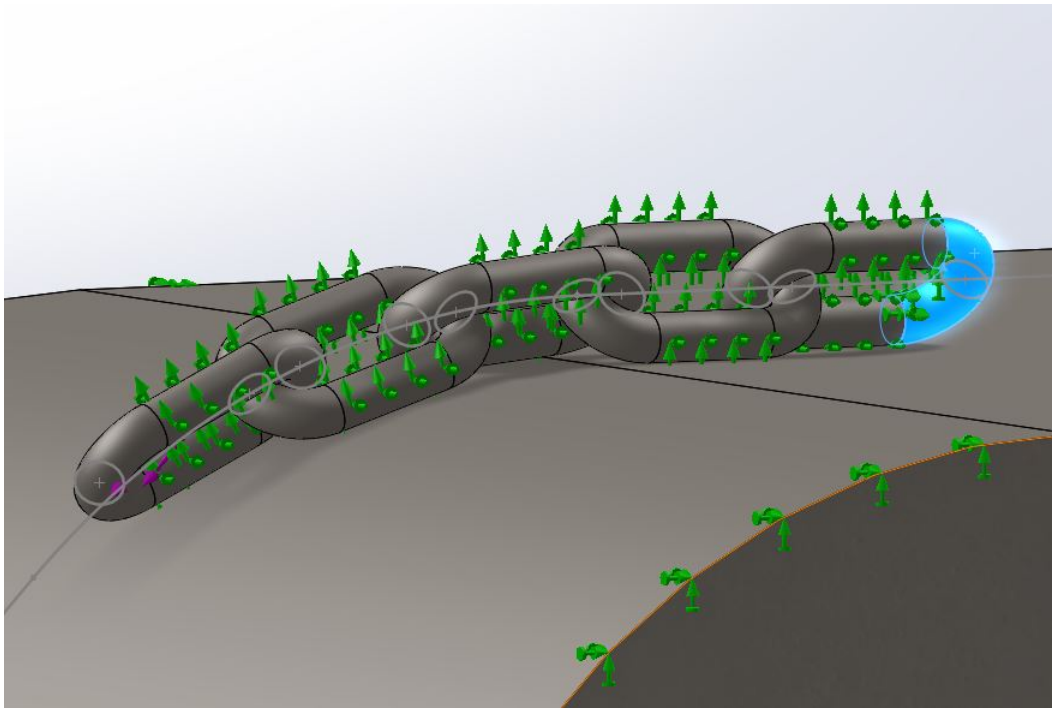

Figure 63: Display of fixtures in SW. Illustrated with green arrows.

To create stability in the system fixtures have to be defined. The blue highlighted area in figure 63 is fixed in all degrees of freedom. This will result in inaccurate stress representation in the link, but as the interesting results will be in the three middle links over the curved geometry, we can neglect stress plots for this link 63.

Fixtures of the on the cylindrical parts of the chain link can also be spotted in figure 63. These fixtures were added after simulations failed in their early stages. As the chain links don't have any initial contact, a lot of rapid events are to be expected as one chain link starts to connect with the other. When the three middle chain links are able to move in all direction, the SW solver has problems solving the chain links positioning as more loading/motion is added. This again prevents the solver from creating an initial stiffness in the system, as the final position of the chain when interlink contact happens, struggle to converge [16]. To help the SW solver , cylindrical sections of the chain links were fixed in their respective radial and axial direction for the first percent of the simulation steps to give the system more predicable movement and help create initial stiffness in the system. This will lead to some inaccurate stresses for the first percent of the simulation, but as only one percent of the force is added while the fixtures are operational, the effects are negligible for the final results.

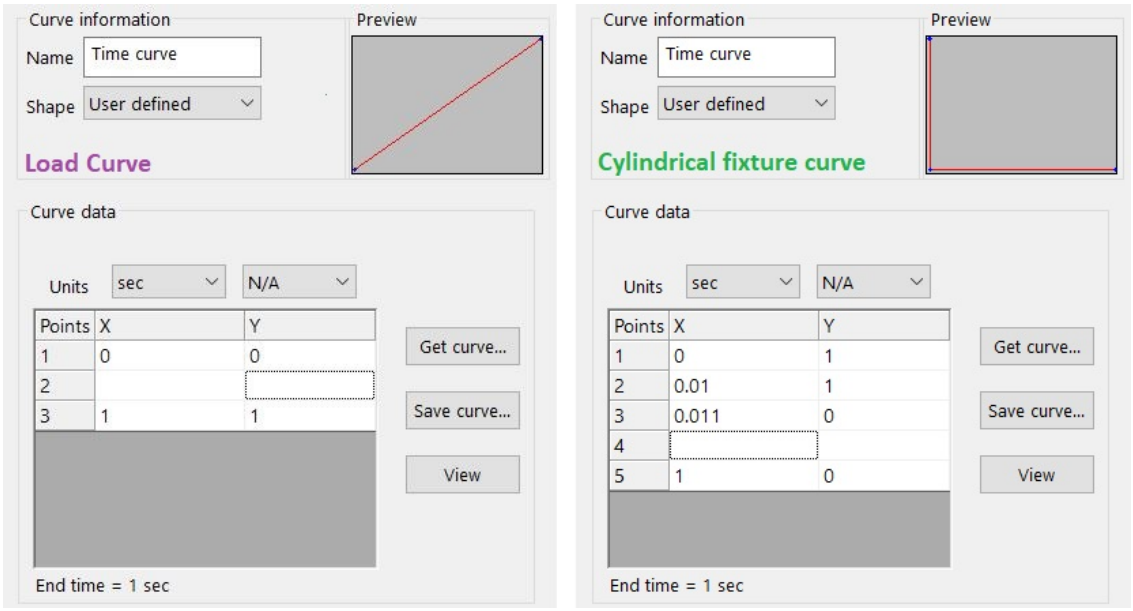

Figure 64: Activity curve for load and cylindrical fixtures in SW.

The magnitude of the load applied was 10% of the chains MBL and was applied linearly (see figure 64). Lower loads and a smooth application makes it easier for the solver.

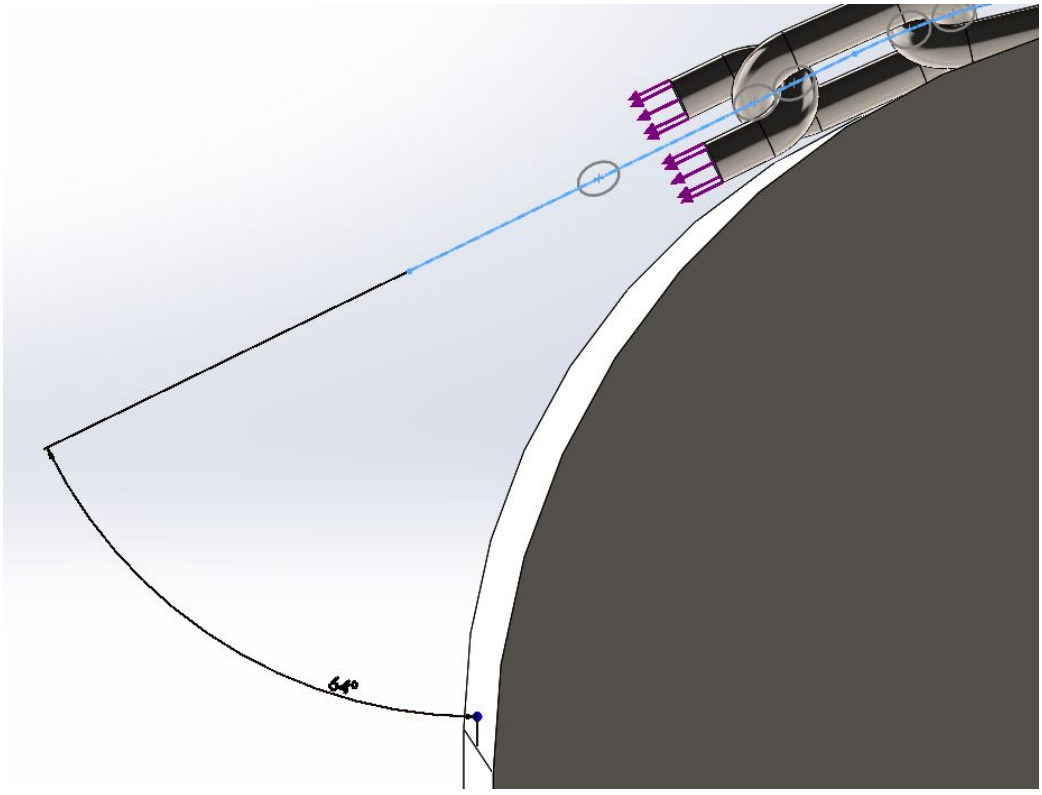

Figure 65: Loading layout in SW.

The angle shown in figure 65 is the resultant angle of a tug pull equal to 52.6% of chains MBL and a water depth of 350 m (base case). The angle for a 10% tug pull is in reality not the same as the one chosen for this analysis. But as Vargas, Hsu and Lee (2004) [29] suggest that SCFs don't change significantly with increased loads for a set geometry, the use of a chain entry angle of $\varphi = 26^{\cdot}$ and a load of 10% MBL is therefore considered an acceptable assumption.

9.3.6 Results in SolidWorks

A total of three months were spent running analyses and tweaking parameters in SW to try and get some sensible results.

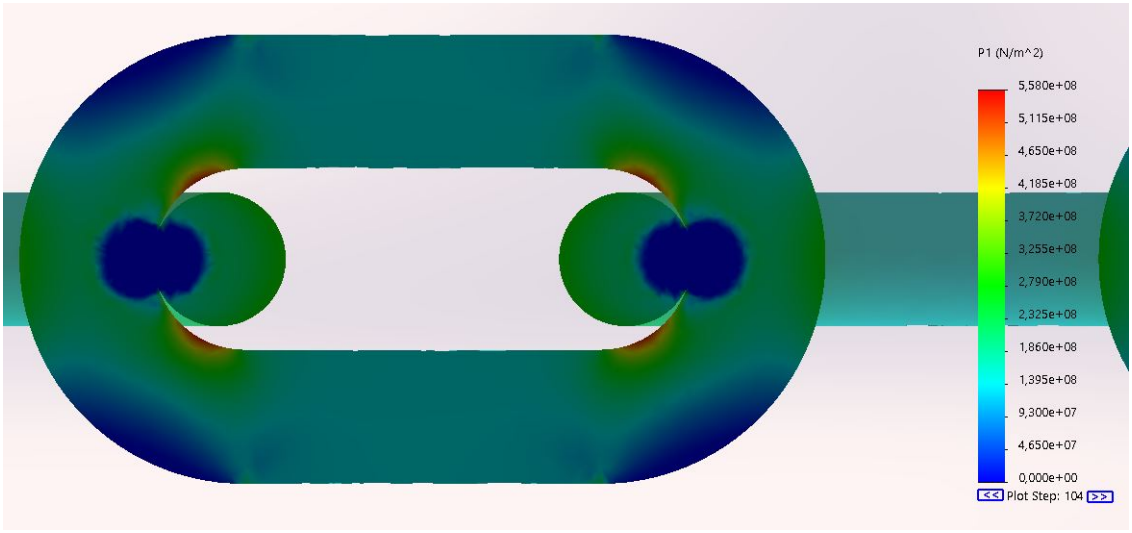

Figure 66: Principal stress distribution for straight chain in SW.

In general, it took an analysis 4 days to complete or crash in SW. Figure shows 66 is just one of many results for a straight chain. All analyses completed shared pretty much the same stress distributions and SCFs. Comparing the stress distribution in figure 66 with the one in figure 28 and the results in Vargas, Hsu and Lee (2004) [29], the resemblance was unfortunately not strikingly similar. The SW results display peak stress in the inner bend of the link, much higher than other than any other area of the link.

10% MBL, straight	Crown	Bend	Straight
SW	4.92	8.50	2.12
Study	4.31	3.73	3.31

Table 13: SCF comparison for straight chain. SW results vs. Vargas, Hsu and Lee (2004) [29].

As the SCFs extracted from SW is not even close to comparable with the ones from Vargas, Hsu and Lee (2004) [29], which makes the validity of the SW results questionable. None of the SCFs collected from SW analyses came closer than the values in table 13. Attempts to run the analyses for the chain over stern roller was conducted even though straight chain simulations produced some worrying results. In short, a single analysis would run for weeks and struggle to converge or fail. Tweaking and professional guidance [16] did seemingly not help. After two months of running simulations on the chain over stern roller geometry without results, it was decided to end further work in SW and start over in Abaqus [19].

9.4 Abaqus

Abaqus is known as one of the best professional FEA software on the marked. Abaqus give users the ability to fine tune analyses by producing unending amounts of options when defining materials, contacts, loads, etc. This is of course optimal for experienced pilots in Abaqus, but can make identification of a faulty setup hard to identify. The most relevant upsides of Abaqus for the analyses in this thesis, is more optimal tools for solving problems with many contact surfaces and rapid events.

9.4.1 Geometry in Abaqus

The straight chain model was completely remade in Abaqus CAD. Importing assemblies to Abaqus from other CAD software is a common procedure as setting up more complex assemblies in Abaqus can be challenging and unnecessarily time consuming. The chain over stern roller assembly made in SW was therefor saved as a STEP-file and imported to Abaqus. The only change made to the model was swapping out the solid stern roller geometry with a analytic rigid surface.

9.4.2 Explicit Solver

Unlike an implicit solver, explicit solver do not require convergence at each step [24] and the analysis time set represents real time. The solver assumes global equilibrium exist, hence there is no iterating for equilibrium and the solver can skip straight to calculating local finite element variables. As there is no convergence criteria to fulfill, the solver will always provide an solution as long as the model and analysis setup is correctly defined [40].

Abaqus itself determine a stable time increment (step size). A step small enough to assume that the global equilibrium simply exists [27]. This step size is naturally very small and hence one typically want explicit problems to unfold in time spaces less than a second (real time) as computational times become increasingly large. The maximal time increment is determined by the time an elastic wave uses to travel through the models smallest finite element, which again is derived from the materials Young modulus, Poisson ratio, material density and element size [40].

9.4.3 Simulation time

A problem that can typically occur for an analysis like the one in this paper is that a lot of dynamics can be introduced if the total time space of the analysis becomes too small. Applying a large load over short period of time to a model with a lot of parts with no initial contact will result in the links colliding and introducing inertia forces not contributing to stress development in the link.

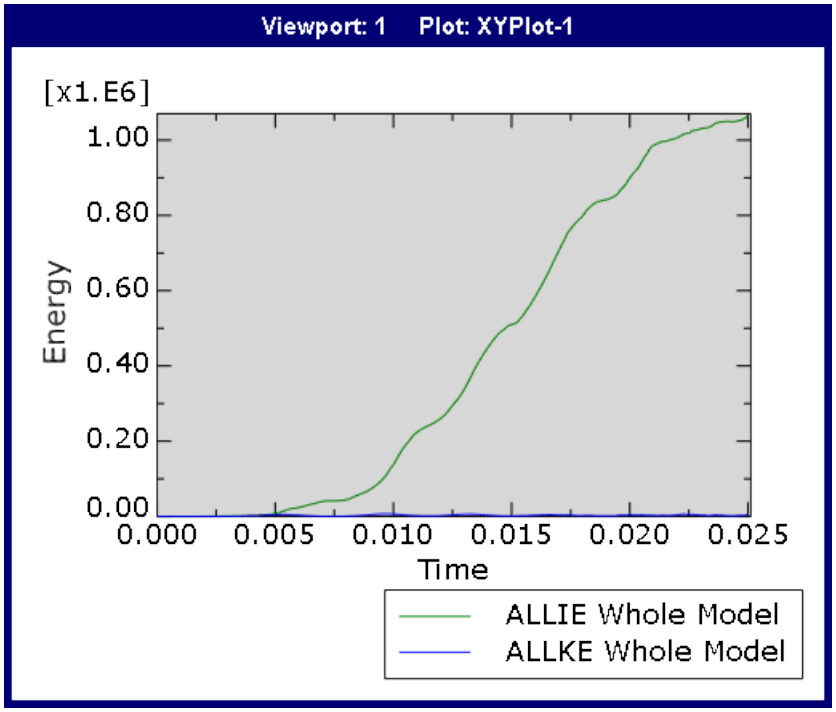

Figure 67: Kinetic energy (blue) vs. internal energy (green) in straight chain analysis (t = 0.025).

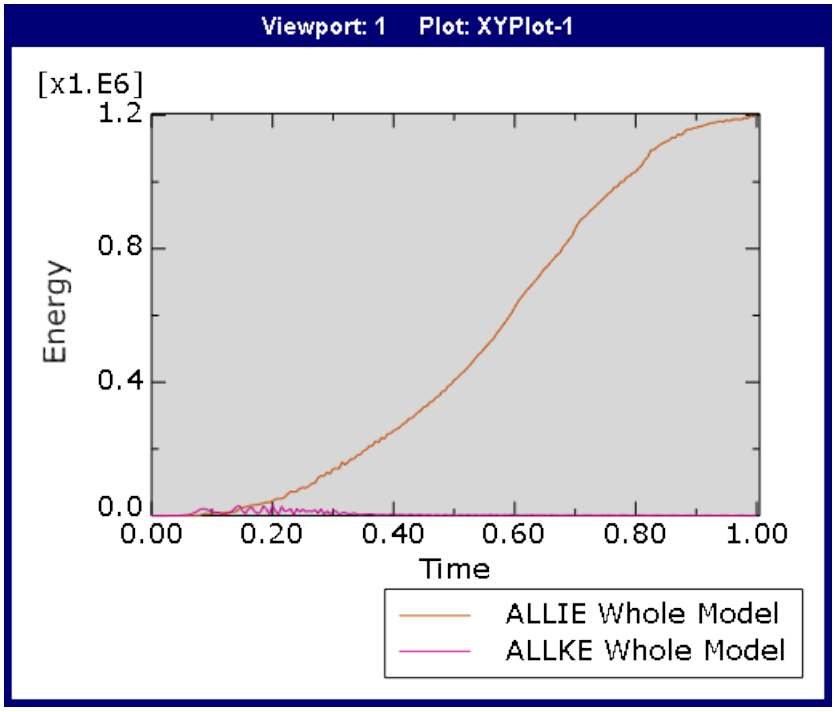

Figure 68: Kinetic energy (pink) vs. internal energy (orange) in chain over stern roller analysis (t = 1).

It is desirable for the problem to be as close to static as possible when the simulation ends. For the straight chain, links are initially close to their final position, hence there is little movement in the system is to be expected and simulation time (t) can be set to a much lower value than for the chain over the stern roller analysis. In figure 67 we can see the kinetic energy is low throughout the analysis, indicating little movement. The internal energy curve is wavy as the links collide and make the system vibrate when the load is applied in such a short time period. Figure 68 have a much smoother internal energy curve, as the load is applied over a time period forty times larger than for the straight chain. But the curve for the kinetic energy in figure 68 is much more spiky. This is because chain over stern rollers (close to) static geometry do not resemble the initial geometry to the same extent as the straight chain. Therefore more motions will present at the earlier stages of the simulation.

Both figure 67 and 68 prove that the simulations times are of adequate length as the kinetic energy is negligible and the internal energy of the model flattens out at the end of the simulations. One could argue that simulation input time could be increased for the straight chain simulation to smoothen the internal energy curve and could be reduced for the chain over stern roller simulation to save time. Analysis time of 0.025 sec for straight chain and 1 sec for chain over stern roller were deemed sufficient [15].

9.4.4 Material Model

In model and analysis verification, analyses were performed with only elastic modulus and Poisson ratio defined (same values as in SW chapter 9.3.2). None of the analyses showed stress over yield magnitude, hence there was no need to define the material further.

9.4.5 Contacts

Abaqus provides powerful contact definition called general contact that scans the model at each step, determining which surfaces that will come in contact [34]. This excludes the need to define contacts for specific surfaces.

9.4.6 Mesh

The mesh was initially made to match the mesh element/chain link ratio in Vargas, Hsu and Lee (2004) [29], using C3D8R cube elements with reduced integration. Edge seeds with a size of 4mm were later applied, giving a finer mesh than in Vargas, Hsu and Lee (2004) [29].

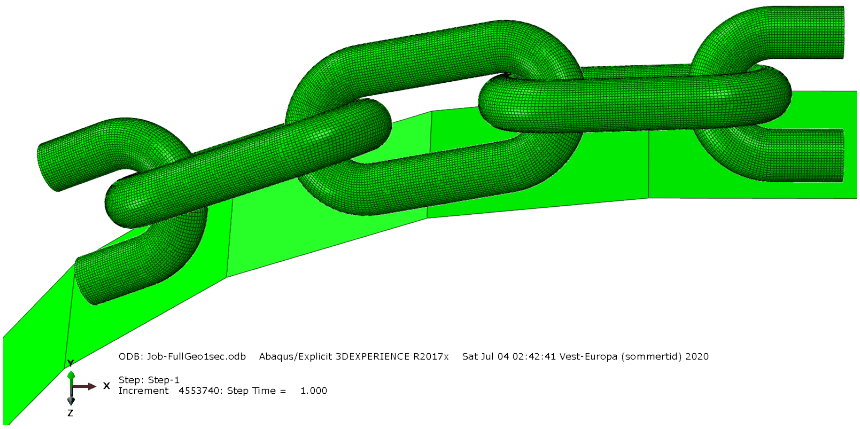

Figure 69: Chain link over stern roller with mesh. Edge seeds = 4 mm

The stern roller geometry was modeled as an analytic rigid surface and do not require meshing.

9.4.7 Fixtures and loads

As spotted in Figure 69, two half links were used in Abaqus at both ends of the chain. Kinematic coupling constraints were defined for both half links.

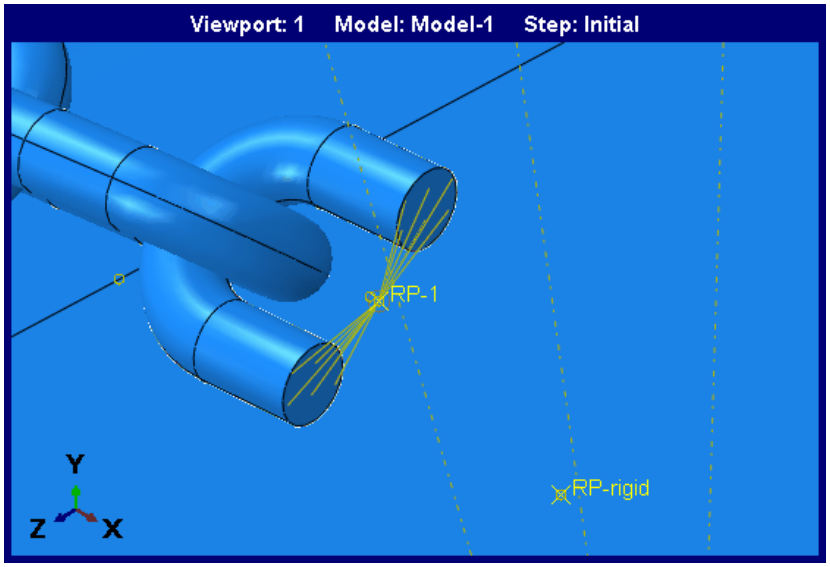

Figure 70: Display of kinematic coupling with reference point at top half link

The kinematic coupling constraint secures the all the nodes of the links end surfaces to a single node's (reference point) rigid body motion [28]. For the top end link a displacement boundary condition was set its kinematic coupling's reference point, locked in all directions. For the end link at the bottom, the same procedure was applied, but the displacement boundary condition was replaced with a load of 600 kN with an entry angle of $\varphi = 26°$.

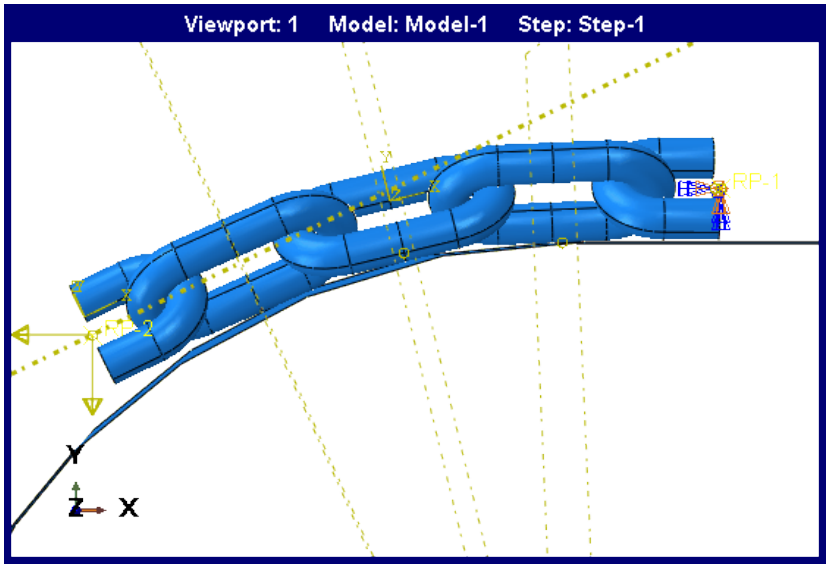

Figure 71: Display of load and fixture set in kinematic coupling constraints

9.4.8 Results for straight chain analysis in Abaqus

The end links were not considered when evaluating stress values as the half link geometry, fixture and load applications lead to misleading results. Element stress at crown, bend and straight sections at the three middle link surfaces were checked.

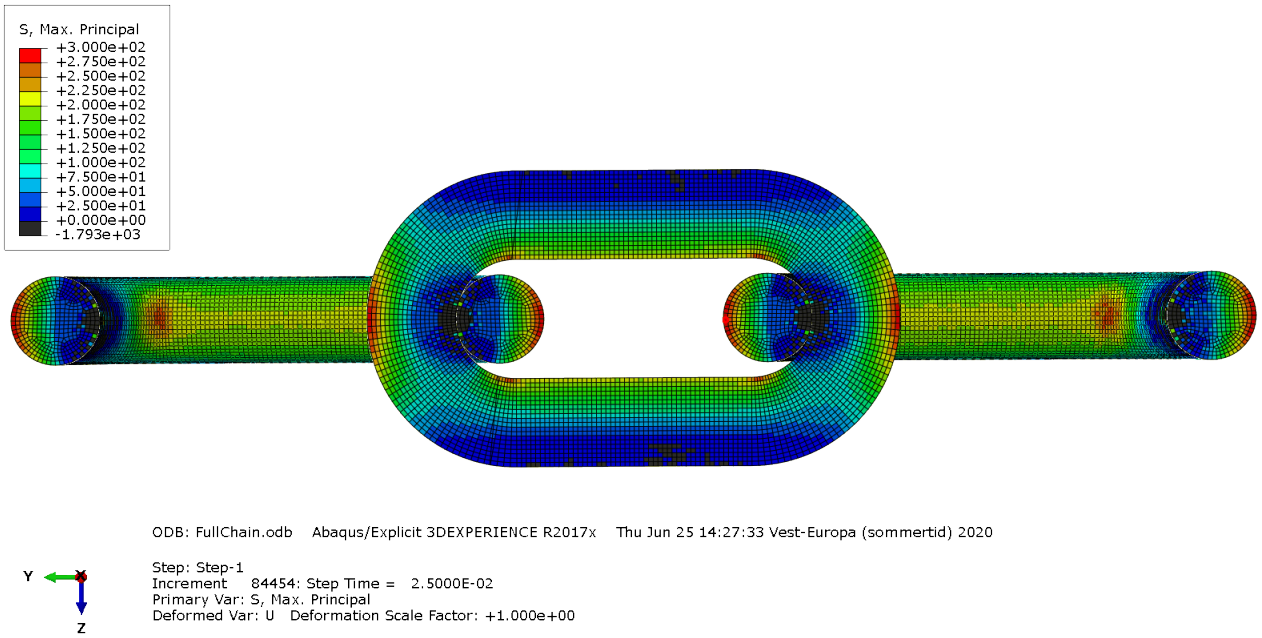

Figure 72: Stress plot for straight chain in Abaqus

Straight chain highest stresses:				SCF:
σ.crown [Mpa]	284.5			4.30
σ.bend [Mpa]	260			3.93
σ.straight [Mpa]	205			3.10

Table 14: Highest stress values at given location and resulting SCF for straight chain in Abaqus.

As expected the, the element stress at the crown, bend and straight sections in the different links, were all of the same magnitude, with only a few MPa difference. Element stresses at crown, bend and straight section was collected for all links, but in calculations of the SCFs, only the highest value at each respective location was used. Comparing SCFs in table 15 with table 24 shows striking similarities, backing the validity of the results for the straight chain analysis.

9.4.9 Results for chain over stern roller analysis in Abaqus

For the same reasons as in chapter 9.4.8 end links were not considered when evaluating stress values. Element stress at crown, bend and straight sections at the three middle link surfaces were checked.

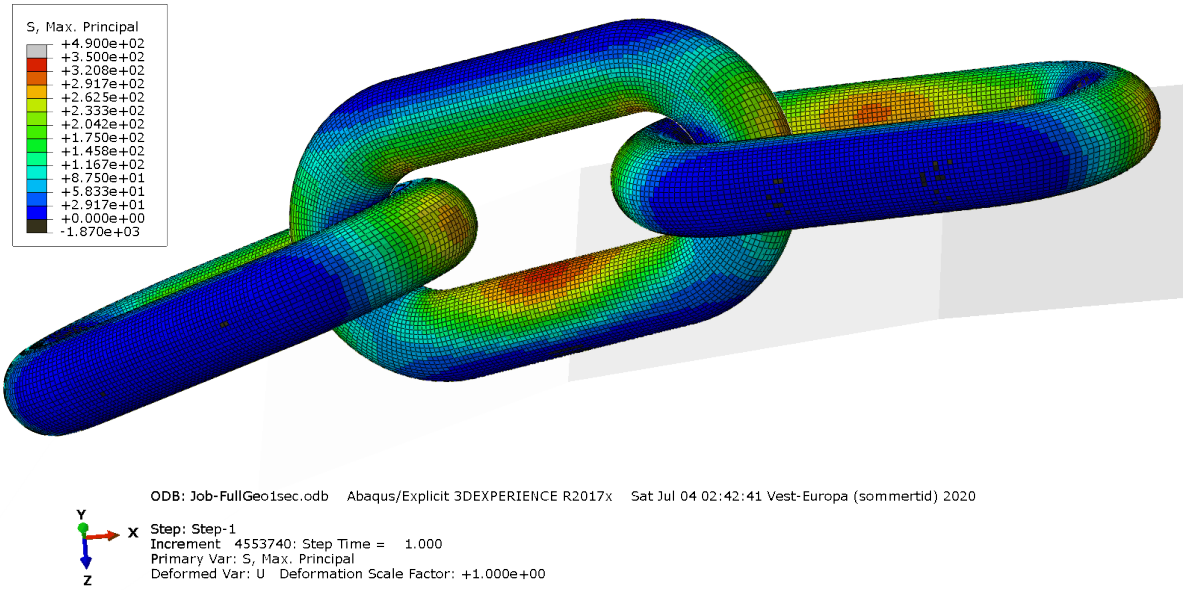

Figure 73: Stress plot for chain over stern roller in Abaqus

The stress distribution shifts quite drastically when the stern roller is introduced into the analysis. The most visual difference in figure 73 compared with figure 72 is the high stress concentrations occurring at the inner straight sections of the links when OPB from stern roller/chain link contact is introduced.

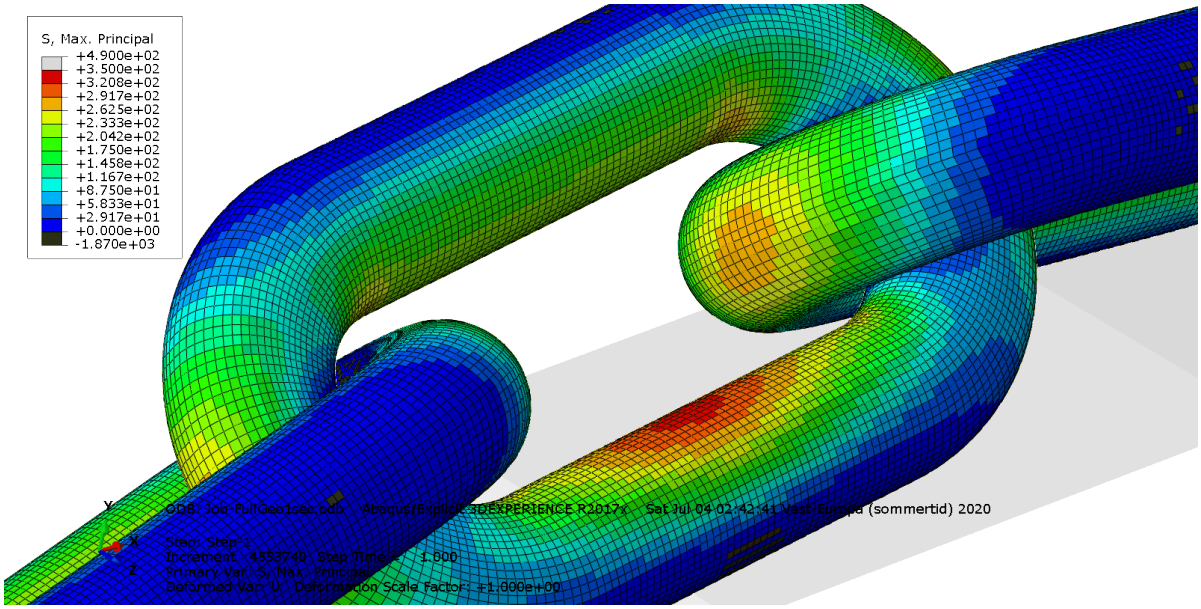

Figure 74: Close up of middle link. Stress plot of chain over stern roller in Abaqus

Highest element stress was located at the straight section of the middle link (329 MPa). The highest bend stress was also found at the middle link. It is located at upper bend to the right in Figure 74 (286 MPa).

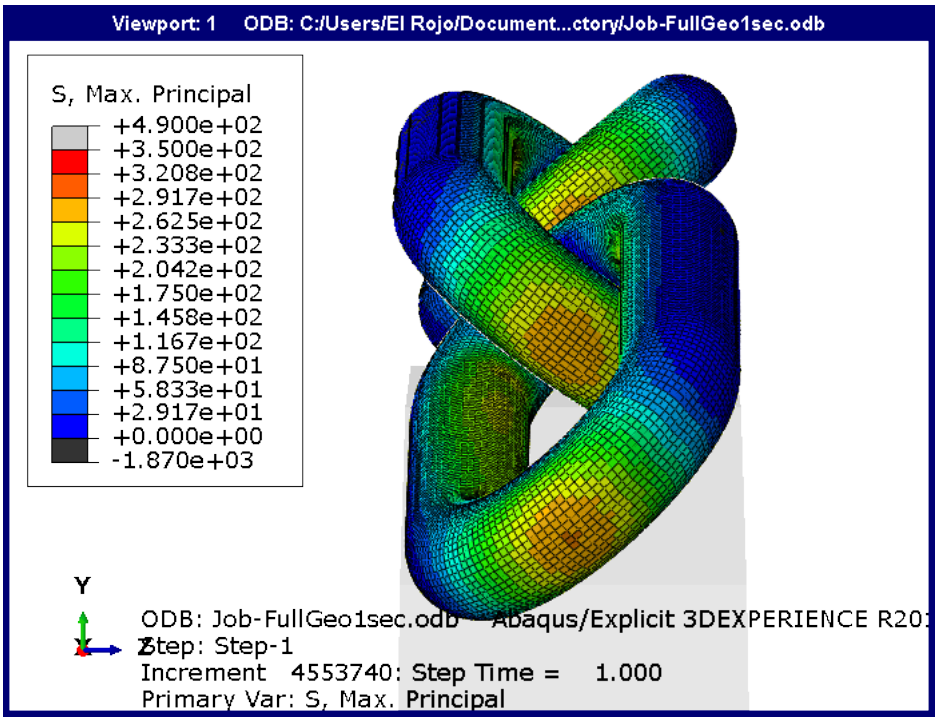

Figure 75: Highest crown stress location for chain over stern roller in Abaqus.

Stress at the crown is not as prominent for the chain over stern roller compared to the straight chain analysis. Highest crown stress is located at the bottom link (293 MPa). The bottom link is not in contact with stern roller.

Chain over stern roller highest stresses:			SCF:
σ.crown [Mpa]	293		4.43
σ.bend [Mpa]	286		4.32
σ.straight [Mpa]	329		4.97

Table 15: Highest stress values at given location and resulting SCF for chain over stern roller in Abaqus.

Location specific SCF increase:	
SCF.crown [Mpa]	1.03
SCF.bend [Mpa]	1.10
SCF.stright [Mpa]	1.60

Table 16: Change in highest location specific SCFs for chain over geometry vs straight chain SCFs.

Table 16 tells us there is small changes in SCFs for the crown and bend caused by the chain/stern roller geometry. Instead the highest stress now occurs at the straight section, where we see a 60% stress increase. This indicate that the critical areas (crown and bend) for normal operation is not much affected by AH handling operations. The Abaqus analyses in this thesis was run with only 10% of the chains MBL. Considering that anchor bedding-in testing is done with 52.6% MBL (SF = 1.9), we will almost certainly exceed the material yield, experience permanent deformations and residual stresses in the links. A compromised link geometry leads to unknown stress distributions when the chain is under normal operation. A more thorough study on the extent and locations of locally damaged/fatigued material from AH operations could help in more accurately quantify fatigue damage. As residual stresses can promote and slow down crack growth, locating and quantifying these as well could be helpful in portraying the fatigue damage from AH operations. Unfortunately, this is outside the scope of this thesis, but it could potentially have a significant impact on fatigue life and should therefore be investigated further.

SCF to account for the stern roller geometry can now be quantified:

$$SCF_{max.FEA} = \frac{SCF_{max.Stern.roller}}{SCF_{max.straight.chain}} = \frac{4.97}{4.3} = 1.156 \tag{63}$$

$SCF_{max.FEA} = SCF\ to\ account\ for\ chain\ over\ stern\ roller\ geometry$
$SCF_{MAXstern.roller} = Highest\ SCF\ from\ chain\ over\ stern\ roller\ analysis$
$SCF_{MAXstraight.chain} = Highest\ SCF\ from\ straight\ chain\ analysis$

$SCF_{max.FEA}$ from Equation (63) is slightly larger than $SCF_{max} = 1.15$ for a chain in fairlead quantified in Vargas, Hsu and Lee (2004) [29]. Even though the SCFs are of similar magnitude, both $SCF_{max.FEA} = 1.156$ and $SCF_{max.fairlead} = 1.15$ will be used in fatigue assessment to get a better picture of SCF impact on fatigue damage.

It is important to note that this $SCF_{max.FEA}$ just accounts for this specific chain over stern roller configuration. In reality, there is no blueprint on how the chain/stern roller layout will end up during AH operations, as each operation differ. It is likely that there is chain/stern roller layouts resulting in higher $SCF_{max.FEA}$ values and different stress distributions in chain links. Defining geometries and running analyses in Abaqus is time consuming, the work of identifying a mean and a worst case value for $SCF_{max.FEA}$ is not included in this thesis, but is recommended as further work.

10 Results and discussion

To quantify the effect on fatigue life of different parameters, a base case is defined for comparison. A good insight can be developed by varying parameters one at a time and comparing it to the defined base case. For this thesis, the base case is set as:

$Corrosion\ grade = 1\ ,\ As\ new/mild\ corrosion$
$Wave\ heading = 180°$
$T_p = 8\ (s)\ ,\ Peak\ wave\ period$
$H_s = 2\ (m)\ Significant\ wave\ height$
$h = 350\ (m)\ ,\ water\ depth$
$T_H = 52.6\%MBL\ = 3157\ (kN),\ Force\ applied\ by\ AH\ vessel$
$SCF_{max} = 1\ ,\ Stress\ concentration\ factor\ to\ account\ for\ chain/stern\ geometry\ (Straight\ pull)$
$T_i = 1800\ (s),\ Duration\ of\ anchor\ bedding - in\ testing$

This represents close to optimal parameters for a anchor bedding-in process. This study has a lot of variables, resulting 5376 different fatigue cases. So all plots are selections to prove the general trends and illustrate the bigger picture. All results and plots, MATLAB scripts and Excel documents can be obtained by contacting author.

SCF = 1

Corrosion grade = 1			**Wave heading = 180 degrees**		
Water depth = 350 m					
	Tp = 5	Tp = 8	Tp = 12	Tp = 14	
Hs = 1	5.66E-10	3.53E-09	9.61E-09	1.31E-08	
Hs = 2	3.96E-09	2.82E-08	7.69E-08	1.04E-07	Mean tension = 20% MBL
Hs = 3	1.34E-08	9.81E-08	2.59E-07	3.53E-07	
Hs = 4	3.17E-08	2.45E-07	6.15E-07	8.36E-07	
	Tp = 5	Tp = 8	Tp = 12	Tp = 14	
Hs = 1	8.75E-10	5.28E-09	3.94E-08	6.91E-08	Mean tension = 29% MBL
Hs = 2	6.18E-09	4.22E-08	3.15E-07	5.53E-07	
Hs = 3	2.09E-08	1.44E-07	1.06E-06	1.87E-06	
Hs = 4	4.95E-08	3.51E-07	2.52E-06	4.42E-06	
	Tp = 5	Tp = 8	Tp = 12	Tp = 14	
Hs = 1	2.24E-09	2.64E-08	8.54E-07	1.70E-06	
Hs = 2	1.68E-08	2.11E-07	6.83E-06	1.36E-05	Mean tension = 52,6% MBL
Hs = 3	5.66E-08	6.65E-07	2.31E-05	4.60E-05	
Hs = 4	1.34E-07	1.39E-06	5.47E-05	1.09E-04	

Table 17: Resulting fatigue damage with varying parameters. Base case in red box.

Table 17 shows clipart the fatigue damage database containing the base case results. Fatigue damage is on a scale from 0-1, where 1 represent chain failure. It is important to note that a safety factor of 5 is recommended by DNVGL-OS-E301 [8], so to conserve safe operations, failure set at a value of 0.2 in this thesis.

10.1 JONSWAP wave spectra

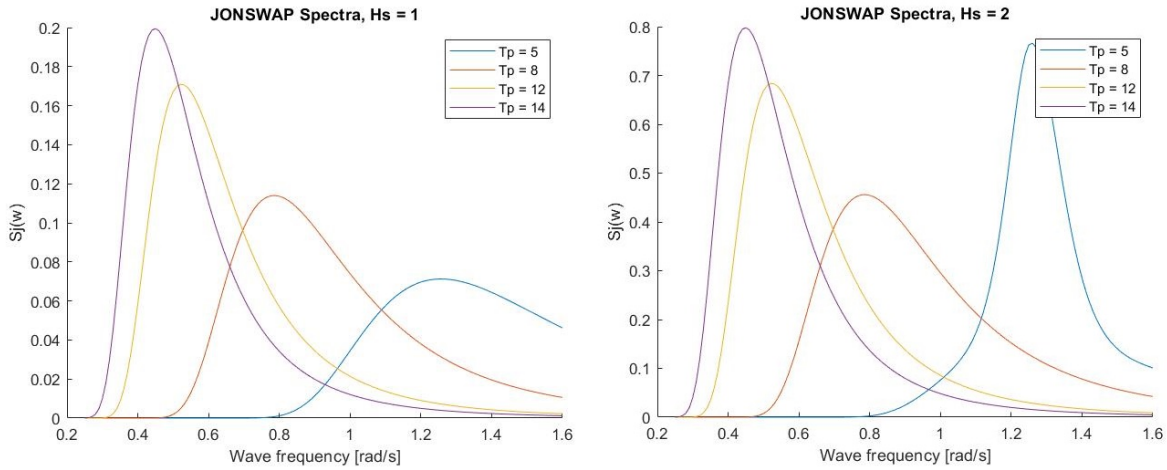

Figure 76: JONSWAP for given T_p and $H_s = 1$ & $H_s = 2$

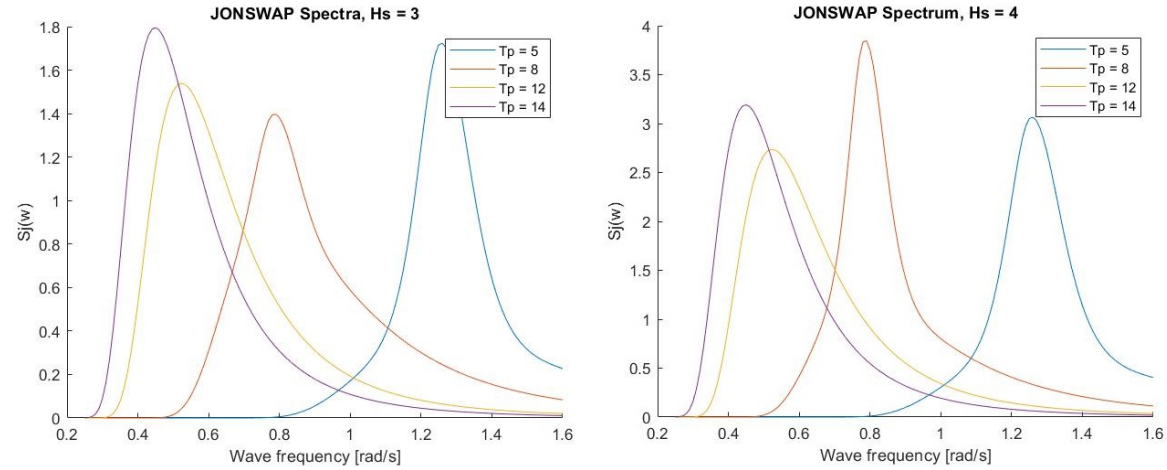

Figure 77: JONSWAP for given T_p and $H_s = 3$ & $H_s = 4$

Figure 76 and 77 display all the JONSWAP spectra used in this thesis.

10.2 Tangential motion at stern roller (ϵ)

In chapter 7.1, tangential motion at stern of AH vessel was discussed. By varying water depth (h), AH vessel pull (T_H) and wave heading, twelve RAOs for the motion ϵ can be defined.

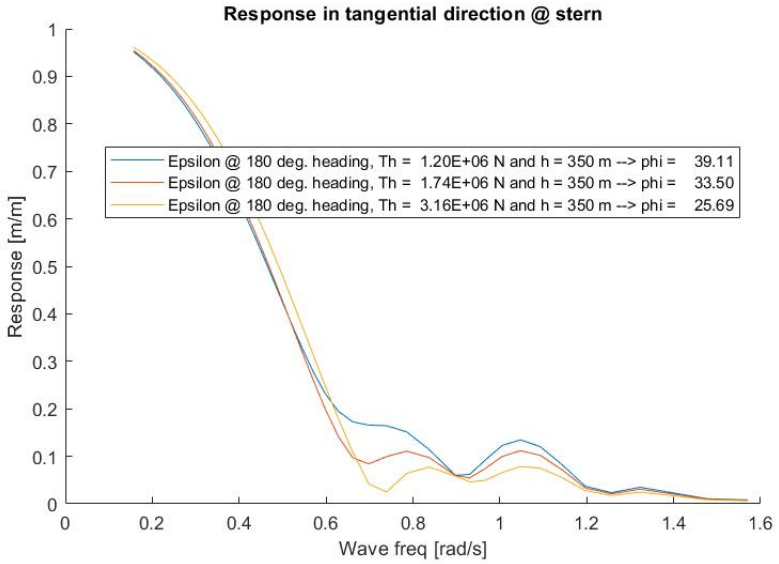

Figure 78: RAOs for vessel motion in tangential direction at stern (ϵ). Wave heading 180° and $h = 350m$

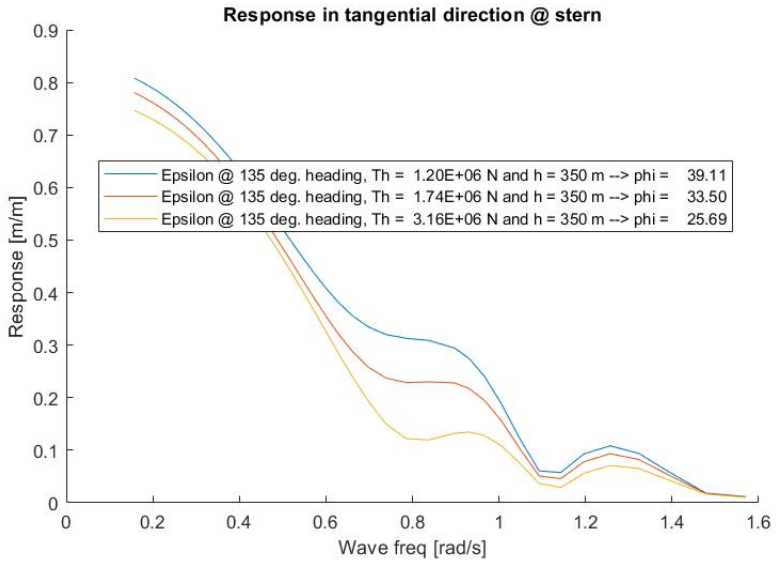

Figure 79: RAOs for vessel motion in tangential direction at stern (ϵ). Wave heading 135° and $h = 350m$

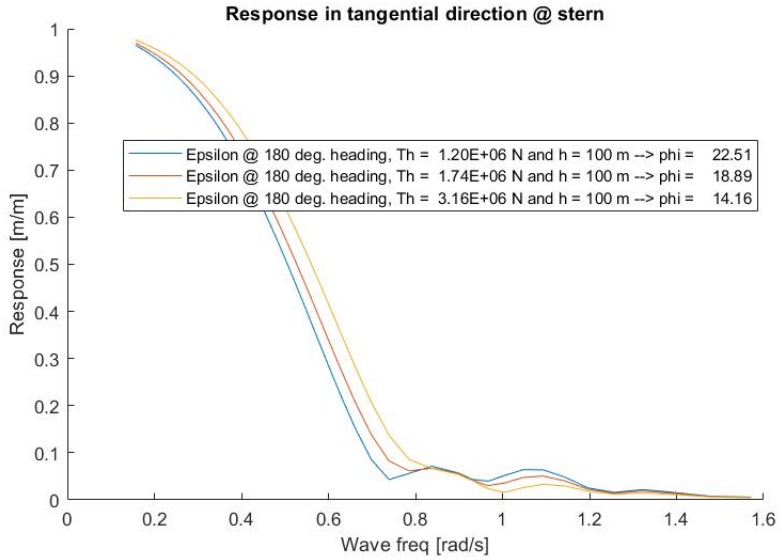

Figure 80: RAOs for vessel motion in tangential direction at stern (ϵ). Wave heading 180° and $h = 100m$

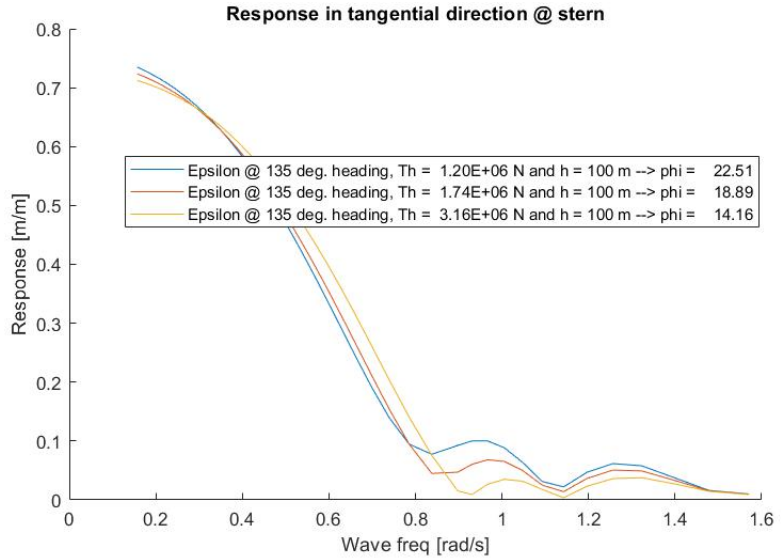

Figure 81: RAOs for vessel motion in tangential direction at stern (ϵ). Wave heading 135° and $h = 100m$

The more significant responses (ϵ) for a all plots occurs for the lower wave frequencies. This is to be expected as a lower wave frequency means bigger waves. A range between 0.15 - 0.6 $\frac{rad}{s}$ is a good approximation of where the more extreme motions are to be expected.

The plots become more spiky for the higher frequencies. The RAO is was handed over by Kjell Larsen (Equinor NTNU) and is produced by model testing. So the so the wave frequency range and steps are not possible to revamp. Spikes carry over in later plots as a result of this.

10.3 Line stiffness

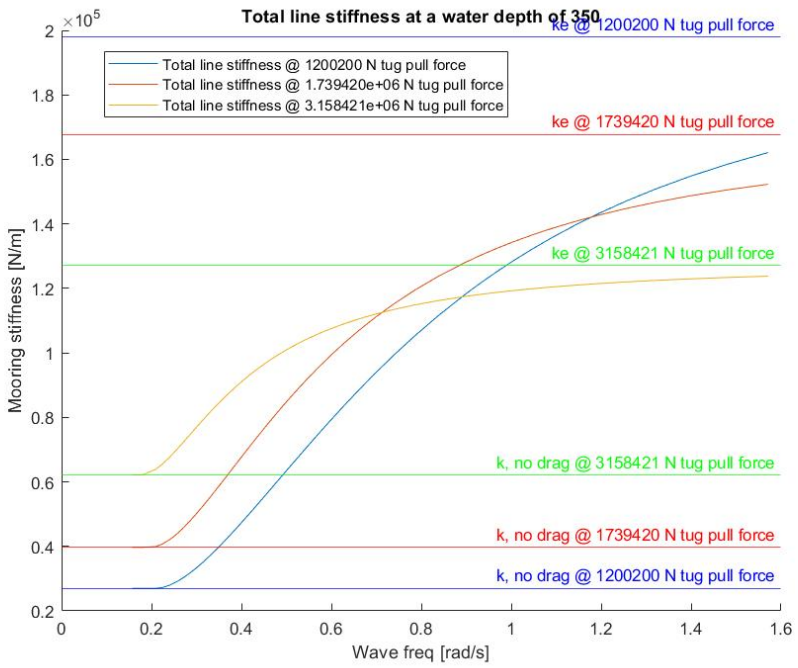

Figure 82: Line stiffness RAOs for $h = 350$ and respective initial tug forces (T_H)

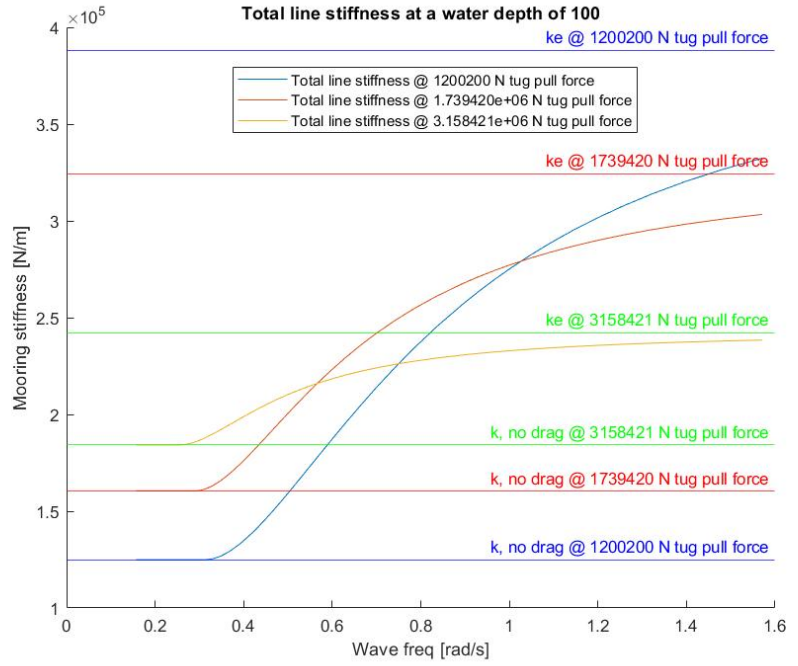

Figure 83: Line stiffness RAOs for $h = 100$ and respective initial tug forces (T_H)

Our calculations takes into account the amount of line lifted from the sea floor at different magnitude tug pulls. As calculations use the suspended length (s) to evaluate elastic stiffness, we get the different thresholds (straight horizontal lines) for the different applied horizontal forces. Using suspended line length instead of full line length is a conservative assumption, because we get a larger elastic stiffness.

With increasing applied tug force, we see all the lower line stiffness thresholds rise. Interesting enough, line stiffness range decreases with increased tug pull force. This is because higher tensions will make the geometric stiffness higher, but as more chain is lifted from the sea floor, upper threshold (k_e) is lower than for lesser magnitude initial line tensions . The impact of water depth on stiffness is also very visible when comparing the magnitudes of line stiffness in figure 82 and 83. The most visual example being the y-axis about doubles when water depth is reduced from 350 to 100 meters.

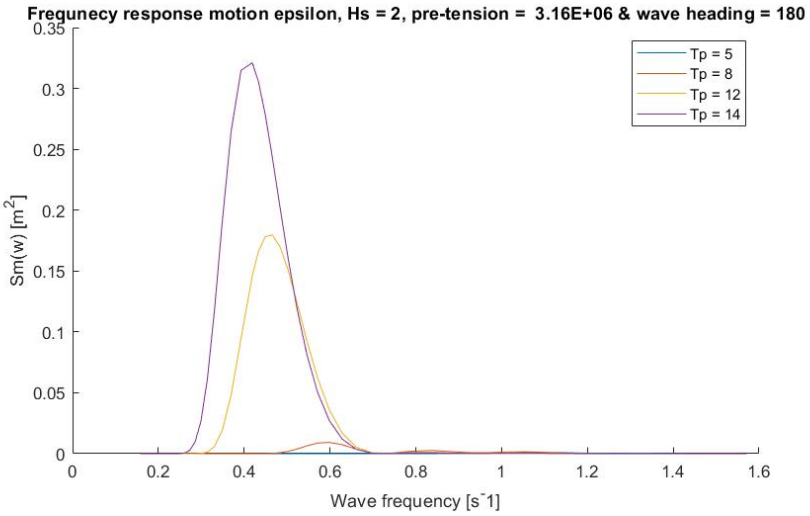

Figure 84: Example plot of motion (ϵ) spectra

Figure 84 shows a plot of a motion (ϵ) spectra. The plots illustrate at what frequency range we can expect to see the largest motions. A good estimation for the range is from around 0.27-0.7 $\frac{rad}{s}$. Looking at this wave frequency range in figure 82 and 83, we can conclude that even if total line stiffness is higher for lower tug pulls forces at higher wave frequencies, the stiffness curve for the highest tug pull force will be the most critical for this thesis' scenario.

Figure 84 is just one of many plots, but as the layout of all the plots share many characteristics and trends, figure 84 is therefore well suited as an example.

Plots including increase in drag to account for marine growth were also made. The drag was increased with a factor of 1.2, which is more than is to be expected for mobile unit chain (DNVGL-OS-E301 [8]). The increase in drag only resulted in an maximum increase in line stiffness of about 5%. Since the increase line stiffness was relatively small compared to a conservative increase in drag caused by marine growth, the results were not included in the rapport.

10.4 Line tension spectra

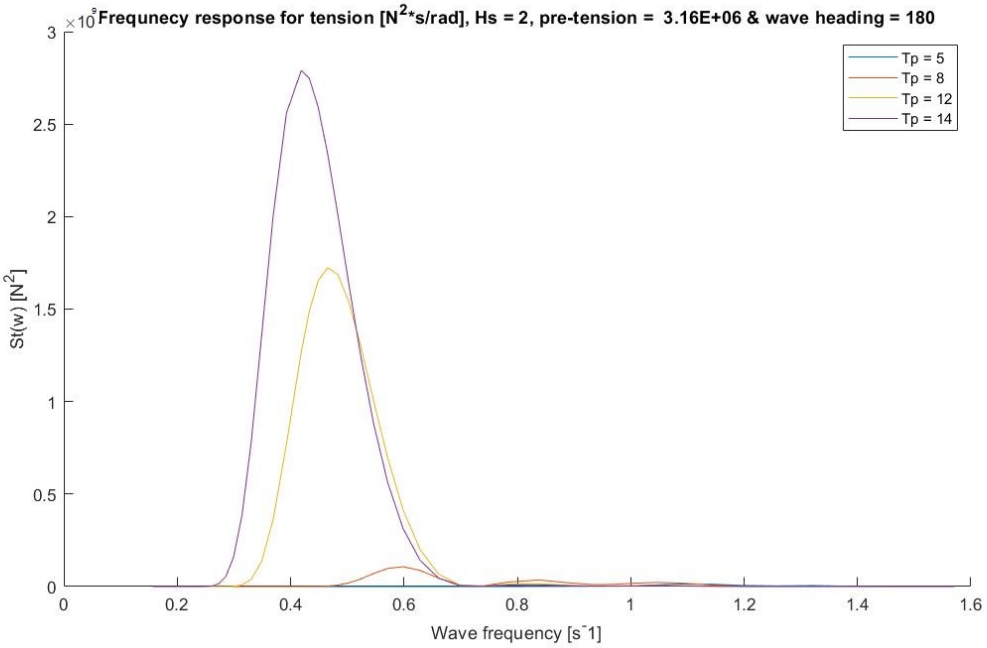

Figure 85: Tension spectra for given parameters, $H_s = 2$ and $h = 350m$. Plot for $T_p = 8$ is the base case

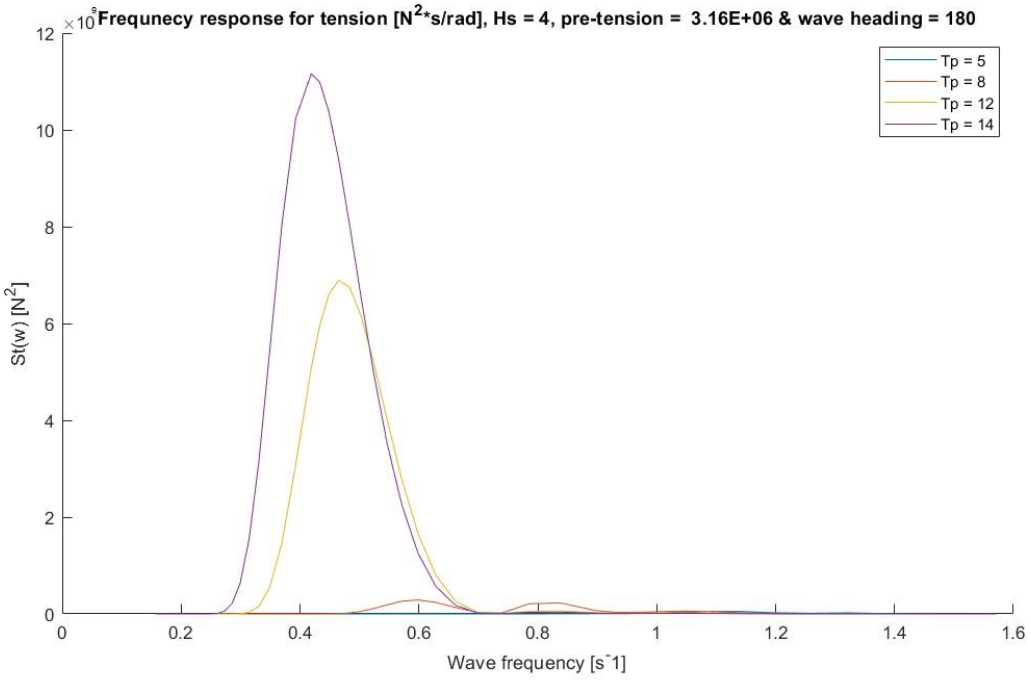

Figure 86: Tension spectra for given parameters, $H_s = 4$ and $h = 350m$

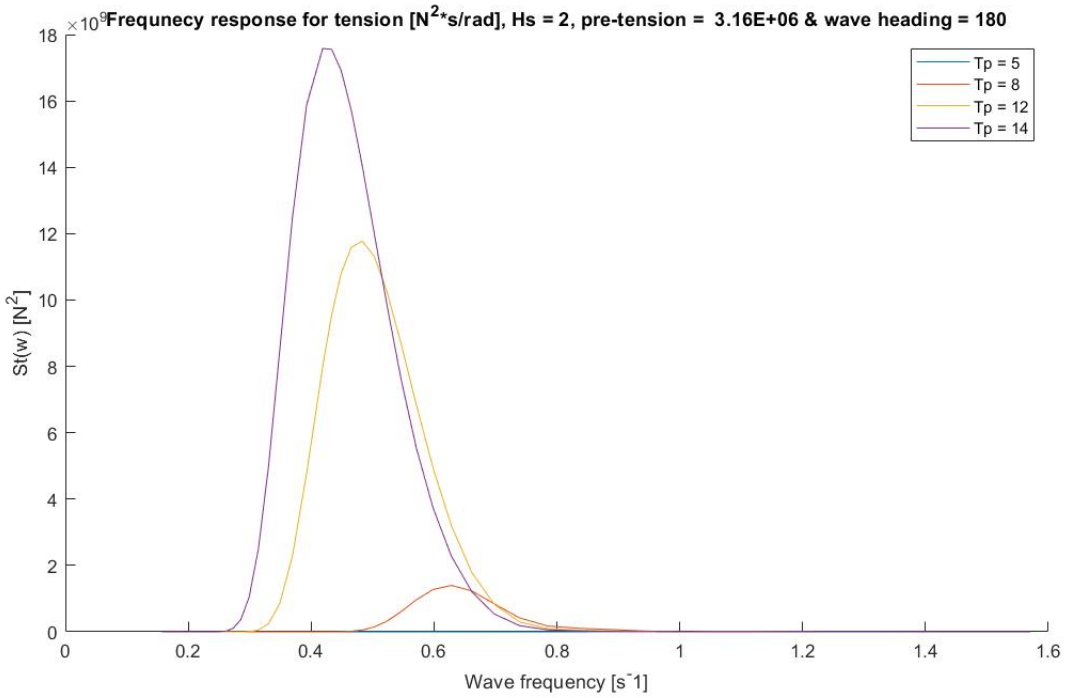

Figure 87: Tension spectra for given parameters, $H_s = 2$ and $h = 100m$

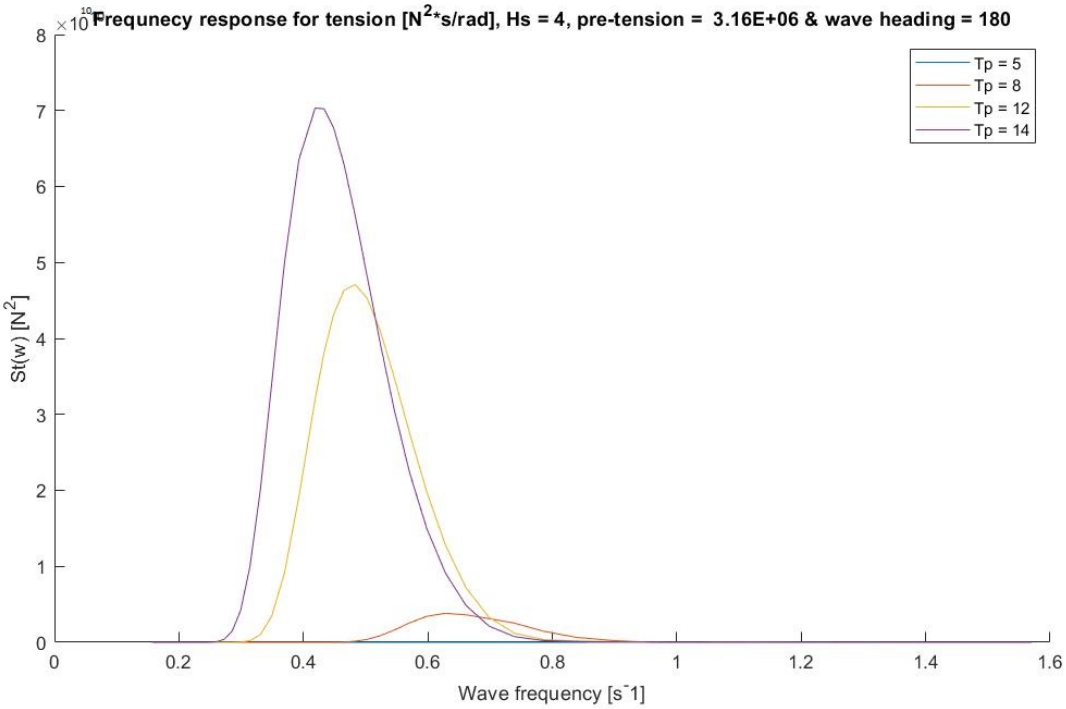

Figure 88: Tension spectra for given parameters, $H_s = 4$ and $h = 100m$

10.5 Fatigue sensitivity to important parameters

10.5.1 Corrosion sensitivity

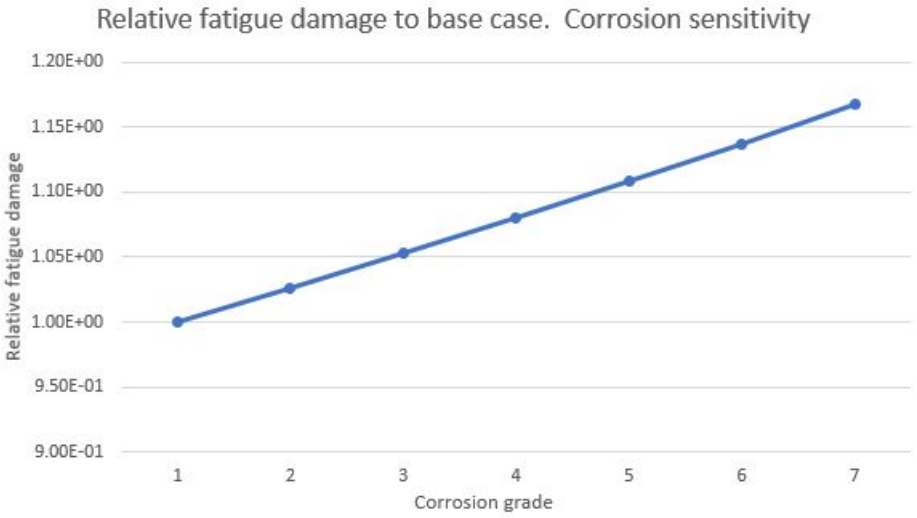

Figure 89: Relative fatigue damage to base case w.r.t. corrosion

As stated earlier, LIFEMOORs fatigue damage correction for corrosion [1] is a work in progress and is not their final product. But from the sensitivity plots we can see a linear increase in fatigue damage as the corrosion grade worsens. The increase in fatigue damage from a brand new chain (corrosion grade 1) to a severely corroded chain (corrosion grade 7) amounts to 16.7%.

10.5.2 Mean Tension sensitivity

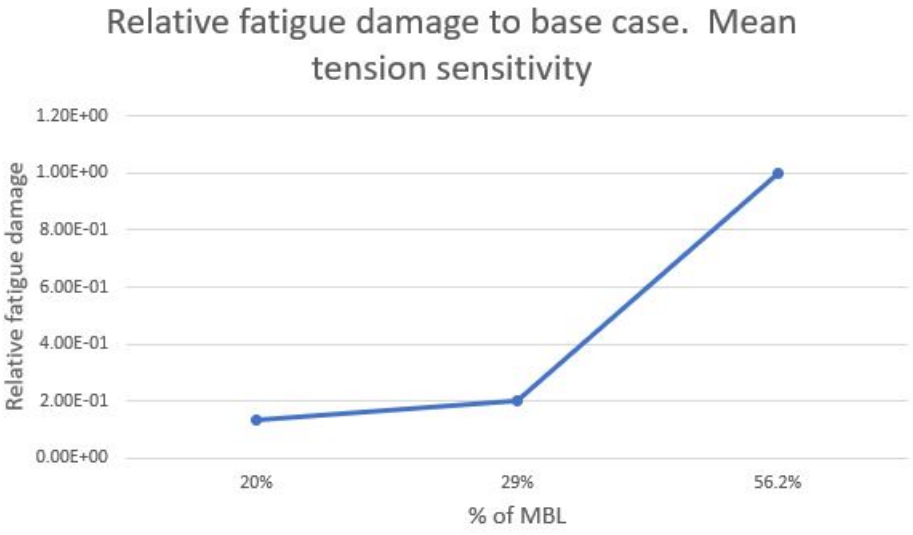

Figure 90: Relative fatigue damage to base case w.r.t. mean tension

Fatigue damage at 56.2% MBL compared to 20% MBL is 7.48 times larger. This makes the impact of corrosion on fatigue life look small in comparison. DNV regulations (as of 23.07.2020) do not account for mean tension. If the NORMOOR JIPs project's correction model for mean tensions effect on fatigue life is correct, new procedures to should be implemented in the DNV regulations as fast as possible.

As the LIFEMOOR project, NORMOOR JIPs mean tension correction project is also a work in progress. This is important to consider, as the mean fatigue correction model for mean tension might be changed in the near future. Also, when mean tension is varied, the entry angle of the chain at the vessel (φ) will as well. This results in minor changes in RAO_ϵ. Varying the entry angle (φ) in ROA provided did not seem to affect the vessel responses significantly and will therefor not be investigated further.

10.5.3 Peak wave period sensitivity

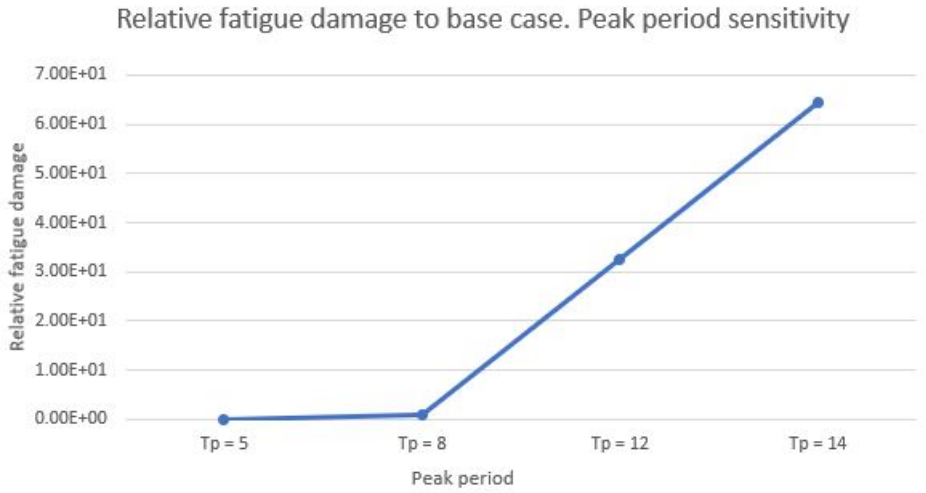

Figure 91: Relative fatigue damage to base case w.r.t. peak period (T_p)

Figure 91 shows a drastic increase in relative fatigue damage with an increasing peak period. Fatigue damage at $T_p = 14$ is 64.6 times larger than the base case. The T_p value is important when defining the JONSWAP spectra and determines at which wave period one expects to see most energy density. Lower T_p-values (0.5 - 8.8 sec) are associated with a sea state consisting of small waves and wavelets [5]. These types of waves typically do not carry enough energy to induce motions in the vessel and are deflected upon contact. It is first after $T_p = 8$ significant responses in the vessel are detected. This corresponds well with the RAOs in figures 78 - 81, which shows vessel response for different wave periods ($\omega = \frac{2\pi}{T}$, T = wave period).

10.5.4 Significant wave height sensitivity

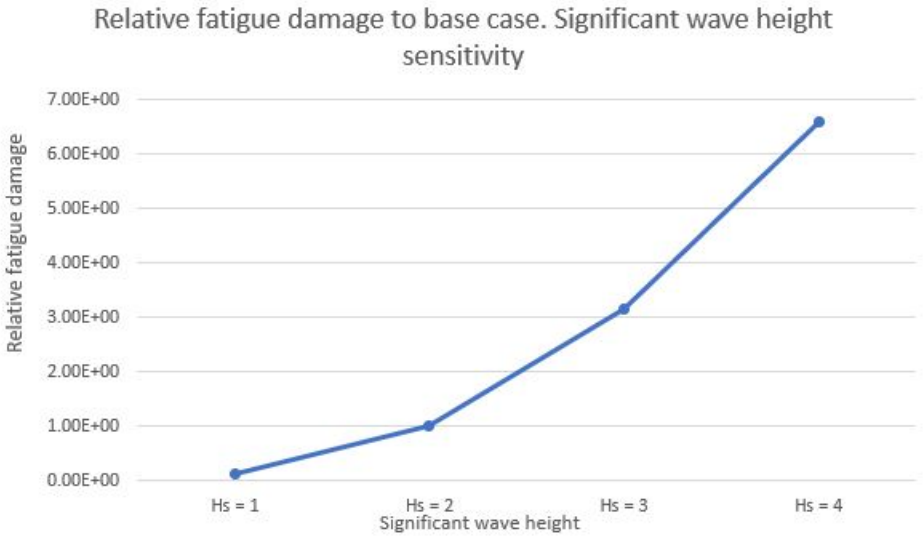

Figure 92: Relative fatigue damage to base case w.r.t. significant wave height (H_s)

Increasing significant wave height (H_s) also increase fatigue damage in a drastic manner. The damage for $H_s = 4$ is 6.6 times larger than for the base case. Looking back at figures 76 and 77, we already know that higher H_s-values increases the magnitude of JONSWAP spectras. As JONSWAP spectras shows energy content and distribution for a given sea state, it is sensible that we would see more fatigue damage as H_s increase.

10.5.5 SCF sensitivity

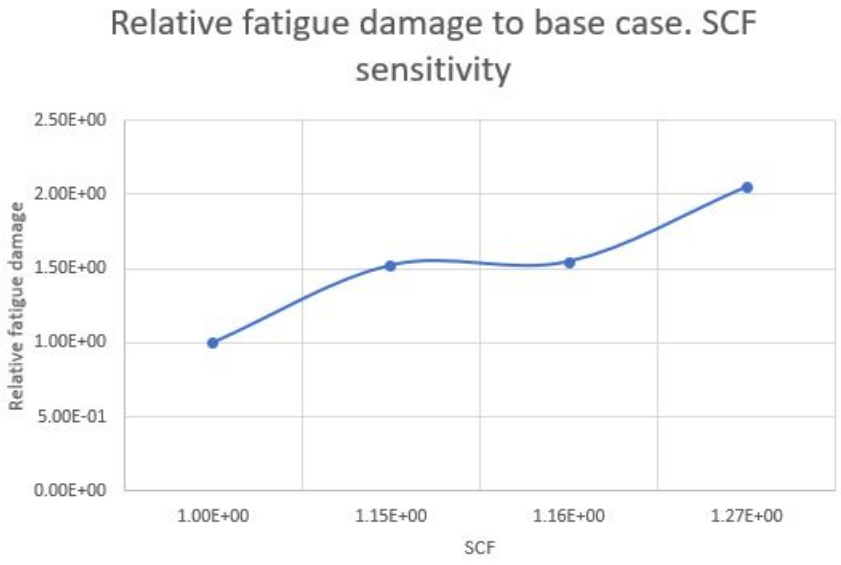

Figure 93: Relative fatigue damage to base case w.r.t. SCF (H_s)

Even though the largest stress increase due to geometry (Vicinay Study (2019) [23]) in this thesis only amounted to 27%, it still just over doubles the fatigue damage (compared to base case). In equation (45), fatigue damage is directly related to the standard deviation of the stress process (σ_{si}), cubed (m = 3). Unraveling why relatively small stress increases lead to quite the increase in fatigue damage.

10.5.6 Water depth sensitivity

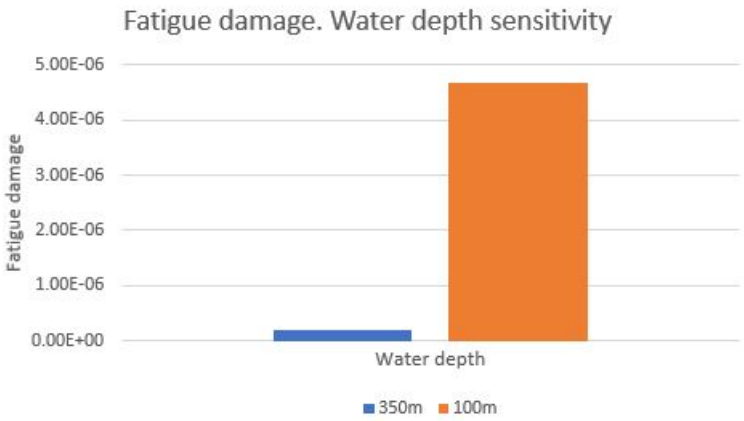

Figure 94: Fatigue damage for water depths of 350 m and 100 m

By reducing operation water depth from 350 m to 100 m, fatigue damage get 22.2 times larger. This proves that shorter mooring lines are much more prone to fatigue damage. As shown in chapter 10.3, water depth has a significant impact on line stiffness. With a higher line stiffness, the tension in the mooring line increase, which again results higher stresses in chain links. As mentioned in chapter 10.5.5, the effect of stress on fatigue is cubed, promoting water depth's effect on fatigue further.

10.5.7 Wave heading sensitivity

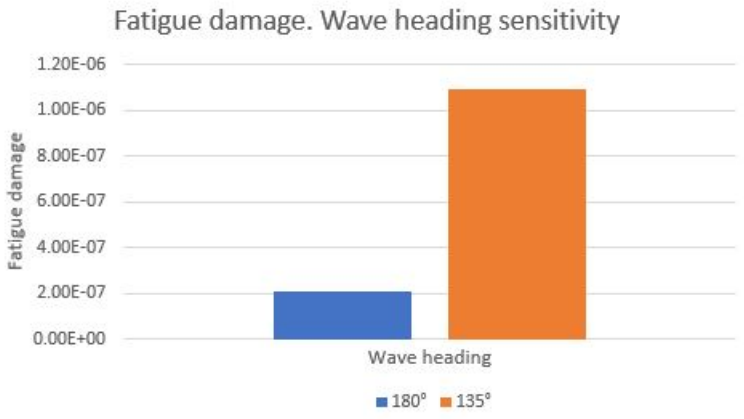

Figure 95: Fatigue damage for wave headings 180° and 135°

For our base case, a wave heading of 135° yields 5.2 times more fatigue damage than a heading of 180°. When processing the fatigue data, it was discovered that a wave heading of 135° always led to more fatigue damage as long as $T_p = 5$ or $T_p = 8$. But if fatigue assessment was run with $T_p = 12$ or $T_p = 14$, a wave heading of 180° yielded the most fatigue.

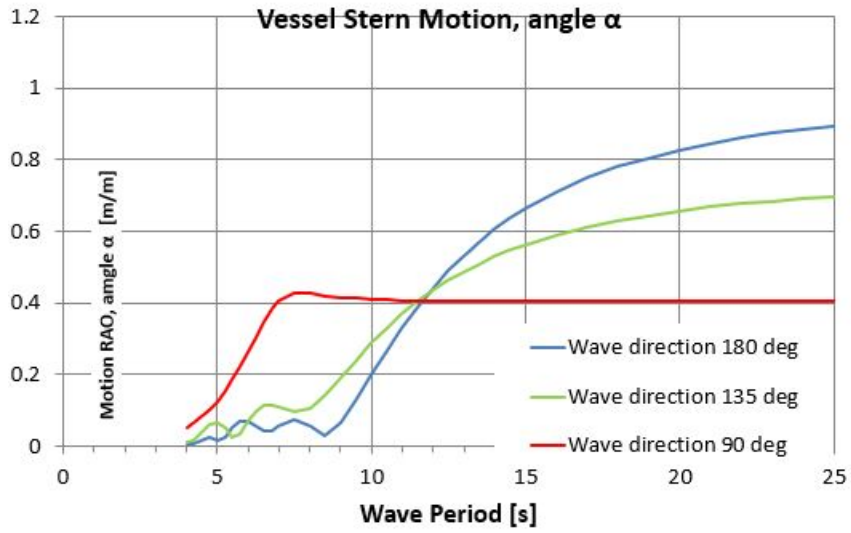

Figure 96: Vessels response in tangential direction to wave periods for different wave headings [19]

Figure 96 is a screenshot from the vessels RAO [19] showing that at approximately a wave period of 11.5 seconds, vessel response for a wave heading of 180° starts to surpass vessel response for a wave heading of 135°. As AH operations usually are scheduled for calm weather, this observation is not that relevant. But should ever one ever have to perform operations under harsher weather conditions, this could potentially be important knowledge. Just remember that the RAOs shown in figure 96 is vessel specific and that all vessels respond differently.

10.6 AH process impact on fatigue life

Life expectation for a 76 mm R4 grade mooring chain used for mobile units is 25 years even with a SF = 5 (FL = 0.2). A chain can see up to 4 retrieval and re-deployments a year. It is assumed that anchor line testing and retrieval is done over a 30 minute period with 52.6% MBL tug pull, resulting in the same fatigue damage for these operations. This is conservative, as the tug pull needed for anchor retrieval depends on the soil at anchor location and often vary. We want to set up some scenarios to see how much fatigue damage contribution from just AH operations can amount to over a year [19].

10.6.1 Base case

Base case:		%	
Fatigue limit:	0.2		Hs = 2
Single AH operation dmg:	0.000000211		Tp = 8
Single AH OP percentage of total life:	0.000001055	0.0001055	Wave heading = 180
			Water depth = 350
Annual dmg:	0.000001688		SCF = 1
Annual percentage of total life:	0.00000844	0.000844	Corrosion grade = 1
25 year dmg from AH OPS:	0.0000422		
Lifetime percent of total life:	0.000211	0.0211	

Table 18: Quantification of fatigue damage for base case

The base case represents close optimal weather and chain conditions. It is also important to note that the SCF chosen represents a straight chain, hence we do not account for the chain over stern roller geometry.

Annual fatigue damage caused by AH OPS under these conditions are negligible. Assuming that the chain is deployed, tested and retrieved four times annually over 25 year, only 0.021% of the chains life is exhausted by AH OPS. The fatigue results from the base case are very modest, even on an annual basis and should not be considered an accurate representation of fatigue damage from AH OPS.

10.6.2 Typical AH operation scenarios

AH case 350m water detph:		%	
Fatigue limit:	0.2		Hs = 2
Single AH operation dmg:	3.43E-07		Tp = 8
Single AH OP percentage of total life:	1.71E-06	1.71E-04	Wave heading = 180
			Water depth = 350
Annual dmg:	2.74E-06		SCF = 1.156
Annual percentage of total life:	1.37E-05	1.37E-03	Corrosion grade = 3
25 year dmg from AH OPS:	6.86E-05		
Lifetime percent of total life:	3.43E-04	3.43E-02	

Table 19: Quantification of fatigue damage for typical AH OPS parameters (350m water depth)

By increasing the corrosion grade and including SCF to account for chain over stern roller geometry found by FEA, we get a more accurate representation of an actual AH OP (ref. figure 19). Still, the fatigue damage is not of significant impact. With an annual fatigue life exhaustion of 0.00137% the damage from operations under these conditions are negligible.

AH case 100m water detph:		%	
Fatigue limit:	0.2		Hs = 2
Single AH operation dmg:	7.61E-06		Tp = 8
Single AH OP percentage of total life:	3.80E-05	3.80E-03	Wave heading = 180
			Water depth = 100
Annual dmg:	6.09E-05		SCF = 1.156
Annual percentage of total life:	3.04E-04	3.04E-02	Corrosion grade = 3
25 year dmg from AH OPS:	1.52E-03		
Lifetime percent of total life:	7.61E-03	7.61E-01	

Table 20: Quantification of fatigue damage for typical AH OPS parameters (100m water depth)

As seen chapter 10.5.6, water depth had the biggest impact on fatigue damage. When running the same scenario as in figure 19 with a water depth of 100m (see figure 20), we get an increase in annual fatigue damage of 2123%. The increase is significant, but still only results in annual fatigue life exhaustion of 0.03%. Still of insignificant magnitude.

10.6.3 Harsh scenario

Harsh case:		%	
Fatigue limit:	0.2		Hs = 3
Single AH operation dmg:	0.000604252		Tp = 12
Single AH OP percentage of total life:	0.003021259	0.302125873	Wave heading = 180
			Water depth = 100
Annual dmg:	0.004834014		SCF = 1.156
Annual percentage of total life:	0.02417007	2.417006981	Corrosion grade = 5
25 year dmg from AH OPS:	0.120850349		
Lifetime percent of total life:	0.604251745	60.42517452	

Table 21: Quantification of fatigue damage for a harsh scenario

The harsh scenario is still within acceptable AH OPS operational limits. Significant wave height for limit is usually between 3-4m and the peak period (T_p) is not taken into account unless operation procedures states otherwise [19].

With an annual exhaustion of fatigue life amounting to 2.42%, damage from AH OPS is now has a significant impact. If this chain were to be deployed, tested and retrieved under these conditions throughout its desired lifespan (25 years), 60.43% of chains fatigue limit would be spent on just AH OPS. If fatigue damage from station keeping were to be added as well, the chain would have to be taken out of operation long before its desired lifespan.

10.6.4 Worst case scenario

Worst Case:		%	
Fatigue limit:	0.2		Hs = 4
Single AH operation dmg:	0.003401257		Tp = 14
Single AH OP percentage of total life:	0.017006287	1.700628682	Wave heading = 180
			Water depth = 100
Annual dmg:	0.027210059		SCF = 1.27
Annual percentage of total life:	0.136050295	13.60502946	Corrosion grade = 7
25 year dmg from AH OPS:	0.680251473		
Lifetime percent of total life:	3.401257364	340.1257364	

Table 22: Quantification of fatigue damage for worst case scenario

The worst case scenario includes bad weather and a short corroded chain. The SCF used is done by visual readings of colored stress plots and is for a studded chain (see chapter 8.4.2). The grade of corrosion would exceed DNV's regulations of allowable diameter loss (5% total diameter) [10]. Corrosion grade 7 is still included as the chain does not automatically fail the re-certification process if the allowable diameter loss criteria isn't met. An operation under these conditions would likely not be performed if the weather and chain conditions were known.

The results still proves that AH OPS can lead to substantial damage if not performed in compliance with regulations. In just one year of AH OPS under unacceptable conditions, 13.6% of the chains life span will have been exhausted. Considering the duration of the AH process is thirty minutes, using 13.6% of a chains fatigue life over a time span of four hours is extreme. The chain would have reached in fatigue limit after 7 years, only accounting for fatigue damage from AH OPS.

10.7 Summary of parameter sensitivities and AH operation scenarios

One can conclude that AH OPS can lead to substantial damage to on mooring chains. All the parameters included in the sensitivity testing led to significant increases in fatigue damage. As the damage from AH OPS under close to optimal conditions is small, setting just one parameter to its most impactful value is not by itself enough to result in significant fatigue damage. But if multiple parameters are varied for the worse w.r.t. fatigue damage, the fatigue damage increases drastically and one can expect to see significant fatigue damage within typical AH OPS operational limits.

One should especially consider the fatigue damage contribution from AH OPS in shallow waters as water depth reduction had one of the most significant impact. In addition the effect of higher wave peak periods are significant and should possibly be considered when planning AH OPS in the future.

Using a tug force of 56.2% MBL in testing anchor bedding-in testing plays a big role in fatigue damage caused by AH OPS. As mentioned in chapter 3, 52.6% of MBL is applied to proof test the chain with a 100 year storm magnitude load. But is it necessary to test the chain several times a year with a load it might not experience during its operational life? There is no doubt that one could reduce fatigue damage from anchor line testing and retrieval by reducing the applied tug pull.

11 Conclusion

The thesis focuses on identifying factors leading to increased fatigue damage on mooring chains for mobile units.

- **Anchor handling:** A mooring chain for mobile units is often retrieved and deployed several times annually. Today, a part of the deployment procedure is to test with a load equal to 52.6% of the chains MBL. This load is typically of a large magnitude and often exceeds what a mooring chain in operation will experience before being retired or break. To make matters worse, the chain is in contact with the anchor handling vessels stern and fairlead while this load is applied. This leads to out of plane bending, which again lead to higher and awkward stress distributions. Huge forces is also needed when retrieving the anchors and during these operations, the chain is also in contact with stern and fairlead. Questions can be raised if a 100 year load (52.6% MBL) really is necessary to test the anchor bedding-in as it clearly promotes fatigue damage of the mooring chain.

- **Inspection and recertification regimes:** The inspection and recertification regimes for mooring chains of mobile units given by DNV-GL can be a bit vague. It can be discussed if it properly identifies the areas that should be inspected with NDT and if the extent of the inspections are good enough. If there is no suspicion that a part of the chain has extensive wear/damage/corrosion, only 5% of the general chain length has to undergo NDT. This is questionable as a chain is only as strong as it's weakest link.

- **Corrosion:** State of the art findings suggest general corrosion with a smooth surface seems to have little to no effect, while pitting and MIC/SRB have clear negative effects. Previous testing also suggest that surface roughness has just as negative effect on fatigue life as pitting and SRB. This is critical, as of now the DNV-GL SN design curve accounts for corrosion just by diameter loss of chain link and do not take into account type of corrosion or surface roughness. Still, varying grades of corrosion using LIFEMOOR's model [1] had the least impact of all the parameters varied in fatigue assessment performed in this thesis. Corrosion still led to noticeable fatigue damage increase, but indications are that chain with significant corrosion might be operational longer than expected if a lower mean tension during operation is assumed.

- **Chain link dimension and material grade:** Stress has a big impact on fatigue life. Papers used for this thesis has performed test w.r.t to MBL, which is a material property. Hence an R5 chain test at 20% MBL will be run with a higher tension than an R4. If run with the same absolute tension, the R5 grade is expected to outperform R4 and lower grades in fatigue testing etc. The same principle goes for dimensions. With a larger diameter, the chain will experience less stress in the chain link and higher fatigue life can be expected for larger dimensions of chains.

- **Mean Tension:** DNV-GLs design SN-curve is based on Noble Denton's testing. These test were run with a mean tension of 20% MBL. DNV-GLs design curve do not take into account what mean tension the chain will experience while operating. Testing indicate that mean tension have a big impact on fatigue life. Considering that most chains operate with a mean load of 5-8% MBL, assuming 20% MBL in DNV-GLs design curve might seem overly conservative. When assessing AH OPS with an applied tension of 52.6% MBL, assuming 20% MBL in the DNV-GL design curves is unconservative. As fatigue assessments run for this thesis showed that an increased mean tension led to a significant increase in fatigue damage. This emphasizes that the current design SN-curve should be revamped to better account for mean tension as it can have a big impact on fatigue life, for better or worse.

- **FEA results:** The location of the highest stress relocated from chain link crown for a straight chain to mid straight section for a chain over stern roller and led to a increase in peak stress of 15.6%. The analyses was performed with an applied force of 10% MBL and results did not include any stresses exceeding material yield. The applied force during AH OPS is 52.6% MBL and will almost certainly lead to stresses exceeding material yield, resulting in permanent deformation, local material damage and residual stresses. The effects of permanent chain link deformations, local material damages and residual stresses on fatigue life is not included in this thesis.

This thesis developed a base case with close to optimal conditions for AH OPS, to create a reference when checking parameter sensitivity:

$Corrosion\ grade = 1\ ,\ As\ new/mild\ corrosion$
$Wave\ heading = 180°$
$T_p = 8\ (s)\ ,\ Peak\ wave\ period$
$H_s = 2\ (m)\ Significant\ wave\ height$
$h = 350\ (m)\ ,\ water\ depth$
$T_H = 52.6\%\ MBL\ = 3157\ (kN),\ Force\ applied\ by\ AH\ vessel$
$SCF_{max} = 1\ ,\ Stress\ concentration\ factor\ to\ account\ for\ chain/stern\ geometry\ (Straight\ pull)$
$T_i = 1800\ (s),\ Duration\ of\ anchor\ bedding - in\ testing$

Increase in relative fatigue damage ref base case:		
Corrosion	Grade 7	16.70 %
Mean tension	52.6% MBL	648 %
Peak wave period	14 sec	6360 %
Significant wave height	4 m	559 %
SCF	1.27	105 %
Water depth	100 m	2120 %
Wave heading	135 degrees	420 %

Table 23: Relative increase in fatigue damage comparing worst case to base case for each parameter, except mean tension where base case value is compared to lowest mean tension

Fatigue damage from the AH base case lead to insignificant fatigue life exhaustion ($1.1 \cdot 10^{-4}$ % of total life). Table 23 show that varying parameters for the worse w.r.t. fatigue damage all lead to significant increases. But still, varying just one parameter by itself is not enough to cause significant fatigue life exhaustion as the damage from the base case is so small. If multiple parameters are varied for the worse, the fatigue damage rack up and we can expect to see significant fatigue life exhaustion within typical AH OP limits. An annual fatigue life exhaustion of 2.42% from just AH was quantified for a harsh AH scenario within typical operational limits. With annual fatigue life exhaustion of 2.43%, the industries life expectation of 25 years would most certainly not be fulfilled. For the worst case scenario set up in thesis (not within typical operational limits), the chain would fail within 2 years, just from AH.

11.1 Recommendations for further work

The MATLAB script should be updated to include full anchor (all of chain length contributing to elastic stiffness). Also a more thorough study into the effect of water depth should be included. This thesis only include relatively shallow water depths and do not look into chains tested in ultra deep waters. If this is performed, alternative models for line stiffness and line tension should be considered.

It could be interesting to look into different chain over stern roller configurations with the full load of 52.6% MBL. The chain has multiple contact points during testing and FEA should be run with fairlead contact and smaller stern rollers dimensions to check the impact.

As mentioned earlier, when a load of 52.6% MBL is applied, we expect to see permanent deformations, local material damage and residual stresses. Hence, FEA with the full load should be performed and a better material model should be implemented (full stress/strain curve). From there, studies on the effects of deformation, material damage and residual stresses on fatigue life should be conducted.

This thesis use NORMOOR and LIFEMOOR projects models to account for mean tension and corrosion. As the NORMOOR and LIFEMOOR projects are ongoing and not final products, future fatigue assessments using the same approach as this thesis should assure that the latest NORMOOR and LIFEMOOR models or other state of the art models are included.

References

[1] Lifemoor 2020. Online: https://prosjektbanken.forskningsradet.no//project/NFR/280705/Sprak=en.

[2] Ramnäs bruk product catalogue. Online document: https://ramnas.com/wp-content/uploads/2012/11/Ramnas-Technical-Broschure.pdf.

[3] Ymv stern rollers for safe anchor handling operations. Online document: http://www.ymvcrane.com/sternroller.html.

[4] R. Baxter and J. Britton. Offshore Cathodic Protection 101: What it is and how it works. Online document: http://www.cathodicprotection101.com, 2013.

[5] S. K. CHAKRABARTI. Handbook of offshore engineering. Volume I, 2005.

[6] S. K. Chakrabarti. Handbook of Offshore Engineering. II, 2015.

[7] Department of Physics Astronomy. Hooke's Law general. Online document: http://labman.phys.utk.edu/phys221core/modules/m3/Hooke%27s%20law.html.

[8] DNV-GL. Dnvgl-os-e301, position mooring. Edition July 2018, 2018.

[9] DNV-GL. Dnvgl-os-e302, offshore mooring chain. Edition July 2018, 2018.

[10] DNV-GL. Dnvgl-ru-ou-0300, fleet in service (offshore units). Edition July 2019, 2019.

[11] DNV-GL. Analysis of chain fatigue test data", report 2020-0386. rev. A, April 4th 2020.

[12] O. Faltinsen. Sea loads on ships and offshore structures. Cambridge Ocean Technology series, 1990.

[13] J. Fernández, W. Storesund, and J. Navas. OMAE2014-23491, FATIGUE PERFORMANCE OF GRADE R4 AND R5 MOORING CHAINS IN SEAWATER. Proceedings of the ASME 2014 33rd International Conference on Ocean, Offshore and Artic Engineering, 2014.

[14] S. Fredheim, S.-A. Reinholdtsen, L. Håskoll, and H. B. Lie. OMAE2013-10609, CORROSION FATIGUE TESTING OF USED, STUDLESS, OFFSHORE MOORING CHAIN. Proceedings of the 32nd International Conference on Ocean, Offshore and Arctic Engineering, 2013.

[15] P. H. Holmström. Personal guidance.

[16] T. R. Jensen. Personal guidance.

[17] Kjell Larsen. Stresses in chain links, Kristin reference and error cases. Internal presentation at Equinor, 2012. Powerpoint without presenter.

[18] A. Kvitrud. OMAE2014-23095, LESSONS LEARNED FROM THE NORWEGIAN MOORING LINE FAILURES 2010-2013. Proceedings of the ASME 2014 33rd International Conference on Ocean, Offshore and Arctic Engineering, 2014.

[19] K. Larsen. Personal guidance.

[20] K. Larsen. Lecture notes in tmr4225, marine operasjoner, 2019.

[21] K. Larsen and P. C. Sandvik. EFFICIENT METHODS FOR THE CALCULATION OF DYNAMIC MOORING LINE TENSION. 1990.

[22] K. Larsen, Øystein Gabrielsen, and S.-A. Reinholdtsen. OMAE2017-61382, FATIGUE TESTING OF USED MOORING CHAIN. Proceedings of the ASME 2017 36th International Conference on Ocean, Offshore and Arctic Engineering, 2017.

[23] V. Marine. Structural analysis of 84 mm r5 stud chain over stern roller and winch drum. Confidential, 2019.

[24] MIT. Choosing between implicit and explicit analysis. Online document: https://abaqus-docs.mit.edu/2017/English/SIMACAEGSARefMap/simagsa-c-absadvexp.htm, 2017.

[25] Murphy oil coorporation. Front page general. Online document: https://www.murphyoilcorp.com/About-Us/Our-History/, 2019.

[26] NDTT. Magnetic particle testing. Online document: http://www.ndttechnologies.com/products/magnetic_particle_testing.html, 2019.

[27] NTNU. 6.3.3 explicit dynamic analysis. Online document: http://ivt-abaqusdoc.ivt.ntnu.no:2080/v2016/books/usb/default.htm?startat=pt03ch06s03at08.html.

[28] NTNU. Kinematic coupling constraints. Online document: https://abaqus-docs.mit.edu/2017/English/SIMACAECSTRefMap/simacst-c-kinematiccoupling.htm.

[29] W. K. L. Pedro M. Vargas, Teh-Min Hsu. Om ae2004-51376, stress concentration factors for stud-less mooring chain links in fairleads. 23rd International Conference on Offshore Mechanics and Arctic Engineering June 20-25, 2004, Vancouver, British Columbia, Canada, 2004.

[30] P. Smedley and D. Petruska. Proc. paper 5.2 comparison of global design requirements and failure rates for industry long term mooring systems (disc, houston, texas, usa, september 16-18, 2014), 2014.

[31] Statoil and Odfjell Drilling. Deepsea Bergen, Scope of Work, Rig move from Mim to Aasgard S, 2017.

[32] Tec science. Dye penetrant inspection. Online document: https://www.tec-science.com/material-science/material-testing/dye-liquid-penetrant-inspection-dpi/, 2019.

[33] Unknown. Magnetic particle testing. Online document: https://inspectioneering.com/tag/magnetic+particle+inspection.

[34] G. Whyte. Solidworks simulation vs simulia abaqus. Online document: https://hawkridgesys.com/blog/solidworks-simulation-vs-simulia-abaqus, 2016.

[35] WunHungLo. "Mooring chain spec?" thread. Online document: http://forums.sailinganarchy.com/index.php?/topic/89841-mooring-chain-spec/, 2009.

[36] Y.-H. Zhang and P. Smedley. OMAE2019-95984, FATIGUE PERFORMANCE OF HIGH STRENGTH AND LARGE DIAMETER MOORING CHAIN IN SEAWATER. Proceedings of the ASME 2018 38th International Conference on Ocean, Offshore and Arctic Engineering, 2019.

[37] S. K. Ås and S. Berge. Fatigue and fracture in marine structures. Compendium Handout, 2017.

[38] Øystein Gabrielsen, K. Larsen, O. Dalane, H. B. Lie, and S.-A. Reinholdtsen. OMAE2019-95083, MEAN LOAD IMPACT ON MOORING CHAIN FATIGUE CAPACITY: LESSONS LEARNED FROM FULL SCALE FATIGUE TESTING OF USED CHAINS. Proceedings of the ASME 2019 38th International Conference on Ocean, Offshore and Arctic Engineering, 2019.

[39] Øystein Gabrielsen, T. Liengen, and S. Molid. OMAE2018-77460, MICROBIOLOGICAL INFLUENCED CORROSION ON SEABED CHAIN IN THE NORTH SEA. Proceedings of the ASME 2017 37th International Conference on Ocean, Offshore and Arctic Engineering, 2018.

[40] Łukasz Skotny. Difference between implicit vs explicit analysis. Online document: https://enterfea.com/implicit-vs-explicit/, 2019.

Appendices

A DNV-GL inspection and recertification regimes for chain link studs and joining shackles

Alternatively, accurate reliable records equivalent to the above markings are to be available onboard. Anchor chains, acceptance criteria and repair.

2.2 Diameter loss due to abrasion and corrosion

2.2.1 Temporary mooring equipment: Links or joining shackles with minimum cross-sectional area less than 81% of the original nominal area are to be rejected. The equivalent reduction in diameter is 10%. Two perpendicular measurements are to be taken and the average compared to the allowable 10% reduction.

2.2.2 Position mooring equipment: Links or joining shackles with minimum cross-sectional area less than 90% of the original nominal area are to be rejected. The equivalent reduction in diameter is 5%. Two perpendicular measurements are to be taken and the average compared to the allowable 5% reduction.

Lengths over five links should be 23.25 *D* as a maximum.

— Missing studs.

Missing studs on stud link chains are not acceptable. Links are to be removed or studs are to be refitted, using an approved procedure.

— Corroded studs.

As guidance, if the measured stud cross-sectional area is less than 40% of the nominal link (bar) cross-sectional area, links should be removed or studs should be refitted using an approved procedure.

— Studs secured by fillet welds.

Grade 3 chains are sometimes fitted with studs secured by fillet welds. In service the welds may crack. The following applies:

- any axial or lateral movement is unacceptable. Links are be removed or studs are to be re-welded using an approved procedure
- links with intact fillet welds but with gaps exceeding 3 mm between the stud and the link should be removed or repaired using an approved procedure. This because the stud welds will eventually crack due to vibrations when chain is running over fairlead at speed during anchor handling
- existing links which are found to have the stud fillet welded at both ends are subject to special consideration
- studs secured by press fitting and mechanical locking.

With this design of stud there is little prospect of the stud falling out even if it is loose. However, loose studs have caused fatigue at the edge of imprints. The following applies:

- axial stud movement up to 1 mm is acceptable
- axial stud movement greater than 2 mm is unacceptable. Links are to be removed or studs are to be pressed using an approved procedure
- acceptance of axial stud movement from 1 to 2 mm shall be evaluated based on the environmental conditions of the unit's location and expected period of time before the chain is again available for inspection
- lateral movement up to 4 mm is acceptable provided there is no realistic prospect of the stud falling out
- welding of studs is not acceptable.

2.2.3 Cracks, gouges, and other surface defects

Defects may be removed by grinding to a depth of 7% of original nominal diameter provided the resulting cross-sectional area is at least 81% (90% for position mooring equipment) of the original nominal area.

The resulting grooves are to have a length along the link of approximately six times the depth and a bottom radius of approximately three times the depth. Grooves are to be blended into the surrounding surface to avoid any sharp contours.

Complete elimination of defects is to be verified by MT or PT.

Rules for classification: Offshore units — DNVGL-RU-OU-0300. Edition July 2019 Page 265
Fleet in service

DNV GL AS

Appendix D

2.2.4 Gross-distortion
Links showing distortion/miss-shape are to be rejected.

2.3 Joining shackle defects and repair

2.3.1 Experience has shown a number of anchors and chains lost due to joining shackle failure. Joining shackle is to be rejected if cracks and other defects are found on the machined surfaces. In addition, all joining shackles on that chain which are of the same design and which have an equal or greater service life are also to be considered carefully with a view to rejection. Cracks and other defects on the remaining surface may be removed by grinding.

2.3.2 Distortion
Shackles showing distortion/miss-shape are to be rejected.

2.3.3 Tapered pins
Tapered pins holding the parts of joining shackles together shall make good contact at both ends and the recess of counter-bore at the large end of the pin holder should be solidly plugged with a peened lead slug to prevent the pin from working out.

2.3.4 Replacement of links and joining shackles
Links or shackles beyond repair are to be replaced with joining shackles in compliance with current rules and guided by the following good marine practice:

- joining shackles should pass through fairleads and windlasses in the horizontal plane
- since joining shackles have much lower fatigue lives than ordinary chain links as few as possible should be used
- if a large number of links meet the discard criteria and these links are distributed in the whole length, the chain should be replaced with new chain.

Any other type of replacement links are subject to special approval.

2.4 Anchors acceptance criteria and repair

2.4.1 The anchor shackle pin shall be renewed if excessively worn or bent.

2.4.2 Bent flukes or shanks may be heated and jacked back in place according to an approved procedure, followed by magnetic particle testing.

2.4.3 If swivels are fitted to the anchor, the threads engaging the swivel nut shall be examined. If significant corrosion is found, the swivel should be removed or replaced.

3 Survey requirements - mooring chain failure

3.1 Inspection scope and acceptance criteria

In case of a mooring chain failure, the inspection shall reveal if the break is due to overload, and to what extent this overload affect the function and/or capacity of the chain. If the inspected chain links do not reveal any findings outside the normal acceptance criteria for chain as per this appendix and DNVGL-OS-E302, the failed link is assumed a local damage and the remainder of the chain is accepted for further use.

Inspection requirements:

B Tables for Weibull distribution

Table 9.1: Table of the complete gamma function.

n	$\Gamma(n+1)$	$\log\Gamma(n+1)$	n	$\Gamma(n+1)$	$\log\Gamma(n+1)$
0.10	0.951350	-0.021659	5.10	142.451	2.153668
0.20	0.918168	-0.037077	5.20	169.406	2.228929
0.30	0.897470	-0.046979	5.30	201.813	2.304949
0.40	0.887263	-0.051947	5.40	240.833	2.381717
0.50	0.886226	-0.052455	5.50	287.885	2.459219
0.60	0.893515	-0.048897	5.60	344.701	2.537443
0.70	0.908638	-0.041608	5.70	413.407	2.616378
0.80	0.931383	-0.030871	5.80	496.606	2.696012
0.90	0.961765	-0.016930	5.90	597.494	2.776333
1.00	0.999999	0.000000	6.00	719.999	2.857332
1.10	1.046485	0.019733	6.10	868.956	2.938998
1.20	1.101802	0.042103	6.20	1050.317	3.021320
1.30	1.166711	0.066963	6.30	1271.423	3.104290
1.40	1.242169	0.094180	6.40	1541.336	3.187897
1.50	1.329340	0.123636	6.50	1871.254	3.272132
1.60	1.429624	0.155222	6.60	2275.032	3.356987
1.70	1.544685	0.188840	6.70	2769.830	3.442453
1.80	1.676490	0.224401	6.80	3376.921	3.528520
1.90	1.827355	0.261822	6.90	4122.709	3.615182
2.00	1.999999	0.301029	7.00	5039.999	3.702430
2.10	2.197620	0.341952	7.10	6169.593	3.790256
2.20	2.423965	0.384526	7.20	7562.288	3.878653
2.30	2.683437	0.428691	7.30	9281.392	3.967613
2.40	2.981206	0.474392	7.40	11405.88	4.057129
2.50	3.323350	0.521576	7.50	14034.40	4.147194
2.60	3.717023	0.570195	7.60	17290.24	4.237801
2.70	4.170651	0.620203	7.70	21327.69	4.328943
2.80	4.694174	0.671559	7.80	26339.98	4.420615
2.90	5.299329	0.724220	7.90	32569.40	4.512809
3.00	5.999999	0.778151	8.00	40319.99	4.605520
3.10	6.812622	0.833314	8.10	49973.70	4.698741
3.20	7.756689	0.889676	8.20	62010.76	4.792467
3.30	8.855343	0.947205	8.30	77035.55	4.886691
3.40	10.136101	1.005870	8.40	95809.45	4.981408
3.50	11.631728	1.065644	8.50	119292.4	5.076613
3.60	13.381285	1.126497	8.60	148696.1	5.172299
3.70	15.431411	1.188405	8.70	185550.9	5.268463
3.80	17.837861	1.251342	8.80	231791.8	5.365098
3.90	20.667385	1.315285	8.90	289867.7	5.462199
4.00	23.999999	1.380211	9.00	362879.9	5.559763
4.10	27.931753	1.446098	9.10	454760.7	5.657782
4.20	32.578096	1.512925	9.20	570499.0	5.756254
4.30	38.077976	1.580673	9.30	716430.6	5.855174
4.40	44.598848	1.649323	9.40	900608.9	5.954536
4.50	52.342777	1.718856	9.50	1133278.	6.054336
4.60	61.553915	1.789255	9.60	1427482.	6.154570
4.70	72.527634	1.860503	9.70	1799844.	6.255234
4.80	85.621737	1.932584	9.80	2271560.	6.356324
4.90	101.270191	2.005481	9.90	2869690.	6.457835
5.00	119.999999	2.079181	10.00	3628799.	6.559763

Figure 9.16: Exceedances of stress ranges represented by the Weibull distribution with different shape parameters. (Equation (9.18)).

Appendix B taken from Fatigue and fracture in marine structures [37]

C Anchor retrieval procedure from "Rig move from Mim to Åsgard S"

9.3 *Recovery of Anchors*

NB! Anchor # 6, #7 and #8 to be recovered away from pipeline!
Stern of AHV shall under no circumstances cross #6-#7-#8 when breaking anchor for these lines.

Break the anchor out of the soil by using maximum 200t tension.
Be aware of heave induced forces when AHV is close to anchor position.

Step 1 AHV to retrieve the pennant wire by the use of a "lasso", recover pennant wire/swivel and connect anchor chain to AHV work-wire.

Step 2 When the vessel has recovered suitable length of chain to its drum, turn 180 degrees on line heading and pull / break anchor out of the soil. Do not secure the anchor chain in shark-jaw when breaking the anchor. Vryhof recommends an angle of 45° when breaking an anchor.

NB! Always keep length behind stern roller above 1.2 x WD when breaking / pulling anchor out of the soil.

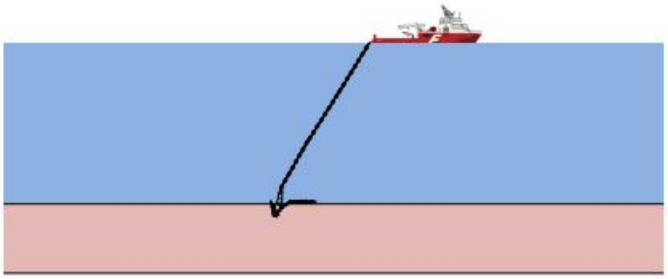

NB! AHV is to move away from pipelines/umbilical when anchors are out of the soil. Anchors shall be recovered minimum 300m away from infrastructure, e.g. pipelines/umbilicals.

D SCF tables from Vargas, Hsu and Lee (2004) [29]

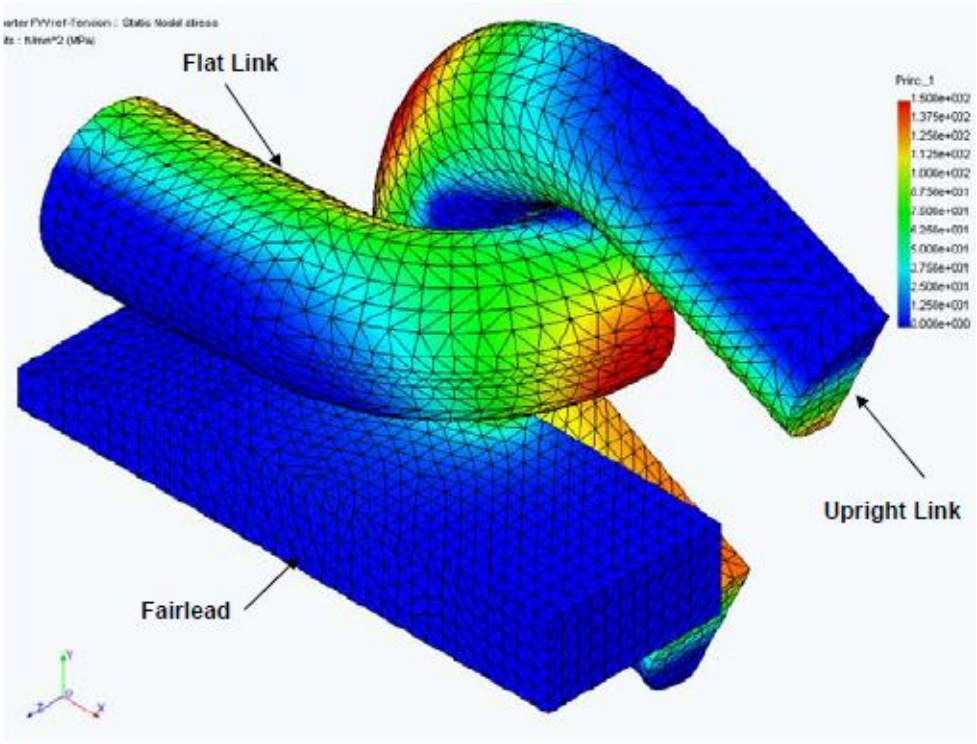

Figure 97: Stress plot in COSMOS FEA with component explanation [29]

Straight Chain Model: Crown Location

% CBL	6.2%	10.0%	30.0%	45.0%	60.0%
ABAQUS medium refinement	154.6	250.0	737.6	1095.4	1445.1
SCF	4.33	4.31	4.24	4.20	4.15
ABAQUS higher refinement	154.2	249.1	735.2	1090.5	1439.4
SCF	4.32	4.29	4.22	4.18	4.14
PUSNES Pro/Engineer	161.0				
SCF	4.51				
CosmosWorks	154.9				
SCF	4.34				
NEL ANSYS		249.3	747.9	1121.8	1495.7
SCF		4.30	4.30	4.30	4.30

Table 2a: Straight Chain Model Crown Section SCF for 5.25" grade R4 Chain

Straight Chain Model: Bend Section Location

% CBL	6.2%	10.0%	30.0%	45.0%	60.0%
ABAQUS medium refinement	133.3	216.2	646.3	967.5	1287.1
SCF	3.73	3.73	3.71	3.71	3.70
ABAQUS higher refinement	133.5	216.6	647.3	968.6	1288.7
SCF	3.74	3.73	3.72	3.71	3.70
PUSNES Pro/Engineer	130.0				
SCF	3.64				
CosmosWorks	134.8				
SCF	3.77				
NEL ANSYS		216.9	650.6	975.9	1301.2
SCF		3.74	3.74	3.74	3.74

Table 2b: Straight Chain Model Bend Section SCF for 5.25" grade R4 Chain

Straight Chain Model: Straight Section Location

% CBL	6.2%	10.0%	30.0%	45.0%	60.0%
ABAQUS medium refinement	121.2	196.3	582.6	867.4	1147.7
SCF	3.39	3.38	3.35	3.32	3.30
ABAQUS higher refinement	121.0	196.1	581.8	866.0	1146.0
SCF	3.39	3.38	3.34	3.32	3.29
PUSNES Pro/Engineer	123.0				
SCF	3.44				
CosmosWorks	121.7				
SCF	3.41				
NEL ANSYS		192.3	576.9	865.4	1153.8
SCF		3.32	3.32	3.31	3.31

Table 2c: Straight Chain Model Straight Section SCF for 5.25" grade R4 Chain

Table 24: SCFs for straight chain model [29]

25.7 angle on fairlead: Crown Location

	% CBL	6.2%	10.0%	30.0%	45.0%	60.0%
Flat	ABAQUS medium refinement	156.3	252.6	751.8	1120.3	1480.6
	SCF	4.38	4.35	4.32	4.29	4.25
	ABAQUS higher refinement	155.2	251.5	748.3	1114.2	1474.7
	SCF	4.34	4.34	4.30	4.27	4.24
	ABAQUS medium w/ friction	153.0	245.2	722.3	1071.8	1415.7
	SCF	4.28	4.23	4.15	4.11	4.07
Upright	ABAQUS medium refinement	155.4	251.7	738.8	1094.5	1443.2
	SCF	4.35	4.34	4.25	4.19	4.15
	ABAQUS higher refinement	154.5	249.4	730.8	1082.8	1424.3
	SCF	4.33	4.30	4.20	4.15	4.09
	ABAQUS medium w/ friction	155.7	252.1	739.8	1090.8	1433.5
	SCF	4.36	4.35	4.25	4.18	4.12

Table 4a: Configuration 1 Fairlead-Chain Link Model Crown Section SCF for 5.25" grade R4 Chain

25.7 angle on fairlead: Bend Section Location

	% CBL	6.2%	10.0%	30.0%	45.0%	60.0%
Flat	ABAQUS medium refinement	130.0	210.7	630.2	943.2	1253.8
	SCF	3.64	3.63	3.62	3.61	3.60
	ABAQUS higher refinement	132.2	214.6	641.8	960.6	1274.7
	SCF	3.70	3.70	3.69	3.68	3.66
	ABAQUS medium w/ friction	127.7	206.6	609.8	905.9	1194.5
	SCF	3.57	3.56	3.50	3.47	3.43
Upright	ABAQUS medium refinement	132.2	214.9	641.9	961.1	1278.7
	SCF	3.70	3.70	3.69	3.68	3.67
	ABAQUS higher refinement	133.6	216.7	646.9	967.8	1286.8
	SCF	3.74	3.74	3.72	3.71	3.70
	ABAQUS medium w/ friction	133.3	216.3	650.4	975.6	1303.1
	SCF	3.73	3.73	3.74	3.74	3.74

Table 4b: Configuration 1 Fairlead-Chain Link Model Bend Section SCF for 5.25" grade R4 Chain

25.7 angle on fairlead: Straight Section Location

	% CBL	6.2%	10.0%	30.0%	45.0%	60.0%
Flat	ABAQUS medium refinement	116.2	188.2	559.2	832.7	1101.5
	SCF	3.25	3.24	3.21	3.19	3.16
	ABAQUS higher refinement	116.6	189.0	561.7	836.6	1105.7
	SCF	3.26	3.26	3.23	3.20	3.18
	ABAQUS medium w/ friction	113.2	183.0	535.4	791.0	1036.1
	SCF	3.17	3.15	3.08	3.03	2.98
Upright	ABAQUS medium refinement	121.5	197.1	584.3	869.8	1150.7
	SCF	3.40	3.40	3.36	3.33	3.31
	ABAQUS higher refinement	121.3	196.4	582.2	866.4	1145.9
	SCF	3.40	3.39	3.35	3.32	3.29
	ABAQUS medium w/ friction	122.5	198.6	592.5	883.7	1173.7
	SCF	3.43	3.42	3.40	3.39	3.37

Table 4c: Configuration 1 Fairlead-Chain Link Model Straight Section SCF for 5.25" grade R4 Chain

Table 25: SCFs for chain in fairlead and fixed link angle ($\beta_1 = \beta 2 = 25.7$) [29]

β_1	β_2	Link		Crown	Bend	Straight
25.7	25.7	Flat	Stress (MPa)	1564.57	1111.88	1109.31
			SCF	***4.46***	***3.19***	***3.18***
		Upright	Stress (MPa)	1594.40	1179.79	1126.60
			SCF	***4.57***	***3.38***	***3.23***
25.7	12.85	Flat	Stress (MPa)	1421.91	1203.37	1065.5
			SCF	***4.07***	***3.45***	***3.05***
		Upright	Stress (MPa)	1444.45	1138.11	1125.61
			SCF	***4.14***	***3.26***	***3.23***
25.7	0	Flat	Stress (MPa)	1509.03	1126.78	1081.00
			SCF	***4.33***	***3.23***	***2.92***
		Upright	Stress (MPa)	1472.87	1162.15	1127.34
			SCF	***4.22***	***3.33***	***3.23***
12.85	12.85	Flat	Stress (MPa)	1587.87	1222.57	1115.11
			SCF	***4.55***	***3.50***	***3.20***
		Upright	Stress (MPa)	1565.87	1196.61	1159.04
			SCF	***4.49***	***3.43***	***3.32***
12.85	0	Flat	Stress (MPa)	1445.65	1200.82	1077.99
			SCF	***4.14***	***3.95***	***3.09***
		Upright	Stress (MPa)	1444.45	1138.13	1125.82
			SCF	***4.14***	***3.26***	***3.23***

Table 3: Configuration 1 Fairlead-Chain Link Model SCF for 5.25" grade R4 Chain, 60% CBL.

Table 26: SCFs for chain in fairlead and varying angles (β_k) [29]

$$\textbf{SCF max} = 4.99 \;\; 4.99/4.33 = 1.15 \tag{64}$$

Max and final $SCF_{geometry}$ obtained in Vargas, Hsu and Lee (2004)

Emil A. Edwin

NTNU
Kunnskap for en bedre verden